AUTOMATIC REPEAT REQUEST PROTOCOLS FOR RADIO CDMA SYSTEMS

A Thesis

Submitted to the College of Graduate Studies and Research

in Partial Fulfilment of the Requirements

for the Degree of

Master Science

in the Department of Electrical Engineering

University of Saskatchewan

Saskatoon

by

Faizal Rochmad Djoemadi

June, 1998

This thesis is dedicated to my wife Silvia P. Dianita and my daughter Fadhila S. Faizal, without whose patience, support, kindness, and love, the last three years would not have been possible

Permission To Use

In presenting this thesis in partial fulfilment of the requirements for a Postgraduate degree from the University of Saskatchewan, I agree that the Libraries of this University may make it freely available for inspection. I further agree that permission for copying of this thesis in any manner, in whole or in part, for scholarly purposes may be granted by the professor or professors who supervised this thesis work or, in their absence, by the Head of Department or the Dean of the College in which my thesis work was done. It is understood that any copying or publication or use of this thesis or parts therefor for financial gain shall not be allowed without my written permission. It is also understood that due recognition shall be given to me and to the University of Saskatchewan in any scholarly use which may be made of any material in my thesis.

Requests for permission to copy or to make other use material in this thesis in whole or part should be addressed to:

Head of the Department of Electrical Engineering,

University of Saskatchewan,

Saskatoon, Saskatchewan,

Canada, S7N 5A9

Abstract

The Industrial, Science, and Medical (ISM) band has been allocated to meet the growing demand for data communications including VSAT tail circuit networks. The users are allowed to share the ISM band by using a particular transmission method known as spectrum spreading. One type of spread spectrum, which is suitable for multiple access radio, is Code Division Multiple Access (CDMA). In the CDMA system, the multiuser interference, multipath fading, and thermal noise result in transmission errors. Automatic-repeat-request (ARQ) protocols are commonly used to mitigate the effect of transmission errors. The stop-and-wait (SW) type of ARQ protocol offers simple implementation but has low throughput. In this thesis, new generalized-stop-and-wait (GSW) protocols that retain the simple implementation feature of the classical SW protocol, while reducing the transmitter's wait state time, are proposed to increase the throughput. The throughput performance of the GSW protocols over a CDMA system is analysed and verified by computer simulation. In particular, four type of GSW simulation methods termed GSW-1 to GSW-4 are analyzed and compared. Both analytical and simulation results show that GSW-4 and GSW-3 protocols are superior under severe channel conditions to somewhat lower complexity protocols such as SW, GBN, GSW-1, and GSW-2. On the other hand, the GSW-1 protocol has the advantage of fairly simple protocol and no buffer. It offers the best solution when thermal noise is the limiting factor. Furthermore, the GSW-2 protocol is comparable in performance to well known GBN protocol under different delay conditions and for different buffer sizes.

Acknowledgments

The author is indebted to Prof. Surinder Kumar for his supervision and constant encouragement throughout this work. His advice and assistance in the preparation of this thesis is thankfully acknowledged.

The author also extends thank to Prof. Eric Salt for his assistance during the analysis and for many hours of useful discussions concerning the simulation. It is a pleasure to acknowledge Prof. Hugh Wood for his guidance during the course work.

The author takes this opportunity to acknowledge the patience, encouragement and moral support provided by his parents, wife, and brothers. The author also wishes to thank to many friends for invaluable suggestions and advices. Particular thanks are due to A. Shamiss, S. Truitt, B. Abolhassani, and J. Panicker.

Financial assistance, in the form of scholarships, was provided by PT. TELKOM, Indonesia. Their support is gratefully acknowledged.

Table Of Contents

List Of Tables

List Of Figures

List of Abbreviations

ARQ	Automatic Repeat Request
AWGN	Additive White Gaussian Noise
BER	Bit Error Rate
BPSK	Binary Phase Shift Keying
bps	Bit per Second
CDMA	Code Division Multiple Access
CRC	Cyclic Redundancy Check
DS-CDMA	Direct Sequence CDMA
FEC	Forward Error Correction
FH	Frequency Hoppers
FM	Frequency Modulation
GBN	Go-Back-N
GSW	Generalized-Stop-and-Wait ARQ Scheme
GSW-1	Generalized-Stop-and-Wait ARQ Scheme Type-1
GSW-2	Generalized-Stop-and-Wait ARQ Scheme Type-2
GSW-3	Generalized-Stop-and-Wait ARQ Scheme Type-3
GSW-4	Generalized-Stop-and-Wait ARQ Scheme Type-4
ISI	Inter-Symbol Interference
ISM	Industrial, Science and Medical
LFSR	Linear Feedback Shift Register
MHz	Mega Hertz
MUI	Multi User Interference
MRC	Maximal Ratio Combiner
NAK	Negative Acknowledgment
PCNs	Personal Communication Networks

PN	Pseudo-Noise
R&D	Research and Development
RMS	Root Mean Square
SNR	Signal-to-Noise-plus-interference-Ratio
SR	Selective-Repeat
SRe	Shift Register
SS	Spread Spectrum
SW	Stop-and-Wait
TF	Transversal Filter
Tx	Transmitter
Rx	Receiver
VSAT	Very Small Aperture Terminal

List of Symbols

β	Random amplitude of the received signal.
$\beta_l^{(k)}$	l^{th} path gain for the k^{th} user.
C_c	Channel capacity.
$\delta(.)$	Unit impulse function.
ϵ	Bit error rate.
E	Average number of time-slots required to transmit the codeword successfully.
$E(\alpha)$	Average number of data blocks to deliver one correct block.
Er	Received signal energy per bit.
η	Throughput efficiency.
f_0	Coherence bandwidth.
f_m	Doppler shift or Doppler spread.
G	Rayleigh constant.
γ_i	Instantaneous signal to noise ratio at the output of the correlator.
$\overline{\gamma_i}$	Signal to noise ratio per combined path.
$h_k(t)$	Equivalent low pass linear filter with a time-invariant impulse response.
i	Transmission index.
k	Information bits.
K	Number of users.
L	Number of path.
M	Number of codeword in a frame.
n	Codewords length in bit.
N	Total round trip delay in codeword.
N_c	Golds codes length.
No	Additive White Gaussian Noise power spectral density.
P	Probability that a received codeword contains a detectable error pattern.

$p(\beta)$ Probability density function of Rayleigh random variable.

$P_k(\tau_l)$ Average received signal power of the multipath for the k^{th} user.

$P_s(i)$ Probability that after i transmission all codewords have been received successfully.

$\Phi_l^{(k)}$ l^{th} path phase for the k^{th} user.

R Information rate .

$S_k(t)$ Transmitted signal for the k^{th} user.

σ_τ Root mean squared delay spread.

T Total round trip delay in second.

T_b Symbol or bit period.

T_c Chip duration.

T_m Maximum excess delay.

T_0 Coherence Time.

$\bar{\tau}$ Mean excess delay.

$\overline{\tau^2}$ Second moment of the power delay profile.

$\tau_l^{(k)}$ l^{th} path delay for the k^{th} user.

θ_k Carrier phase for the k^{th} user.

W Transmitted bandwidth.

$\lfloor x \rfloor$ The largest integer that is less than or equal to x.

1. Introduction

1.1 Background

The 902 to 928 MHz spectrum band has been allocated by the frequency regulatory agencies to meet the growing demand for commercial data communication in the Industrial, Science and Medical (ISM) fields. The users are allowed to share the ISM band without a license by limiting their transmitted power to less than one watt and by using a particular transmission method known as spectrum spreading [1, 4]. This frequency slot can be used for a wide variety of applications such as Personal Communication Networks (PCNs), wireless local area networks for personal computers, wireless fire and security systems, and a Very Small Aperture Terminal (VSAT) tail circuit network. The name VSAT implies that these satellite systems use Earth-terminal antennas that are relatively small, i.e., 1.8 metres in diameter or less. The VSAT tail circuit network consists of a point to point communication link connecting a VSAT station with a remote terminal as shown in Figure 1.1.

If the distance between the VSAT and the remote terminal is not large, a cable can be used to make the connection. The research work reported in this thesis is concerned with the replacement of this cable with a spread spectrum wireless radio in the ISM band. This allows the distance between the VSAT station and a remote terminal to be extended to several kilometres. An important factor in the design of a VSAT tail circuit network using wireless communications is the presence of multipath propagation.

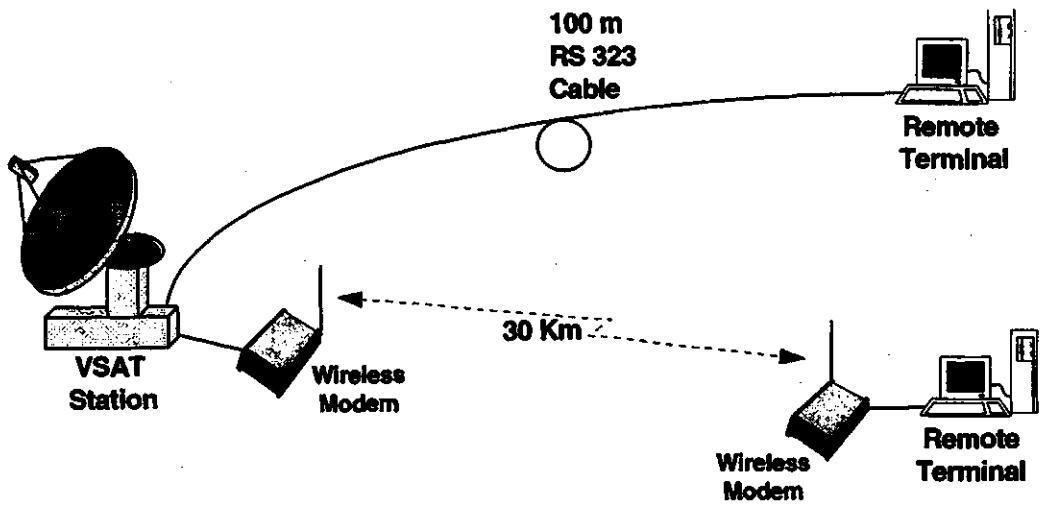

Figure 1.1 VSAT Tail Circuit Network.

Multipath propagation occurs when the height of the remote stations is below the height of surrounding structures, thus there is no single line-of-sight path to the VSAT station. Even when a line-of-sight path exists, some multipath propagation still occur due to reflections from the ground and surrounding structures. The signal received by the remote terminals may consist of a large number of plane waves that have randomly distributed amplitude, phase, and angle of arrival. These multipath components combine vectorially at the receiver antenna, and they can cause the signal received by the remote station to fade.

One well known method of mitigating the multipath effect is to use spread spectrum modulation. For a Spread Spectrum (SS) system, the transmission bandwidth W is much larger than the minimum bandwidth required to transmit the information. This inherent redundancy can be employed to overcome the effect of multipath fading. Another well known feature of a spread spectrum system is the ability to let multiple users transmit simultaneously in the same bandwidth as long as different users employ orthogonal codes to implement spectrum spreading. This is called Code Division Multiple Access (CDMA). The data sent using spread spectrum modulation can be recovered by a receiver, provided

that the receiver uses a Pseudo-Noise (PN) code that is identical to that used for spreading the particular SS signal that is to be demodulated.

In the CDMA system, the signals from other simultaneous channel users appear as an additive interference [5]. The level of interference varies, depending on the number of users at any given time. The multiuser interference and multipath fading are two primary effects that cause performance degradation in a CDMA system. A third source is the thermal noise at the front end of the receiver. The thermal noise has a Gaussian distribution and is distributed throughout the radio communication band. The overall effect of the multiuser interference, multipath fading, and thermal noise is the occurrence of transmission errors in the data. The error correction coding and error control strategies are commonly employed to mitigate the effect of transmission errors.

Two basic error control strategies commonly used in CDMA systems are Automatic Repeat Request (ARQ) and Forward Error Correction (FEC). Both methods require error detection. The error detection codes are based on the principle that by encoding the bit sequence prior to transmission so as to introduce certain redundant information, the presence of errors can be detected by the receiver. If a feedback channel is possible, a request for retransmission of information-in-error is employed in the ARQ protocols. Such retransmission continues until the codeword is successfully received and delivered to the user. On the other hand, in the FEC protocols, an error-correcting code is used to combat transmission errors. When the receiver detects the presence of errors in a received word, the receiver attempts to locate and correct the errors. After the error correction has been performed, the decoded word is delivered to the user. Since no retransmission is required in the FEC protocols, there is no need for a feedback channel. The Automatic Repeat Request (ARQ) strategy requires error detection and request for retransmission when an error is detected. In the Forward Error Correction (FEC), error detection is followed by error correction.

With ARQ protocols, erroneous data is delivered to the user only if the receiver fails to detect the presence of errors. Using a proper error-detecting code, the probability of an undetected error can be made very small [6-8]. ARQ protocols require a simple decoder, while they provide high system reliability. However, the throughput efficiency, defined as the ratio of the average number of information bits successfully accepted by the receiver per unit time to the total number of bits that could be transmitted per unit time, is not constant and the throughput efficiency decreases as the channel error rate increases. In the FEC protocols, when a received word is detected as being in error, it must be decoded, and the decoded word must be delivered to the user, regardless of whether it is correct or not. Since the probability of incorrect decoding is much greater than the probability of undetected error [6], it may be difficult to achieve high system reliability. For many applications, ARQ is preferred over FEC for error control in data communication, provided the feedback channel is available. The primary focus of this thesis is the study of ARQ methods for the CDMA systems.

The ARQ methods are categorized based upon retransmission strategies. There are three basic types of ARQ protocols, namely, Stop-and-Wait (SW) ARQ, Go-Back-N (GBN) ARQ, and Selective-Repeat (SR) ARQ. In a SW ARQ protocol, the transmitter sends a codeword and waits for acknowledgment (ACK) from the receiver. Once the acknowledgment of error-free reception has been received, the next codeword is sent. A negative acknowledgment (NAK) from the receiver indicates that the codeword is not correctly received. In the case of a NAK, the transmitter resends the codeword and waits for the acknowledgment. The other two ARQ methods mentioned above, the GBN and SR, are continuous transmission methods. In both protocols, the codewords are sent from the transmitter to the receiver without interruptions. In the GBN protocol, the transmitter can send N codewords without waiting for acknowledgment. Whenever the transmitter receives a NAK, it stops transmitting new codewords, returns to the erroneous codeword, and retransmits the codeword and (N-1) succeeding codewords. The receiver discards the

erroneously received codeword and all (N-1) subsequent codewords, whether they are error-free or not. The SR protocol transmits codewords continuously and only those containing errors are retransmitted.

The SW protocol is simple to implement, but is inherently inefficient because of the idle time spent waiting for acknowledgment. The GBN protocol gives a better throughput efficiency, as there is no idle channel. However, the main drawback of GBN protocol is that whenever a received word is detected to be in error, the receiver also rejects the next (N-1) received codewords, even though many of them may be error free. As a result, the throughput performance dips sharply when error rates and/or round-trip delays increase. Of these methods, the SR protocol gives the best performance, but the cost of implementation and complexity is higher as the SR protocol theoretically requires an infinite buffer at the receiver side [9].

Because of the shortcomings of the three ARQ methods discussed above, improved ARQ protocols are required. The research problem may be defined in general terms as the study and investigation of ARQ methods for CDMA systems.

1.2 Previous Work and Thesis Objectives

A number of references currently exist in literature, for the CDMA system performance over multipath fading channels. A good reference is the analysis of the Bit Error Rate (BER) performance for the direct sequence spread spectrum multiple access communication system by M. B. Pursley et al [10, 25]. The effect of multipath fading in the DS-CDMA has been derived in [11, 12]. A well-known method to mitigate the effect of multipath fading is the use of a coherent RAKE receiver, and the performance results for such a system are covered quite well in a text by Proakis [5]. The throughput performance of some new types of ARQ protocols over satellite channels has been studied in [9, 13-15]. The objectives of this thesis may be listed as

1. Analyze different ARQ error correction methods for the CDMA systems. Identify/ propose an ARQ method that is particularly suitable for CDMA.

2. Using computer simulation, verify the analysis results of the first objective. Based on the analysis and simulation perform a comparison of various ARQ methods for CDMA.

1.3 Thesis Outline

In Chapter 2, a brief introduction to direct sequence spread spectrum and CDMA is presented. This is followed by a discussion of the channel model. In Chapter 3, error detecting codes and different types of error control strategies are discussed in some depth. Bit Error Rate (BER) analysis of the CDMA system over multipath fading channel is developed in Chapter 4. Performance analysis of the various types of generalized ARQ methods is presented in Chapter 5. The simulation method as well as simulation results are included in Chapter 6. Conclusions and suggestions for further research are presented in Chapter 7.

2. CDMA Systems

2.1 Introduction

During World War II, the spread spectrum systems were developed to meet the demand for secure communications. Such communication and navigation systems have to perform in presence of deliberate jamming [17]. Until the early 1980s, spread spectrum techniques were used almost exclusively in military communications systems, and Research and Development (R&D) in these areas were performed primarily with such applications in mind. However, in 1983, the U.S. Federal Communication Commission (FCC) opened three frequency bands, 902-928 MHz, 2400-2483.5 MHz, and 5725-5850 MHz for commercial spread spectrum systems [18]. Unlicensed operation with up to one watt transmitter power levels was permitted using spectrum spreading. The number of users that might operate within any of these bands was not specified and there is a possibility that many users will operate simultaneously in the same location. As mentioned in the last chapter, spread spectrum systems allow multiple users to simultaneously use a common channel for information transfer using orthogonal spreading codes. Such an access method is known as the Code Division Multiple Access or CDMA.

In this chapter, various components of a CDMA system are briefly described. To start with the Binary Phase Shift Keying (BPSK) carrier modulation technique and the Spread Spectrum (SS) concepts are discussed. This is followed by codes for spectrum spreading and their properties. The channel parameters that influence the transmitted signal are discussed. The receiver structures for a CDMA system are examined.

2.2 Binary Phase Shift Keying Modulation

The source information needs to be mapped into a high frequency bandpass signal in order to transmit over a radio channel. This mapping process is called bandpass modulation. Bandpass modulation can be defined as the process whereby the amplitude or frequency or phase of an RF carrier, or a combination of them, is varied in accordance with the information to be transmitted. The general form of the carrier wave, $s(t)$, can be represented by [27]:

$$s(t) = A(t)\cos(\omega_0 t + \theta(t)), \tag{2.1}$$

where $A(t)$ is the time-varying amplitude, ω_0 is the radian frequency of the carrier wave, and $\theta(t)$ is the instantaneous phase. In the Binary Phase Shift Keying (BPSK) modulation, the modulating data signal switches the phase of the carrier to one of the two states, 0° or 180°. The BPSK modulated carrier signal may be written as

$$s_i(t) = A\cos(\omega_0 t + \theta_i(t)) \qquad \begin{matrix} 0 \le t \le T \\ i = 1,2, \end{matrix} \tag{2.2}$$

where $\theta_i(t) = \pi i$, $i = 1, 2$. Figure 2.1(a) shows a typical BPSK waveform for the modulating data stream of 1 0 1 1. The signal waveforms can be also represented as vectors in a polar plot as shown in Figure 2.1(b).

2.3 Spread Spectrum Communication Systems

As stated in the last chapter, in a Spread Spectrum (SS) system, the transmitted signal is spread over a wide frequency band; much wider than the minimum bandwidth required to transmit the information being sent. For example, a voice signal can be sent with amplitude modulation in a bandwidth only twice that of the information itself [16]. A spread

spectrum, on the other hand, often takes a baseband signal (such as a voice channel) with a bandwidth of only a few kilohertz, and spreads it over a band that may be tens or even hundreds of KHz wide. This is accomplished by using a wide band coding signal.

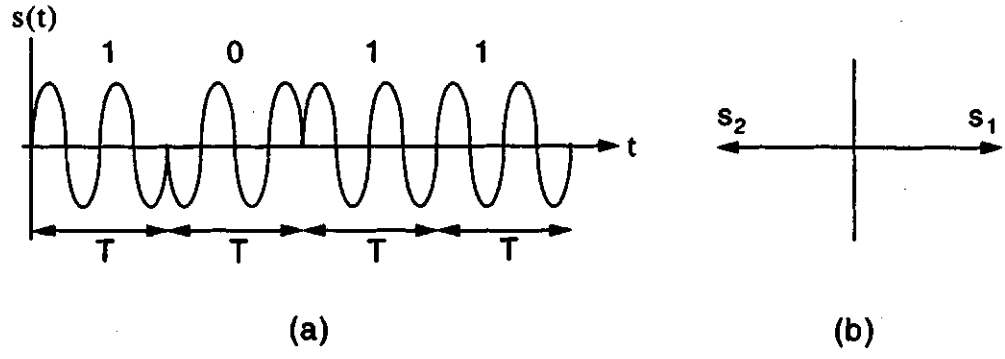

Figure 2.1 BPSK modulation. (a) BPSK signal waveform (b) BPSK signal vector representation.

The bandwidth expansion factor, or processing gain, is denoted by $N_c = R_c/R$, where R_c is the spreading code rate and R is information rate. For spread spectrum signal N_c, of course, is much greater than unity.

The bandwidth expansion factor in a spread spectrum technique results in quite a few useful properties such as:

- Combating interference that includes self interference caused by multipath propagation and cross interference caused by other users of the same bandwidth. An interference signal is a wide band signal existing in the same band as the spread signal. In the receiver, when the received signal containing an interference signal is multiplied by the de-spreading code, the spectrum of the desired signal is converted into the narrow information bandwidth. On the other hand, the spectrum of the interference signal will not be de-spread to a narrow bandwidth unless a synchronized spreading code corresponding to that of the wide band interference signal is used. This results in a major portion of the energy in the information

bandwidth being due to the desired signal and only a small portion being due to interference.

- Hiding a signal by transmitting with low power, and thus, making it difficult for an unintended listener to detect the presence of background noise.

There are three types of spread spectrum signaling methods that are commonly used today. They are as follows:

- Modulation of a carrier by a digital code sequence with a bit rate much higher than the information signal. This spreading method is called direct sequence modulation and is the method analyzed in this thesis.
- Carrier frequency shifting in discrete increments in a pattern dictated by a code sequence. This method is called Frequency Hopping (FH). In this implementation, the transmitter jumps from frequency to frequency within some predetermined set and the order of frequency usage is determined by a code sequence.
- Pulsed-FM or "chirp" modulation in which a carrier is swept over a wide band during a given pulse interval. This type of SS modulation does not necessarily employ coding but does use a wider bandwidth than the minimum required so that it can realize processing gain.

2.3.1 Direct Sequence Spread Spectrum

In Direct Sequence Spread Spectrum (DS-SS), the spectrum spreading is achieved by multiplying the information signal $b(t)$ with a Pseudo-Noise (PN) code $a(t)$ that has much wider bandwidth compared to that of the information signal. The information and wide band signals have two possible amplitudes, +1 and -1, and these amplitudes are periodically switched, in a pseudo-random manner. The combined signal is used as the

modulating signal for BPSK carrier modulation as shown in Figure 2.2 (a).

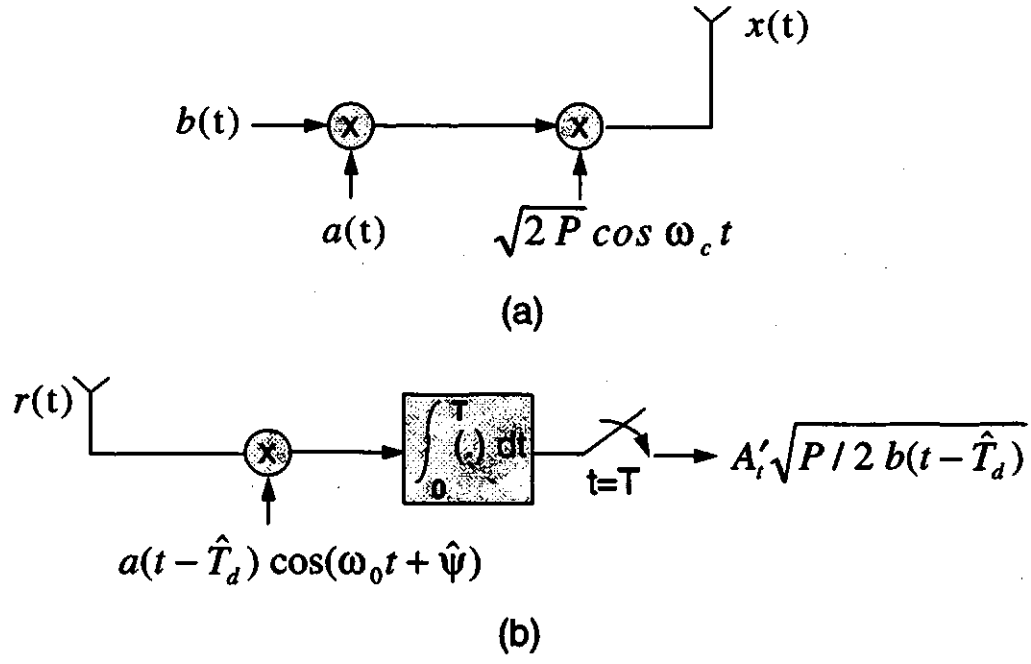

Figure 2.2 Direct Sequence Spread Spectrum System (a) Transmitter (b) Receiver.

The transmitted SS BPSK modulated signal $x(t)$ can be described mathematically as follows:

$$x(t) = \sqrt{2P_c}\, b(t)\, a(t) \cos\, \omega_0 t, \qquad (2.3)$$

where P_c is the average carrier power. A 1 Ohm system resistance is assumed. At the receiver, the received signal consists of a desired signal, interference signals from other user and Additive White Gaussian Noise (AWGN), $n(t)$. Therefore, the received signal may be described as

$$r(t) = A_t \sqrt{2P_c}\, b(t-T_d)\, a(t-T_d) \cos[\omega_0(t-T_d) + \theta(t)] + MUI + n(t), \qquad (2.4)$$

where *MUI* is Multi User Interference, A_t is the attenuation of the channel, $\theta(t)$ is the instantaneous phase, and T_d is the propagation delay. The signals from other users appear as an additive interference [5] so that $MUI + n(t)$ can be replaced by $\acute{n}(t)$. Thus, equation (2.4) may be written as,

$$r(t) = A_t \sqrt{2P_c}\, b(t-T_d)\, a(t-T_d) \cos[\omega_o t + \psi] + \acute{n}(t), \qquad (2.5)$$

where $\psi = \omega_0 T_d + \theta(t)$.

In Figure 2.2(b), the receiver has to be able to estimate the delay and phase of the received signal in order to recover the information. Assuming perfect delay and phase estimates, the received signal is multiplied by $a(t-T_d)\cos(\omega_0 t + \psi)$ and passed through a matched filter. The matched filter consists of an integrate and dump circuit. The output of the matched filter is a scaled version of the information signal that may be written as $A_t'\sqrt{P_c/2}\; b(t-T_d)$. A direct sequence implementation of the CDMA is briefly introduced in the next section.

2.3.2 Code Division Multiple Access

The enhancement in performance obtained from a DS-SS signal through the processing gain can be used to enable many DS-SS signals to occupy the same channel bandwidth, provided that each signal has its own distinct PN sequence, as shown in Figure 2.3. Thus, it is possible to have several users transmit messages simultaneously over the same channel bandwidth. This type of digital communication, in which each user (transmitter-receiver pair) has a distinct PN code for transmitting over a common channel bandwidth, is called Code Division Multiple Access (CDMA).

In the demodulation of each PN signal, the signals from other simultaneous users of the channel appear as additive interference. The level of interference depends on the

number of users at any given time. In the CDMA system, the limit as the users allowed to communicate over the same channel depends on the level of total interference that can be tolerated [17].

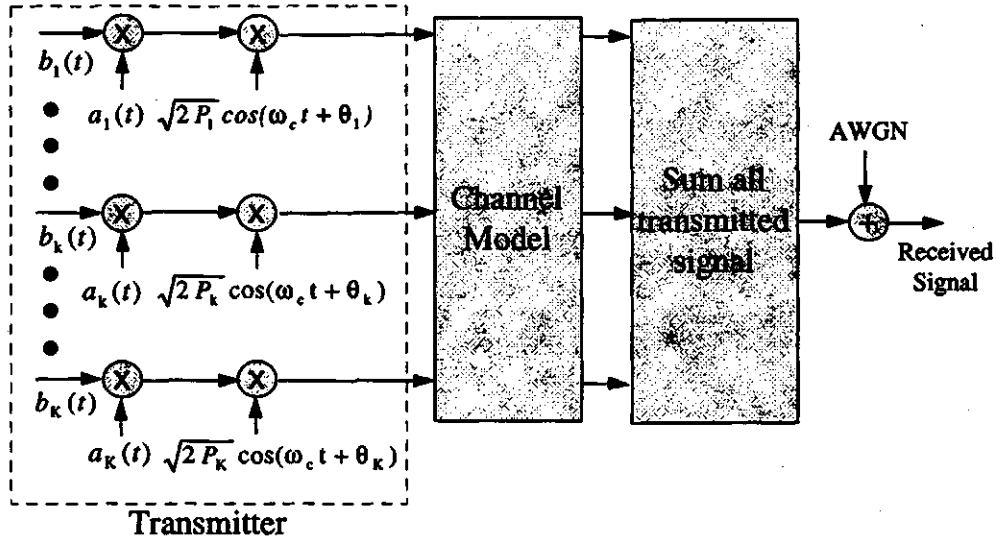

Figure 2.3 Code Division Multiple Access with Direct Sequence Spread Spectrum.

2.4 Spread Spectrum Codes

As stated above, Pseudo-Noise (PN) code is used to spread the signal spectrum. To de-spread the signal, the receiver needs a replica of the transmitted sequence (in almost perfect time synchronism). Desirable characteristics of the spreading code include ease of generation, randomness of sequences, and long period. Sequences generated using a Linear Feedback Shift Register (LFSR) possess all these properties [19]. This generation method is shown in Figure 2.4. It consists of n binary storage elements (boxes) that transfer their contents to the right, after each clock pulse. The contents of the register are linearly combined and are fed back to the first stage.

The length of the sequence depends on the initial state and on the feedback taps. The code is said to have a maximal length, when its length is $2^n - 1$, where n is number of

registers. An example is shown for a five-state register. For an initial 11111 state, the sequence output is 11111 00100 11000 01011 01010 001110 which is a maximal length code which repeats every 31 bits.

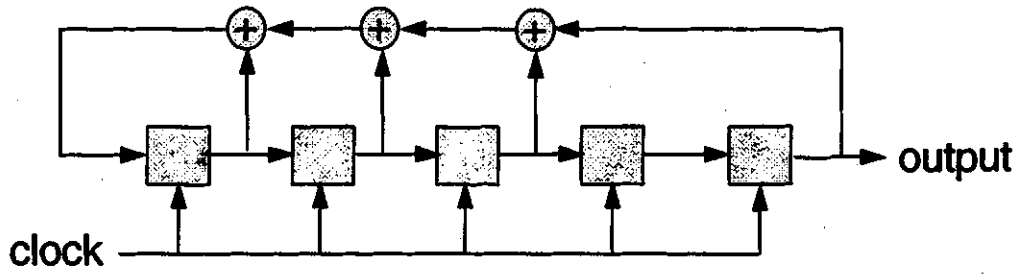

Figure 2.4 Linear Feedback Shift Register (LFSR) generator.

The maximal length sequences (m-sequences) have the following desirable properties:

- There is an approximate balance of zeros and ones (2^{n-1} ones and $2^{n-1} - 1$ zeros).
- In any period, half of the runs of consecutive zeros or ones are of length one, one-fourth are of length two, one-eight are of length three, etc.
- A modulo-2 addition of maximal linear code with a phase-shifted replica of itself results in another replica with a phase shift different from either of the original codes.
- Auto-correlation of maximal linear code is such that for all values of phase shift greater than a chip, the correlation value is -1. For the 0 ± 1 chip phase shift area, the correlation varies linearly from -1 to $2^n - 1$. A 31-chip maximal code, therefore, has a peak to minimum auto-correlation value 31; a range of 15 dB.

The cross-correlation of two codes is of similar importance. Cross-correlation is the

measure of agreement between two different codes. Unfortunately, cross-correlation values among any m-sequences are relatively high [16]. When a large number of users in CDMA with different m-sequence codes, transmit at the same time, a significant amount of interference is generated which deteriorates the received signal. Therefore, a better code that has better cross-correlation properties must be used. Codes, known as the Gold codes, have better cross-correlation properties than m-sequences and these codes are most commonly used. The next section is concerned with a description of these codes.

2.4.1 Gold Codes

Gold codes, invented by R. Gold [23, 24], can be generated by the modulo-2 addition of a pair of preferred maximal linear sequences **a** and **b**, shown in Figure 2.5. The code sequences are added chip-by-chip by synchronous clocking. An example of Gold codes generation is given below

m-sequence of **a:** 11111000110111010100000100101100

m-sequence of **b:** 11111001001100001011010100011110

Gold Code: 00000001111011011111011101000010

Gold codes for different users in CDMA can be generated by changing the phase shift between the two m-sequence generators. For example by giving one-chip-shift to the m-sequence **b** in the above examples, a new Gold code shown below may be generated

m-sequence of **a:** 11111000110111010100000100101100

m-sequence of **b:** 11110010011000010110101000111011

New Gold Code: 00001010101111000010100001100001

Using the above example of 5 register maximal length codes, 33 different Gold codes for up to 33 users can be generated.

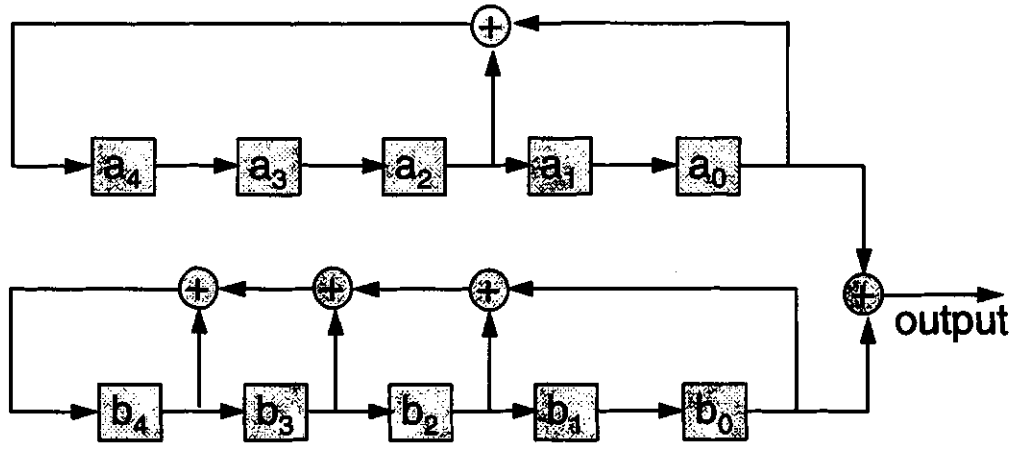

Figure 2.5 Gold code generation with generator $\mathbf{a}(X)=X^5+X^3+1$ and $\mathbf{b}(X)=X^5+X^4+X^3+X^2+1$ generators.

In addition to their advantage in generating large numbers of codes, the Gold codes are chosen because they have better periodic cross-correlation properties than m-sequences [5]. The Gold codes have a three-valued cross correlation function with values $\{-1, -t(n), t(n)-2\}$, where

$$t(n) = \begin{cases} 2^{(n+1)/2}+1 & (odd\ n) \\ 2^{(n+2)/2}+1 & (even\ n). \end{cases} \qquad (2.6)$$

For example, if $n = 5$ then $t(5) = 2^3 + 1 = 9$, and the three possible values of the periodic cross correlation function are {-1, -9, 7}.

2.5 Channel Model

As shown in Figure 2.6, a signal can travel from transmitter (Tx) to receiver (Rx) over multiple paths. No single line-of-sight path exists between transmitter and receiver as when the height of the antenna is below the heights of surrounding structures. This

phenomenon is referred to as multipath propagation. Even when a line-of-sight path exists, multipath propagation still occurs due to the reflection from the ground and the surrounding structures. At the receiver, the incoming radio waves arrive from different directions with different propagation delays. At any time, the signal received by the antennas may consist of a large number of plane waves with randomly distributed amplitudes, phases, and angles of arrival. These multipath components combine vectorially at the receiver antenna, and can cause the signal received by the mobile to fade. In the case of a fixed radio, the received signal may also fade due to the movement of surrounding objects.

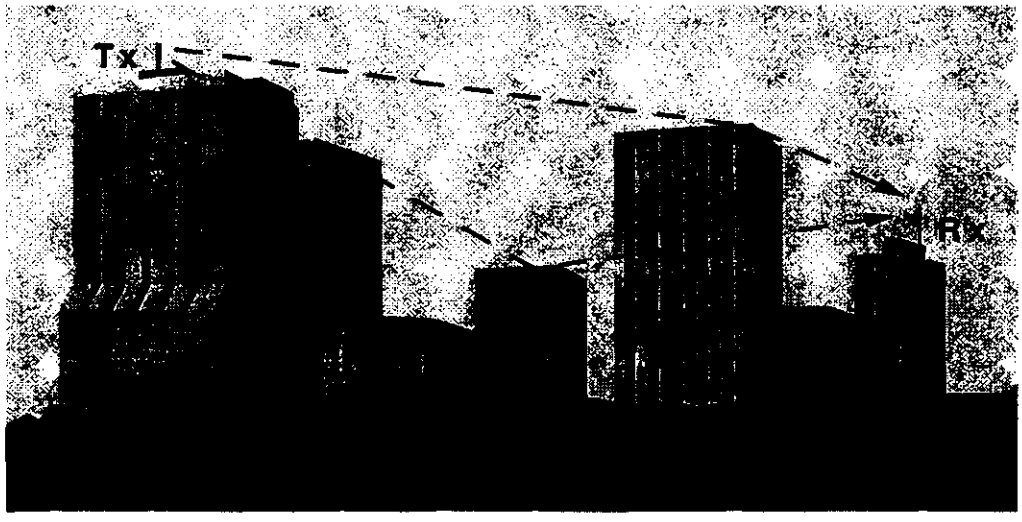

Figure 2.6 An example of multipath in an urban radio propagation.

2.5.1 Impulse Response

The multipath phenomenon can be directly related to the impulse response of the radio channel. The impulse response is a form of wide band channel characterization and it essentially contains all the information necessary to simulate or analyze the radio transmission through the channel. The impulse response stems from the fact that a fixed radio channel may be modeled as an equivalent low pass linear filter with a time-invariant impulse response $h(t)$ given by [5]

$$h(t) = \sum_{l=0}^{L-1} g_l \, \delta(t-t_l) \, e^{j\phi_l}, \tag{2.7}$$

where L is the number of paths, g_l, t_l, and ϕ_l are random amplitude, delay and phase of the l^{th} path respectively and $\delta(.)$ is the unit impulse function. In Figure 2.7, with transmitted signal, denoted by $x(t)$, the received signal $r(t)$ can be expressed as convolution of $x(t)$ with $h(t)$ and adding noise $n(t)$ as follows,

$$\begin{aligned} r(t) &= x(t) * h(t) + n(t) , \\ &= \int_{-\infty}^{\infty} x(\tau) h(t-\tau) d\tau + n(t) . \end{aligned} \tag{2.8}$$

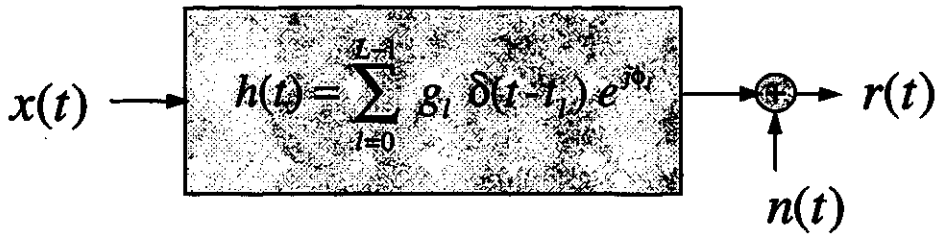

Figure 2.7 Mathematical model of the fixed radio channel.

The bandpass transmitted signal $x(t)$ can be expressed in terms of an equivalent low pass transmitted signal $s_l(t)$ as $x(t) = Re\{ s_l(t) \exp[j\omega_0 t] \}$. For a channel with L multipaths, the received signal is given by $r(t) = Re\{ \rho(t) \exp[j\omega_0 t] \}$, where $\rho(t)$ is an equivalent low pass received signal that may be written as

$$\rho(t) = \sum_{l=0}^{L-1} g_l s(t-t_l) e^{j\phi_l} + n(t). \tag{2.9}$$

2.5.2 Delay Spread and Coherence Bandwidth

One result of multipath medium is the time spreading of the signal transmitted through the channel. In practice, the time spread is measured by transmitting very narrow pulses [1]. In Figure 2.8, the power delay profile of a multipath propagation is shown. One of the important parameters shown in the power delay profile is the maximum excess delay, T_m. This is defined to be the time delay between the first and last received components. The last component is the component for which the multipath energy falls below the threshold level. The threshold level could be chosen at 20 dB below the level of the strongest expected component.

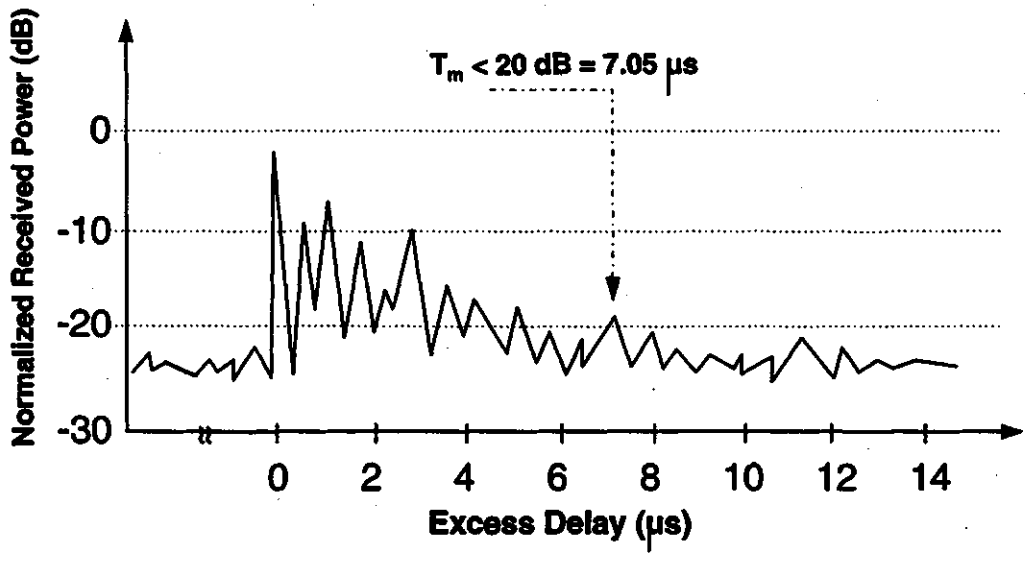

Figure 2.8 Power delay profile of the urban radio propagation.

Another important parameter, namely Root Mean Squared (RMS) delay spread, is commonly used. This is defined as

$$\sigma_\tau = \sqrt{\overline{\tau^2} - (\overline{\tau})^2}, \tag{2.10}$$

where $\bar{\tau}$ is the mean excess delay and is defined to be

$$\bar{\tau} = \frac{\sum_l P(\tau_l)\,\tau_l}{\sum_l P(\tau_l)} \tag{2.11}$$

and $\overline{\tau^2}$ is the second moment of the power delay profile and is defined as

$$\overline{\tau^2} = \frac{\sum_l P(\tau_l)\,\tau_l^2}{\sum_l P(\tau_l)}\,. \tag{2.12}$$

Where $P(\tau_l)$ is the power of the received signal arriving with delay τ_l. At 900 MHz, the typical reported values of the urban radio maximum excess delay T_m and RMS delay spread σ_τ are 7.05 μs and 1300 ns respectively [3, 20, 26].

The fading channels are categorized into two categories of frequency selective and flat fading channels. A channel exhibits frequency selective fading if $T_m > T_b$, where T_b is symbol time. This condition occurs whenever the received multipath components extend beyond the symbol duration, thus causing channel-induced inter-symbol interference (ISI). On the other hand, in flat fading, $T_m < T_b$ and there is no inter-symbol interference due to multipath fading. Therefore, T_m sets an upper limit on the information rate that can be used without incorporating an equalizer for frequency selective fading. For a 64 Kbps urban radio, the fading is essentially flat fading.

A completely analogous characterization of multipath channels in the frequency domain can be done using the concept of coherence bandwidth. The coherence bandwidth is a statistical measure of the range of frequencies over which the channel passes all spectral components with approximately equal gain and linear phase [21]. Thus, the coherence

bandwidth represents a frequency range over which frequency components have a strong potential amplitude correlation. Note that the coherence bandwidth f_0 and T_m are reciprocally related. As an approximation, it is possible to say that $f_0 \approx 1/T_m$. Another commonly used approximation of f_0 can be obtained by using RMS delay spread as [1]

$$f_0 \approx \frac{1}{5\sigma_\tau} . \tag{2.13}$$

When viewed in the frequency domain, a channel is referred to as frequency-selective if f_0 is less than the transmitted bandwidth W. If f_0 is more than W, then the channel experiences flat fading. If DS-SS is used to modulate 64 Kbps digital information using a 31 chip PN sequence, then the spread spectrum bandwidth is about 2 MHz. The RMS delay spread of the urban radio channel is 1300 ns, thus the coherence bandwidth of the channel is approximately 154 KHz, which is less than the spread spectrum bandwidth. Therefore, the channel can be categorized as frequency-selective with respect to the basic signaling element, namely, the chip. It is clear that there is inter-chip interference due to different path components arriving simultaneously. The spread-spectrum processing gain allows the system to endure such interference at the chip level. It also shows that a DS-SS system operating over a frequency-selective channel at chip level does not necessarily experience frequency-selective distortion at the symbol level.

2.5.3 Doppler Spread and Coherence Time

The movement of surrounding objects in the fixed radio channel results in the time-varying behavior for the channel. Doppler spread f_m and coherence time T_0 are parameters used to describe the time varying nature of the channel.

The Doppler spread or fading rate is defined as the range of frequencies over which the received signal spectrum is essentially non-zero. When a pure sinusoidal tone of frequency f_c is transmitted, the received signal spectrum will have components in the range

of $f_c - f_d$ to $f_c + f_d$, where f_d is the Doppler shift. The amount of the Doppler spread is a function of the relative velocity of the moving objects.

Coherence time is a statistical measure of time duration, over which the channel impulse response is essentially invariant. In other words, coherence time is the time duration over which two received signals have a strong potential for amplitude correlation. If the coherence time is defined as the time over which the time correlation function is above 0.5, then it can be approximated by [1]

$$T_0 \approx \frac{9}{16\pi f_m} . \tag{2.14}$$

where $f_m = \upsilon/\lambda$. υ and λ are relative velocity and signal wavelength, respectively.

A channel is referred to as fast fading if the symbol rate $1/T_s$ is less than the fading rate f_m. Conversely, a channel is referred to as slow fading if the signaling rate is greater than the fading rate, or the symbol period T_s is less than coherence time T_0.

For a 900 MHz fixed radio, the channel has a maximum Doppler shift of approximately 10 Hz [5]. For an information rate of 64 Kbps, the channel can be categorized as a slow fading channel. As a result of this slowly fading channel, channel attenuation and phase shift can be considered to be constant over the duration of a signaling interval.

2.5.4 Rayleigh Fading

The Rayleigh fading is widely used to describe multipath fading in absence of a strong path component [5, 20-22]. The multipath fading will cause rapid amplitude fluctuations that are randomly distributed over the signaling interval. This random fluctuation has a Rayleigh distribution, with probability density function (pdf) given by [1]

$$p(\beta) = \frac{\beta}{\sigma^2} e^{-\beta^2/2\sigma^2} \qquad \beta \geq 0, \tag{2.15}$$

where β is the random amplitude of the received signal, and σ^2 is the pre-detection mean power of multipath or Rayleigh constant that may be written as

$$\sigma^2 = \frac{1}{2} E(\beta^2), \tag{2.16}$$

where $E(\beta^2)$ is the average power of the received signal amplitude.

2.6 CDMA Receiver

The inherent redundancy in the DS-SS can be used to mitigate the effect of multipath fading described in the previous section. Further, for a DS-SS radio, a RAKE receiver may be used for providing diversity by coherently combining multipath components that would otherwise be lost. Therefore, instead of multipath being just a source of performance degradation, the multipath can be used to realize diversity and thereby improve performance.

2.6.1 RAKE Receiver

The name RAKE Receiver apparently taken from the action of a rake with a number of teeth pulling in a number of items simultaneously [22]. In Figure 2.9, the RAKE Receiver is modeled by a tapped delay line or a Transversal Filter (TF) with statistically independent time-variant tap weight $\{ a_l(t) \}$. The tapped delay line model with statistically independent, tap weights indicates that L diverse signals are available at the receiver. Hence, a receiver that processes the received signals in an optimum manner will achieve the performance of an equivalent L^{th} -order diversity.

This Transversal Filter (TF) incorporates a T_m seconds long delay line, which is tapped at least every T_c (chip duration) seconds. The input to TF is the output envelope of a matched filter. The output of the TF is a weighted sum of certain tap outputs, with the taps that are included in the sum depending on the delay estimates $\hat{t}_l$. The weight of the tap amplifier is set to be proportional to the associated strength estimates $\hat{a}_l$, where $\hat{a}_l$ is the conjugate of the estimate of the magnitude $\hat{g}_l$ and the phase $\hat{\phi}_l$, which is the low-pass-equivalent channel impulse response in the equation (2.7). The equivalent low pass tap weight amplifier can be written as:

$$\hat{a}_l = (\hat{g}_l \, e^{j\hat{\phi}_l})^* \, . \tag{2.17}$$

To achieve a significant improvement in performance, the RAKE receiver needs an accurate estimation of the tap delay as well as magnitude and phase of the channel impulse response. In this thesis, it is assumed that the receiver has means to do that and there are no errors due to imperfect estimates.

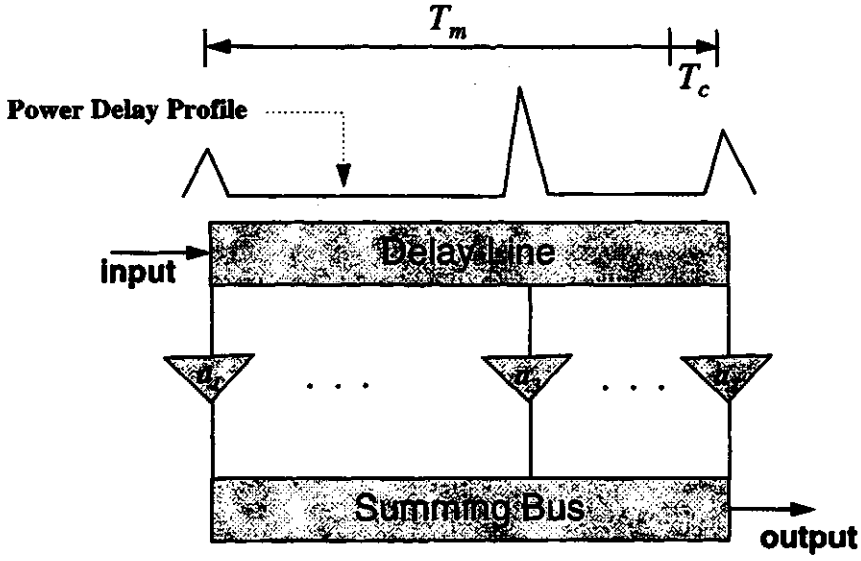

Figure 2.9 RAKE Receiver.

2.7 Summary

The fundamental concepts for a direct sequence spread spectrum radio were introduced in this chapter. Desirable features of Gold codes for implementing a code division multiple accessing system with direct sequence spread spectrum radios were introduced. This is followed by a description of the multipath channel model. For a 64 Kbps radio, the channel can be considered to be a flat fading channel. The multipath nature of the channel can be used advantageously in implementing multipath diversity with a RAKE receiver. The subject of error control coding is addressed next in Chapter 3.

3. Error Control Coding

3.1 Introduction

Error control coding is employed to deliver information from a source to a destination with a minimum of errors. As such error control coding can be seen as a branch of information theory and has its origins in Shannon's work in 1948 [28]. Shannon's work showed that any communication channel could be characterized by a capacity at which information could be reliably transmitted. At information transmission rate R up to the channel capacity C, it should be possible to transfer information with error rates that can be reduced to any desired low level. Error control can be provided by introducing redundancy in the transmission. This means that redundant symbols are added to the message with the result that only certain patterns at the receiver correspond to valid transmissions. Once an adequate degree of error control has been introduced, the error rates can be made as low as required by extending the length of the codes.

Present-day systems do not use codes as a way of obtaining the theoretical channel capacity but instead use these to achieve improvement over the systems with no coding. Thus, the use of coding may increase the operational range of a communications system, reduce the transmitted power requirements or obtain a blend of both benefits.

A typical communication system incorporating coding is shown in Figure 3.1. In this figure, information sequence **u** is given as a digital representation. The encoder transforms the information sequence **u** into a discrete encoded sequence **v**, which is called a codeword. The modulator, the channel model, and the demodulator are all combined into the coding channel block. The output **r** in the coding channel will be different from the input **v** because

of the noise and interference experienced in the channel. The decoder transforms the received sequence **r** into a binary sequence $\hat{\mathbf{u}}$, called the estimated sequence. Ideally, $\hat{\mathbf{u}}$ will be a replica of the information sequence **u**, although the noise may cause some decoding errors.

A major goal is to control transmission errors so that error-free data can be delivered to the user. The error control codes used to achieve this goal are introduced in the next section.

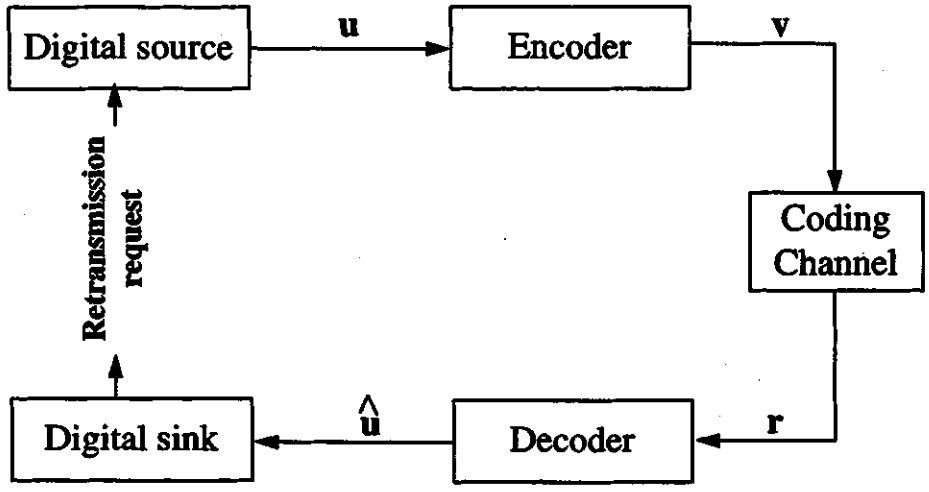

Figure 3.1 A block diagram of a typical data communication.

3.2 Types of Codes

There are two different types of codes used for the transmission error control strategies: error-correcting codes and error-detecting codes. The most complex techniques fall into the category of error-correcting codes, where errors are detected and corrected. An alternative strategy is to use error-detecting codes only and request a retransmission if an error is detected. The research work reported in this thesis is concerned with the use of the second strategy, i.e., error detection followed by retransmission. The Cyclic Codes are commonly used for error detection applications [6-8,27,28] and the next section contains

a brief description of these codes.

3.3 Cyclic Codes

Cyclic codes form an important subclass of linear block codes. A linear system is one in which the principles of superposition and scaling are satisfied. If two signals are added together at the input of a linear system, the output is the sum of the two corresponding outputs. If the input is multiplied by a scalar factor, the output is also multiplied by the same factor. The superposition and scaling principles can be used for implementation of the coding system. If two information sequences are added together, symbol by symbol, before going into a linear encoder, the resulting codeword should be the sum of two codewords that correspond to the individual information sequences. Similarly, if the input is scaled by any symbol value, the codeword output should consist of the original codeword output similarly scaled. For binary codes, binary symbol values are only 0 and 1 and the scaling property is not important.

A linear block code encoder divides the information sequence into message blocks of k information bits each. A message block is represented by the binary k-tuple $\mathbf{u} = (u_1, u_2, \ldots, u_k)$ called a message. There are a total of 2^k different possible messages. The encoder transforms each message $\mathbf{u}$ independently into n-tuple $\mathbf{v} = (v_1, v_2, \ldots, v_n)$ of discrete symbols, which is called a codeword. Therefore, corresponding to the 2^k different possible messages, there are 2^k different possible codewords at the encoder output. This set of 2^k codewords of length n is called an (n,k) block code.

An (n,k) block code is called a cyclic code if a cyclic shift of a codeword results in another codeword. This does not mean that all codewords can be produced by shifting a single codeword. However, it does mean that all codewords can be generated from a single sequence by the process of shifting and addition. For example, it is possible to generate a cyclic code of length 7 from a generator sequence of 0001011 [28]; bearing in mind that

the all-zeros sequence is also a codeword. The constructed codewords are shown in Table 3.1.

Table 3.1: Cyclic Code length 7

Seq.	Notes	Codeword	Seq.	Notes	Codeword
1	all zeros	0000000	9	sequence 2 + 3	0011101
2	generator	0001011	10	shift sequence 9	0111010
3	shift	0010110	11	2nd shift	1110100
4	2nd shift	0101100	12	3rd shift	1101001
5	3rd shift	1011000	13	4th shift	1010011
6	4th shift	0110001	14	5th shift	0100111
7	5th shift	1100010	15	6th shift	1001110
8	6th shift	1000101	16	sequences 2 + 11	1111111

The code starts from the second sequence and six left shifts give the first seven codewords. Sequence 2 and 3 are added to give a new sequence. The six cyclic shifts of the new sequence give the next six codewords. The 16th codeword is obtained by addition of second and eleventh codewords.

The encoding, the syndrome computation and the decoding of cyclic codes are all easily implemented using a shift register with feedback connections [7, 27, 28]. This is further described in the next section.

3.3.1 Encoding of Cyclic Codes

The special methods of encoding, syndrome computation and decoding are implemented by the use of an algebraic formula in which a polynomial is used to represent the sequences. In the polynomial representation, a multiplication by X represents a shift to the right, i.e., to next position in the sequence. The message vector is represented by polynomial $\mathbf{u}(X)$ as follows [7]:

$$\mathbf{u}(X) = u_0 + u_1 X + u_2 X^2 + \ldots + u_{k-1} X^{k-1}. \tag{3.1}$$

Shifting $\mathbf{u}(X)$ by $(n-k)$ positions results in

$$X^{n-k}\mathbf{u}(X) = u_0 X^{n-k} + u_1 X^{n-k+1} + \ldots + u_{k-1} X^{n-1}. \tag{3.2}$$

If Equation 3.2 is divided by generator polynomial $\mathbf{g}(X)$ used to generate the code, where

$$\mathbf{g}(X) = 1 + g_1 X + g_2 X^2 + \ldots + g_{n-k-1} X^{n-k-1} + X^{n-k}, \tag{3.3}$$

the result can be expressed as

$$\frac{X^{n-k}\mathbf{u}(X)}{\mathbf{g}(X)} = \mathbf{q}(X) + \frac{\mathbf{rem}(X)}{\mathbf{g}(X)}, \tag{3.4}$$

where $\mathbf{q}(X)$ is called the quotient polynomial that can be written as $\mathbf{q}(X) = q_0 + q_1 X + \ldots + q_{k-1} X^{k-1}$ and $\mathbf{rem}(X)$ is called remainder that can be written as

$$\mathbf{rem}(X) = rem_0 + rem_1 X + rem_2 X^2 + \ldots + rem_{n-k-1} X^{n-k-1}. \tag{3.5}$$

Each valid codeword has zero remainder when divided by the generator polynomial. Equation 3.5 can also be written as

$$\mathbf{rem}(X) = X^{n-k}\mathbf{u}(X) \text{ modulo } \mathbf{g}(X). \tag{3.6}$$

Addition of **rem**(X) in modulo-2 arithmetic to both sides of Equation 3.4 results in

$$\mathbf{rem}(X) + X^{n-k}\mathbf{u}(X) = \mathbf{q}(X)\mathbf{g}(X) = \mathbf{v}(X), \tag{3.7}$$

where modulo-2 addition or subtraction are equivalent to the logical exclusive or. Consequently, $\mathbf{rem}(X) + \mathbf{rem}(X) = 0$.

The left-hand side of Equation 3.7 is recognized as a valid codeword polynomial, since it is a polynomial of degree $n-1$ or less, and when divided by $\mathbf{g}(X)$, there is a zero remainder. This codeword can be expanded into its polynomial terms as follows:

$$\begin{aligned}\mathbf{rem}(X) + X^{n-k}\mathbf{u}(X) = {} & rem_0 + rem_1 X + \ldots + rem_{n-k-1}X^{n-k-1} \\ & + u_0 X^{n-k} + u_1 X^{n-k+1} + \ldots + u_{k-1}X^{n-1}.\end{aligned} \tag{3.8}$$

The right-hand side of Equation 3.7 is the codeword polynomial $\mathbf{v}(X)$ corresponding to the code vector **v** that can be written as

$$\mathbf{v} = \mathbf{rem}\ \mathbf{u}, \tag{3.9}$$

where $\mathbf{rem} = rem_0, rem_1, \ldots, rem_{n-k-1}$ is $n-k$ parity bits vector and $\mathbf{u} = u_0, u_1, \ldots, u_{k-1}$ is k message bits vector.

To further clarify the above encoding process, an example of a (7,4) codeword can be considered using a message vector **u** = 1 0 1 1. In polynomial form, the message vector may be written as $\mathbf{u}(X) = 1 + X^2 + X^3$. Division of $X^3\mathbf{u}(X)$ by $\mathbf{g}(X) = 1 + X + X^3$ using polynomial division, the quotient $\mathbf{q}(X)$ and the remainder $\mathbf{rem}(X)$ can be obtained; so that

$$\begin{aligned} X^3\mathbf{u}(X) &= \mathbf{q}(X)\mathbf{g}(X) + \mathbf{rem}(X) \\ X^3+X^5+X^6 &= (1+X+X^2+X^3)(1+X+X^3) + 1. \end{aligned} \tag{3.10}$$

The resulting codeword $\mathbf{v}(X)$ is obtained as

$$\begin{aligned} \mathbf{v}(X) &= \mathbf{rem}(X) + X^3\mathbf{u}(X) = 1+X^3+X^5+X^6 \\ \mathbf{v} &= 100 \quad 1011, \end{aligned} \tag{3.11}$$

where 1 0 0 are the parity bits and 1 0 1 1 are the message bits.

The cyclic code encoding operation explained above is accomplished by a division circuit using an $(n-k)$-stage shift register with feedback connections as shown in Figure 3.2. The circuit feedback connections corresponds to the coefficients of the generator polynomial g_i.

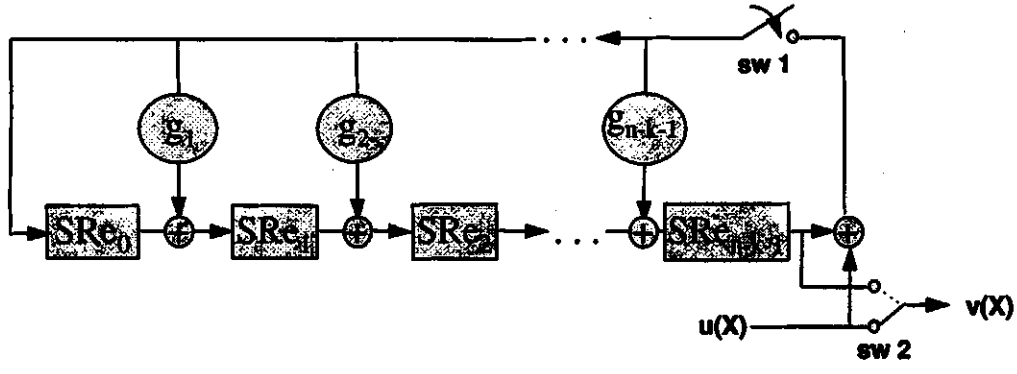

Figure 3.2 A dividing circuit with feedback connection.

For the above example of the (7,4) codeword, the codeword generation process using the shift register is explained in Figure 3.3 and Table 3.2.

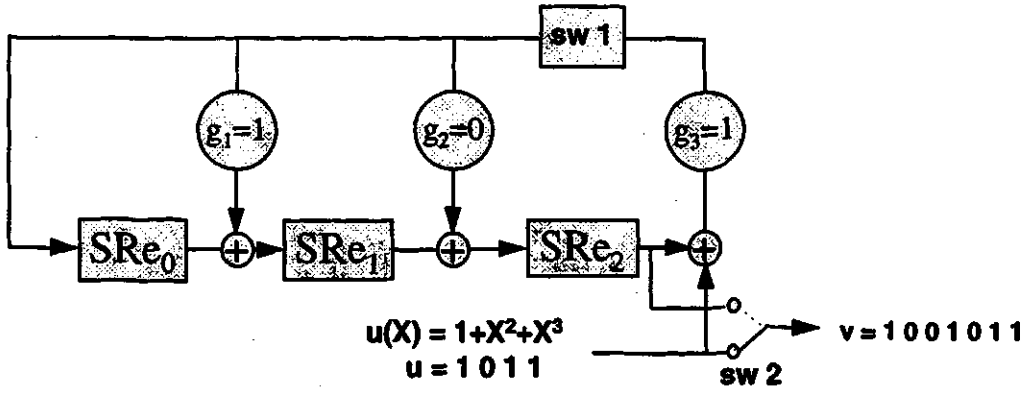

Figure 3.3 An encoder with generator polynomial $g(X)=1+X+X^3$, where $g_1=1$, $g_2=0$, and $g_3=1$.

Table 3.2: 3-stage encoding shift register

Input queue	Shift number	Register contents			Output
u		SRe_0	SRe_1	SRe_2	**v**
1 0 1 1	0	0	0	0	-
1 0 1	1	1	1	0	1
1 0	2	1	0	1	1
1	3	1	0	0	0
-	4	1	0	0	1
		Remainder **r**			

After the fourth shift, switch 1 is opened, switch 2 is moved to the up position, and the parity bits contained in the last register are shifted to the output as a remainder vector. The output code vector is **v** = 1 0 0 1 0 1 1, or in polynomial form, $v(X) = 1 + X^3 + X^5 + X^6$.

3.3.2 Syndrome Computation and decoding of Cyclic Code

The remainder obtained by the division of a codeword by the generator polynomial

is called the syndrome. The transmitted codeword $\mathbf{v}(X)$ may be perturbed by noise and interference as explained in Chapter 2. The vector received codeword $\mathbf{r}(X)$ is a corrupted version of the transmitted codeword. From the algebraic properties of a cyclic code [6], the transmitted codeword $\mathbf{v}(X)$ can be obtained by multiplying the message polynomial $\mathbf{u}(X)$ by the generator polynomial $\mathbf{g}(X)$, so that

$$\mathbf{v}(X) = \mathbf{u}(X)\mathbf{g}(X). \tag{3.12}$$

$\mathbf{r}(X)$, the corrupted version of $\mathbf{v}(X)$, may be written as

$$\mathbf{r}(X) = \mathbf{v}(X) + \mathbf{e}(X), \tag{3.13}$$

where $\mathbf{e}(X) = e_0 + e_1 X + \ldots + e_{n-1} X^{n-1}$ is the error polynomial. The decoder performs a test to find out whether $\mathbf{r}(X) = r_0 + r_1 X + \ldots + r_{n-1} X^{n-1}$ is a codeword polynomial or not, that is, whether it is divisible by $\mathbf{g}(X)$, with a zero remainder. This is accomplished by calculating the syndrome of the received polynomial. An all-zero syndrome indicates that the received sequence $\mathbf{r}(X)$ is correct. Any other syndrome indicates the presence of errors. The syndrome $\mathbf{s}(X)$ is the remainder resulting from dividing $\mathbf{r}(X)$ by $\mathbf{g}(X)$, that is,

$$\mathbf{r}(X) = \mathbf{q}(X)\mathbf{g}(X) + \mathbf{s}(X), \tag{3.14}$$

where syndrome $\mathbf{s}(X)$ is a polynomial of degree $n-k-1$ or less. Thus, the syndrome is an $(n-k)$-tuple. By combining Equations 3.12 to 3.14, the error polynomial can be obtained as

$$\mathbf{e}(X) = [\mathbf{u}(X) + \mathbf{q}(X)]\mathbf{g}(X) + \mathbf{s}(X). \tag{3.15}$$

A comparison of Equations 3.14 and 3.15, shows that the syndrome $\mathbf{s}(X)$ is obtained as the remainder of $\mathbf{r}(X)$ modulo $\mathbf{g}(X)$. In other words, the syndrome is the same as the parity bits recalculated from the received information plus the received parity bits. Equation 3.15 also shows that the syndrome is actually equal to the remainder resulting from dividing the error pattern by the generator polynomial. This means that $\mathbf{s}(X)$ is a zero vector only if either the error polynomial $\mathbf{e}(X) = 0$ or it is identical to a codeword. If $\mathbf{e}(X)$ is identical to a codeword, $\mathbf{e}(X)$ is an undetectable error pattern.

The syndrome calculation is accomplished by a division circuit that is almost identical to the encoding circuit. An example of syndrome calculation with an $n-k$ shift register is shown in Figure 3.4, using the received code vector $\mathbf{r}$ generated in the previous section. Switch 1 is initially closed and switch 2 is open. The received vector is shifted into the register input, with all stages initially set to zero. After the entire received vector has been entered into the shift register, the contents of the register give the syndrome. Switch 1 is then opened and switch 2 is closed, so that the syndrome vector can be shifted out of the register. The operational steps of the decoder for the received vector $\mathbf{r} = 1001011$ are illustrated in Figure 3.4 and Table 3.3.

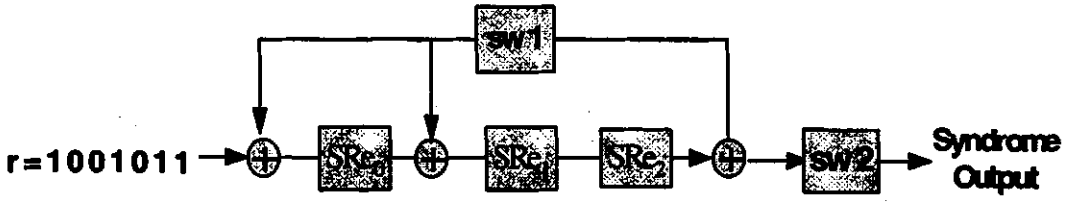

Figure 3.4 A decoder with generator polynomial $\mathbf{g}(X)=1+X+X^3$.

If the syndrome is an all-zeros vector, the received vector is assumed to be a valid code vector. Therefore, the estimated message vector $\hat{\mathbf{u}}(X)$ can be extracted using the last four bits of the received vector $\mathbf{r}(X)$. If the syndrome is non-zero, the received vector is

a perturbed code vector and errors have been detected. Such errors can be corrected by sending a negative acknowledgment to the transmitter with a request to resend the erroneous message . This type of error control strategy is explained in the next section.

Table 3.3: 3-stage decoding shift register

Input queue	Shift number	Register contents			
r		SRe_0	SRe_1	SRe_2	
1001011	0	0	0	0	
100101	1	1	0	0	
10010	2	1	1	0	
1001	3	0	1	1	
100	4	0	1	1	
10	5	1	1	1	
1	6	1	0	1	
-	7	0	0	0	Syndrome s

The commonly used cyclic codes are Cyclic Redundancy Check (CRC) codes or *S*-bit CRC, where S denotes the number of bits over which parity is generated. To generate a (n, k) codeword, CRC codes require $S = n - k$ parity bits in addition to the k information bits. The 10-bit CRC, the 12-bit CRC, the 16-bit CRC, and the 32-bit CRC are commonly used for error detection [8,28]. In this thesis, a (400, 386) codeword, in conjunction with the 16-bit CRC or CRC-16, will be used to perform error detection. The generator polynomial of the CRC-16 used in this thesis is $g(X) = 1 + X^2 + X^{15} + X^{16}$ [28].

3.4 Error Control Strategies

As mentioned before, the two commonly used error control strategies are the Forward Error Control (FEC) protocol and the Automatic Repeat Request (ARQ) protocol [7]. In the FEC protocols, an error-correcting code is used. In such method, when the

receiver detects the presence of errors, it attempts to determine the error locations and then correct the errors. If exact locations of errors are determined, the received codeword can be correctly decoded. Obviously, if the receiver fails to determine the exact locations of errors, the received codeword will be decoded incorrectly and erroneous data will be delivered to the users. In the ARQ protocols, a code with good error-detecting capability is used. At the receiver, the syndrome of the received codeword is computed. If the syndrome is zero, the received codeword is assumed to be error-free and is accepted by the receiver. At the same time, the receiver notifies the transmitter, via a return channel, that the transmitted codeword has been successfully received. However, if the syndrome is not zero, errors are detected in the received codeword. Then, the transmitter is instructed to retransmit the same codeword through the return channel. Retransmission continues until the codeword is successfully received. With this system, erroneous data gets delivered to the data sink only if the receiver fails to detect the presence of errors. Using a proper linear code, the probability of undetected error can be made very small [8]. The primary focus of this thesis is the study of ARQ protocols for the CDMA systems.

3.5 Automatic Repeat Request Protocols

In the ARQ protocols, the throughput efficiency, defined as the ratio of the average number of information bits successfully accepted by the receiver per unit time to the total number of bits that could be transmitted per unit time, is not constant and it decreases as the channel error rate increases. In the FEC protocols, when an error is detected in a received word, it must be decoded and the decoded word must be delivered to the user, regardless of whether it is correct or not. Since the probability of incorrect decoding is much greater than the probability of undetected error [6], it may be difficult to achieve high system reliability. Because of its simple implementation and high reliability, ARQ is often preferred over FEC for error control in data communication systems, provided a feedback channel is available. The performance of an ARQ error-control system, normally measured by its reliability and

throughput efficiency and these topics are addressed in the next section.

3.5.1 Reliability and Throughput Efficiencies

In an ARQ protocol, the receiver commits a decoding error whenever it accepts a received codeword with undetected errors. Such an event is called an error event. The reliability performance depends on the probability of an error event which is denoted by P(E). Clearly, for an ARQ protocol to be reliable, the P(E) should be made very small.

Assuming that a cyclic code is used for error detection in an ARQ protocol, the following probabilities can be defined

P_c = probability that a received n-bit word contains no error.

P_d = probability that a received word contains a detectable error pattern.

P_e = probability that a received word contains an undetectable error pattern.

where $P_c + P_d + P_e = 1$. Probability P_c depends on the channel error. For a random error channel such as CDMA system with Bit Error Rate (BER) ϵ, P_c can be found using a binomial distribution. The probability of getting exactly e errors in an n bit codeword is given by

$$P_n(e) = \binom{n}{e} \epsilon^e (1-\epsilon)^{(n-e)}. \tag{3.16}$$

Thus, the probability that a received n-bit word contains no error is

$$\begin{aligned} P_c &= P_n(0) \\ &= (1-\epsilon)^n. \end{aligned} \tag{3.17}$$

For an (n, k) codeword, the probability of undetected error P_e has the following upper bound [29]:

$$P_e \leq [1-(1-\epsilon)^k]\, 2^{-(n-k)}. \tag{3.18}$$

A received word is accepted by the receiver only if it either contains no errors or contains an undetectable error pattern which results in an error event. Since an undetectable error pattern can occur in the initial or in any retransmission, the P(E) may be written as

$$\begin{aligned} \mathrm{P(E)} &= P_e + P_d P_e + P_d^2 P_e + \ldots \\ &= P_e(1 + P_d + P_d^2 + \ldots) \\ &= P_e \frac{1}{1-P_d} = \frac{P_e}{P_c + P_e}. \end{aligned} \tag{3.19}$$

As stated before, a (400, 384) codeword is employed for error detection in this work. For a bit error rate $\epsilon = 10^{-3}$, $P_c \approx 6.70\times10^{-1}$, $P_e \leq 4.86\times10^{-6}$ and $\mathrm{P(E)} \leq 7.26\times10^{-6}$. An error event occurs approximately every one million received codewords at this bit error rate. This shows that a high system reliability can be achieved by an ARQ error-control protocol using very little parity overhead. As P_e is relatively small, $P_c + P_d \approx 1$. This assumption will be used throughout this thesis.

There are three main types of ARQ protocols called the Stop-and-Wait (SW) ARQ, Go-Back-N (GBN) ARQ and Selective-Repeat (SR) ARQ protocols[13]. The latter two are sometimes grouped together under the heading continuous ARQ protocols. Each of these protocols has different throughput efficiency. These ARQ protocols are next described starting with Stop-and-Wait ARQ protocol.

3.5.2 Stop-and-Wait ARQ Protocol

The Stop-and-Wait ARQ protocol is the simplest protocol and in this protocol, the transmitter sends a codeword to the receiver and waits for an acknowledgment from the

receiver as shown in Figure 3.5. A positive acknowledgment (ACK) from the receiver gives a signal that the codeword has been successfully received (i.e., no errors being detected) and the transmitter starts sending the next codeword. A negative acknowledgment (NAK) from the receiver indicates that the codeword three has been detected in error and the transmitter resends the erroneous codeword. Retransmission continues until an ACK is received by the transmitter. The SW-ARQ scheme is simple and is used in many communication systems. However, it is inherently inefficient because of the idle time spent waiting for acknowledgment for each transmitted codeword.

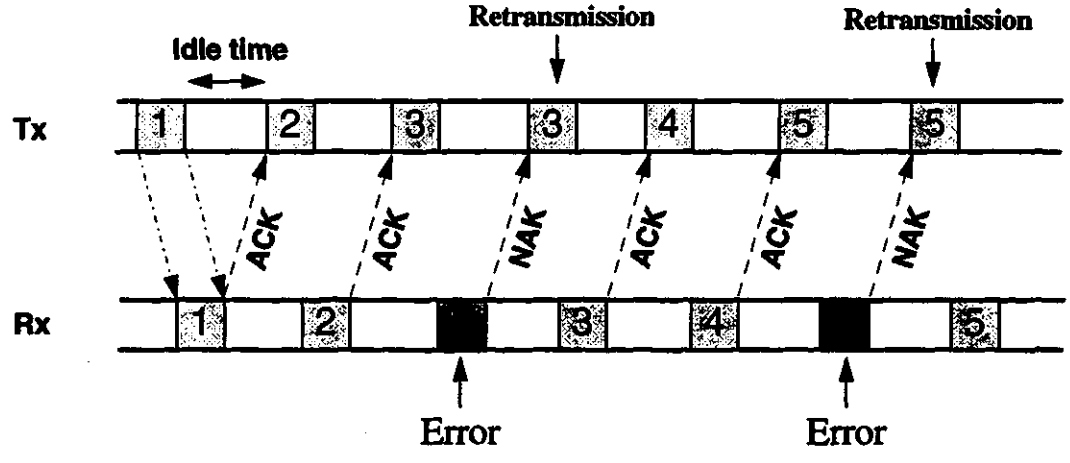

Figure 3.5 Stop-and-Wait ARQ protocol.

The SW throughput efficiency η may be expressed as $\eta = k/E$, where E is the average number of time-slots required to transmit a codeword successfully and is given by

$$E = \sum_{i=1}^{\infty} n_i \, P_s(i) \; . \tag{3.20}$$

In this expression, i is the transmission index and n_i is the number of time slots required to transmit a codeword after i transmission. $P_s(i)$ is the probability that after i

transmissions, the codeword has been successfully received. Let T be the total round trip delay of the system in seconds defined as the time interval between the beginning of the transmission of a codeword and the reception of the acknowledgment for that codeword and R be the rate of transmission in bit per seconds. In one round trip delay time, the transmitter could transmit $n+RT$ bits, where n is the codeword length in bits. To simplify the notation, the detection probability P_d is denoted by P.

The computation of E of Equation 3.20 is illustrated in Table 3.4. In this table, $P_t(i)$ and $P_p(i)$ are the probability that a codeword is received correctly after i transmission and the probability that some codewords were received in error after i transmission, respectively. The number of positively and negatively acknowledged codewords after i^{th} transmission are denoted by $pac(i)$ and $nac(i)$, respectively.

Table 3.4: $P_s(i)$ computation for Stop-and-Wait ARQ protocol

i	n_i	$pac(i)$	$P_t(i)$	$nac(i)$	$P_p(i)$	$P_s(i)=P_t(i)P_p(i)$
1	$(n+RT)$	1	$(1-P)$	0	P^0	$(1-P)$
2	$2(n+RT)$	1	$(1-P)$	1	P^1	$(1-P)P$
3	$3(n+RT)$	1	$(1-P)$	2	P^2	$(1-P)P^2$
4	$4(n+RT)$	1	$(1-P)$	3	P^3	$(1-P)P^3$
...						
j	$j(n+RT)$	1	$(1-P)$	j-1	$P^{(j-1)}$	$(1-P)P^{(j-1)}$

From table 3.4, $P_s(i)=(1-P)P^{i-1}$ and $n_i=i(n+RT)$, so that from equation 3.20

$$
\begin{aligned}
E &= \sum_{i=1}^{\infty} i(n+RT)\ (1-P)\ P^{(i-1)} \\
&= (1-P)\ (n+RT) \sum_{i=1}^{\infty} iP^{(i-1)} \\
&= \frac{n+RT}{1-P} .
\end{aligned}
\tag{3.21}
$$

Therefore, the throughput efficiency η or simply throughput of a stop and wait ARQ protocol is given by

$$
\eta = \frac{k(1-P)}{(n+RT)} . \tag{3.22}
$$

3.5.3 Go-Back-N ARQ Protocol

In a go-back-N ARQ protocol, codewords are transmitted continuously. The transmitter does not wait for acknowledgment after sending a codeword. As soon as it has completed sending one, it begins sending the next codeword as shown in Figure 3.6. The acknowledgment for a codeword arrives after a round trip-delay. If T denotes round-trip delay and R denotes the transmission rate, the number of codewords that can be transmitted during the round-trip delay is $N = \lfloor TR/n \rfloor + 1$ where $\lfloor x \rfloor$ denotes the largest integer that is less than or equal to x. During the round-trip delay interval, $N-1$ other codewords have also been transmitted. When a NAK is received, the transmitter backs up to the codeword that is negatively acknowledged and resends that codeword along with the $N-1$ succeeding codewords that were transmitted during round trip delay (i.e., the transmitter pulls back and resends N codewords). The buffer must be provided at the transmitter for these codewords. At the receiver, following an erroneously received codeword, the $N-1$ received vectors are discarded, regardless of whether they are error-free or not. Therefore, the receiver needs to store only one received codeword at a time. The GBN is more effective than SW ARQ and

it can be implemented at a moderate cost. However, it becomes ineffective when round trip delay is large and data transmission error rate is high.

The throughput efficiency of GBN protocol is given by [6]

$$\eta = \frac{k}{nE} . \tag{3.23}$$

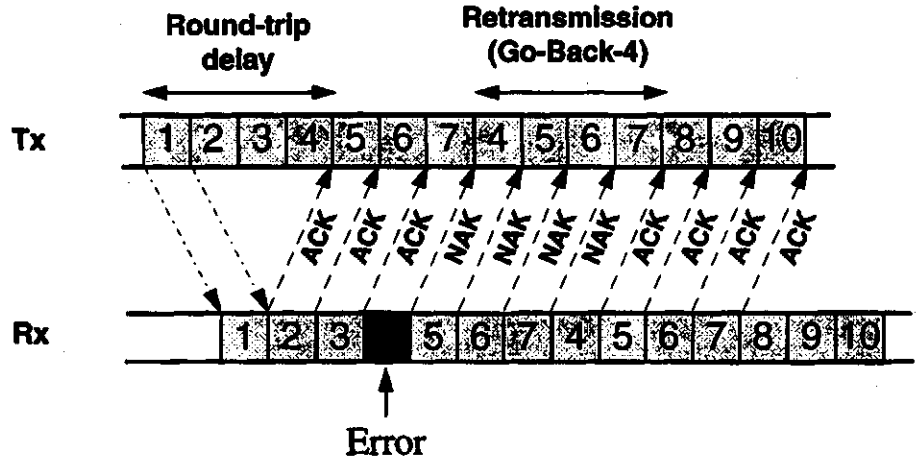

Figure 3.6 Go-Back-N ARQ Protocol.

As for Stop-and-Wait protocol, $P_s(i)$ is shown in tabular form in Table 3.5.

Table 3.5: $P_s(i)$ computation for Go-Back-N ARQ protocol

i	n_i	$pac(i)$	$P_f(i)$	$nac(i)$	$P_p(i)$	$P_s(i) = P_f(i)P_p(i)$
1	*(N-1)*	1	*(1-P)*	0	P^0	*(1-P)*
2	*2N-(N-1)*	1	*(1-P)*	1	P^1	*(1-P)P*
3	*3N-(N-1)*	1	*(1-P)*	2	P^2	$(1-P)P^2$
4	*4N-(N-1)*	1	*(1-P)*	3	P^3	$(1-P)P^3$
...						
j	*jN-(N-1)*	1	*(1-P)*	j-1	$P^{(j-1)}$	$(1-P)P^{(j-1)}$

Thus $P_s(i) = (1-P)P^{i-1}$, $n_i = (i-1)N+1$. By combining Equation 3.23 and the result from Table 3.5, E can be written as

$$\begin{aligned} E &= \sum_{i=1}^{\infty} n_i \, P_s(i) \, , \\ &= (1-P) \sum_{i=1}^{\infty} ((i-1)N+1) \, P^{(i-1)} \, , \\ &= 1+\frac{NP}{1-P} \, . \end{aligned} \tag{3.24}$$

Finally the throughput efficiency of GBN can be written

$$\eta = \frac{(1-P) \; k/n}{(1-P)+PN} \, . \tag{3.25}$$

3.5.4 Selective-Repeat Protocol

This method is a modified form of GBN protocol. In Selective Repeat (SR) ARQ protocol, codewords are also transmitted continuously. However, the transmitter only resends those codewords that are negatively acknowledged, as shown in Figure 3.7. Since codewords are ordinarily delivered to the user in correct order, a buffer must be provided at the receiver to store the error-free received codewords following a received codeword detected in error. When the first negatively acknowledged codeword is successfully received, the receiver releases the error-free received codewords in consecutive order until the next erroneously received codeword is encountered. Sufficient receiver buffer must be provided, otherwise buffer overflow may occur and data may be lost. Of the three ARQ protocols, SR ARQ is the most efficient protocol. However, it is also the most complex protocol to implement.

For an ideal SR ARQ protocol, the receiver has infinite buffer to store the error-free codewords. $P_s(i)$ is once again computed from Table 3.6.

Table 3.6: $P_s(i)$ computation for SR ARQ protocol

i	n_i	$pac(i)$	$P_f(i)$	nac(i)	$P_p(i)$	$P_s(i) = P_f(i)P_p(i)$
1	*1*	1	*(1-P)*	0	P^0	*(1-P)*
2	*2*	1	*(1-P)*	1	P^1	*(1-P)P*
3	*3*	1	*(1-P)*	2	P^2	$(1-P)P^2$
4	*4*	1	*(1-P)*	3	P^3	$(1-P)P^3$
...						
j	*j*	1	*(1-P)*	j-1	$P^{(j-1)}$	$(1-P)P^{(j-1)}$

Thus $P_s(i) = (1-P)P^{i-1}$, $n_i = i$. For a codeword to be successfully accepted by the receiver, the average number of time-slots required to transmit a codeword successfully E is given by

$$\begin{aligned} E &= \sum_{i=1}^{\infty} n_i \, P_s(i) \\ &= (1-P) \sum_{i=1}^{\infty} i \, P^{(i-1)} \\ &= \frac{1}{(1-P)} . \end{aligned} \tag{3.26}$$

Therefore, the throughput efficiency of SR ARQ protocol is given by

$$\eta = (1-P) \frac{k}{n} . \tag{3.27}$$

3.6 Summary

In this chapter, the encoding and decoding of the cyclic codes was introduced. A (400, 386) code termed as CRC-16 is used for ARQ analysis in this thesis. A low probability of undetected codeword error ($1 x 10^{-6}$ at bit error rate of 10^{-3}) can be obtained using CRC-

16. A CRC-16 based ARQ gives a rugged system and this error detection method is assumed for comparative analysis of the ARQ protocols used in this thesis.

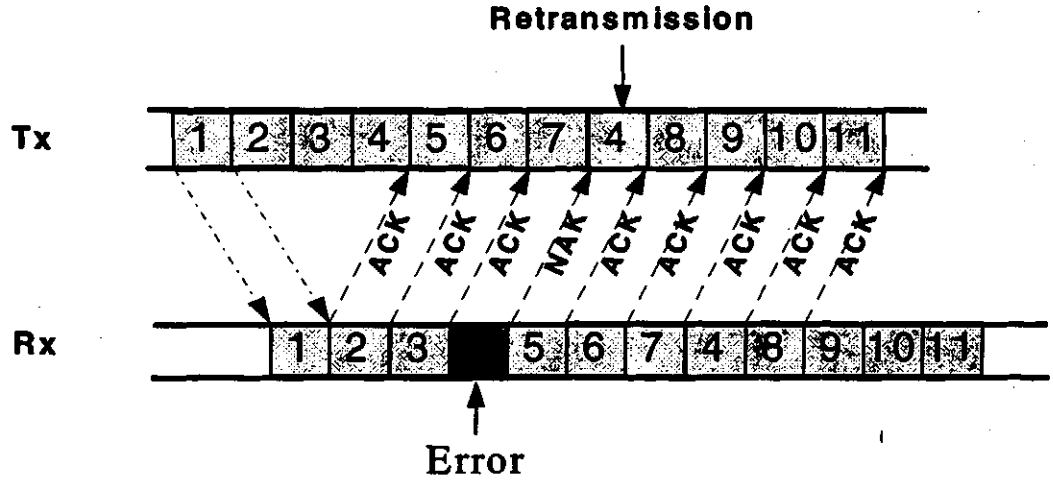

Figure 3.7 Selective-Repeat ARQ Protocol.

The performance of an ARQ error-control system is normally measured by its throughput efficiency. An expression for throughput efficiency (or simply throughput) for three types of ARQ protocols was derived. Using these expressions, the throughput efficiency is plotted in Figure 3.8 as a function of average probability of error ϵ for various ARQ protocols. To simplify the notation, the average probability of error ϵ is denoted by P(e). The performance of SW protocol degrades as the round-trip delay of the channel increases. The GBN protocol gives a better throughput as there is no idle time. However, the main drawback of GBN protocol is that whenever a received word is detected in error, the receiver also rejects the next (N-1) received codewords, even though many of them may be error free. As a result, the throughput performance dips sharply when bit error rate and/or round trip delay increases. Of these methods, the SR protocol gives the best performance. The price is a higher implementation cost and complexity, as it requires theoretically an infinite buffer at the receiver side.

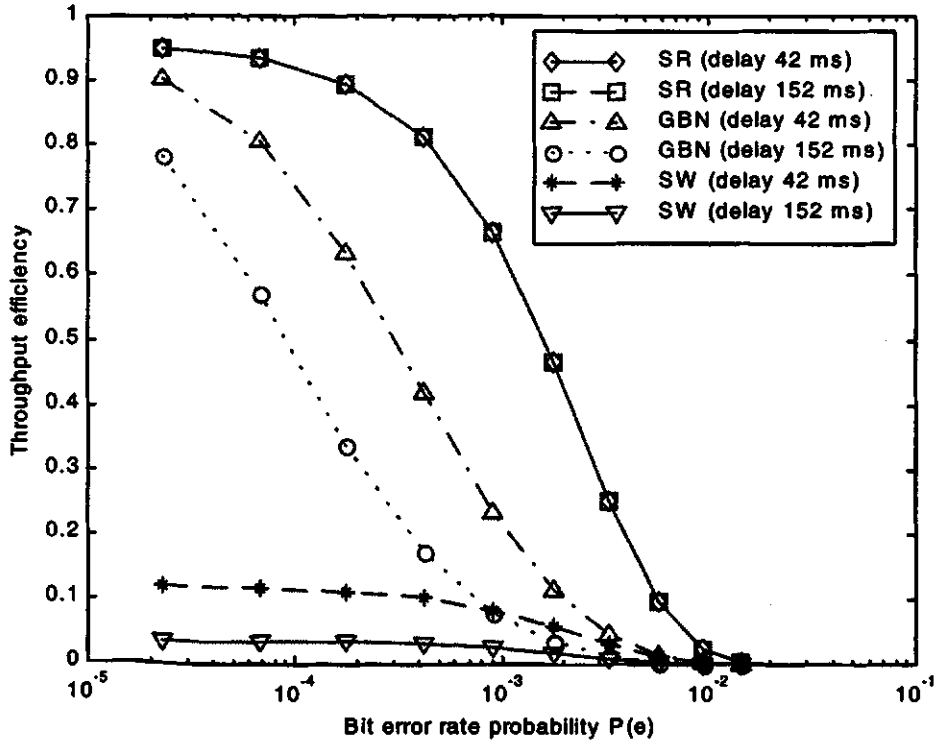

Figure 3.8 A comparison of throughput efficiencies of the SW, GBN, and SR ARQ protocols for two values of delay.

4. Performance Evaluation for a BPSK DS-CDMA Communication System

4.1 Introduction

This chapter is concerned with the performance evaluation for an asynchronous Direct Sequence - Code Division Multiple Access (DS-CDMA) communication system that employs Binary Phase Shift Keying (BPSK) modulation radio in an urban environment. The performance evaluation of interest is the average probability of error or average Bit Error Rate (BER). The average error probability is evaluated by first obtaining the average of the Signal-to-interference-plus-Noise Ratio (SNR). The self interference due to multipath fading and Multi User Interference (MUI) are modeled as Gaussian processes and this method is, therefore, called the Gaussian approximation method.

The RAKE receiver is employed for path diversity thus taking advantage of the multipath fading. As the fading is sufficiently slow, it is assumed that the RAKE receiver can perfectly estimate the gain and phase of each path and any errors due to imperfection estimation are not considered. It is also assumed that perfect power control is used by all active users. Perfect power control means that all active user signals arrive at the receiver with the same average power.

The derivation of the probability of error consists of two steps. First, the probability of error conditioned on a fixed set of fading attenuation factor is obtained. Then, the conditional probability of error is averaged over the probability density function of the fading attenuation factors.

4.2 Transmitter Model

The transmitter, shown in Figure 4.1, consists of K users. Each user spread spectrum signal employs BPSK DS-SS modulation. Assuming a data rate of 1/T bits per second, the baseband and the spread spectrum signal for the k^{th} user may be written as

$$b_k(t) = \sum_{n=-\infty}^{\infty} b_n^{(k)} p_T(t - nT) \tag{4.1}$$

and

$$a_k(t) = \sum_{n=-\infty}^{\infty} a_n^{(k)} p_{T_c}(t - nT_c), \tag{4.2}$$

where $p_\tau(t)$ is a unit rectangular pulse with width τ, $b_n^{(k)}$ is one symbol of the k^{th} transmitted signal and $a_n^{(k)}$ is the k^{th} user's code sequence. Both of these symbols take on value of -1 or 1. The PN sequence is repeated every one symbol period so that $a_n^{(k)} = a_{n+N_c}^{(k)}$ for all n and k and for some integer $N_c = T/T_c$, where T is the bit interval duration and T_c is the chip duration (or the duration of the code bit bandpass signal).

Let $s_k(t)$ denote the transmitted signal for the k^{th} user. Then,

$$s_k(t) = \mathrm{Re}\{u_k(t)e^{j\omega_c t}\}, \tag{4.3}$$

where the low-pass equivalent transmitted signal is given by

$$u_k(t) = \sqrt{2P_k}\, b_k(t)\, a_k(t)\, e^{j\theta_k}. \tag{4.4}$$

P_k is the k^{th} user signal power and θ_k is the carrier phase for the k^{th} user.

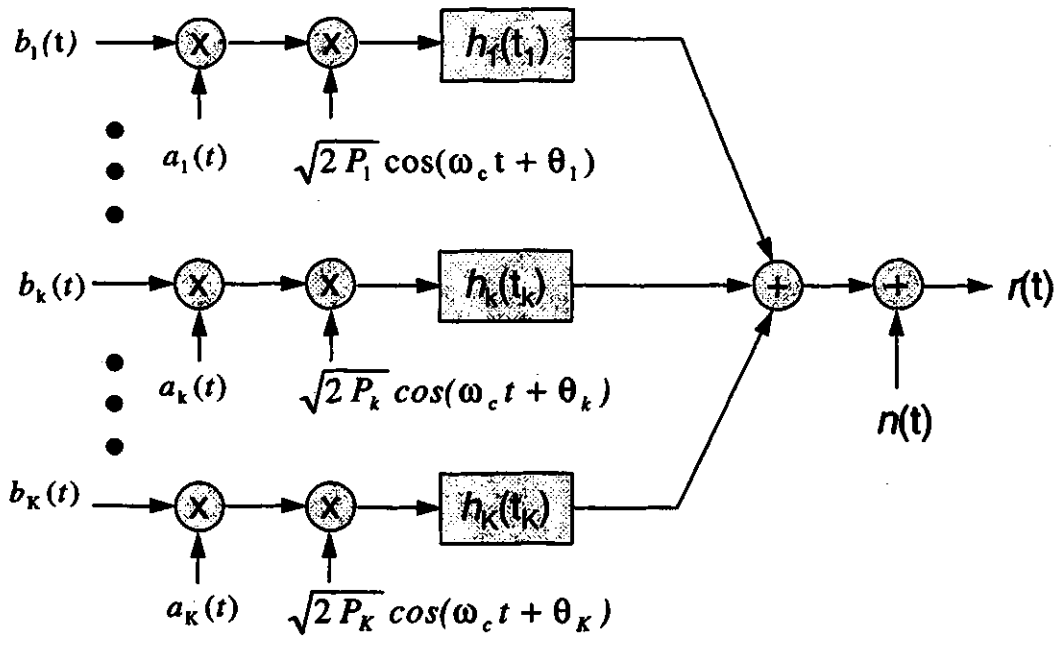

Figure 4.1 The transmitter for K user system with Code Division Multiple Access using BPSK Direct Sequence Spread Spectrum modulation.

4.3 Channel Model

In Chapter 2, it was shown that for the data rate of 64 Kbps, the multipath Rayleigh-fading can be considered to be slow fading. The channel parameters do not change significantly over two consecutive bit intervals. It was also explained in Chapter 2 that the maximum multipath delay spread, T_m, is less than the signaling interval, T, so that the signal does not experience significant Inter Symbol Interference (ISI). The channel can be considered to consist of fixed number of independently fading paths. The maximum number of faded paths L may be calculated as

$$L = \left\lfloor \frac{T_m}{T_c} \right\rfloor + 1, \tag{4.5}$$

where L is the maximum number of resolved paths for a maximum multipath delay spread of T_m seconds and $\lfloor x \rfloor$ is the largest integer that is less than or equal to x.

Due to slowly varying fading characteristics, the channel can be modeled as a linear filter with a time-invariant impulse response given by

$$h_k(t) = \sum_{l=1}^{L} \beta_l^{(k)} \delta(t - \tau_l^{(k)}) e^{j\Phi_l^{(k)}}, \tag{4.6}$$

where $\beta_l^{(k)}$, $\tau_l^{(k)}$, and $\Phi_l^{(k)}$ are the l^{th} path gain, delay, and phase for the k^{th} user. It is assumed that for each l and k, the path delay $\tau_l^{(k)}$ is an independent random variable that is uniformly distributed over $[0, T]$. The path phase $\Phi_l^{(k)}$ is also assumed to have a uniform random variable over $[0, 2\pi]$. As stated in Chapter 2, the multipath fading, without a strong path component causes a rapid path gain fluctuations. The path gain $\beta_l^{(k)}$ can be considered to be an independent random variable with a Rayleigh distribution for all k and l. Therefore, the average path power of the path gain is given by

$$E[(\beta_l^{(k)})^2] = G, \tag{4.7}$$

where $G/2$ is the Rayleigh constant of Equation 2.16.

The multiuser received signal $r(t)$ for this multipath channel may be written as

$$r(t) = \sum_{k=1}^{K} \int_{-\infty}^{\infty} h_k(\tau)\, s_k(t-\tau) d\tau + n(t). \tag{4.8}$$

From Equations 4.1 to 4.4 and 4.6, the received signal may be written as

$$
\begin{aligned}
r(t) = & \sqrt{2P_1}\,\beta_1^{(1)} b_1(t-\tau_1^{(1)})\, a_1(t-\tau_1^{(1)}) \cos(\omega_c t + \varphi_1^{(1)}) \\
& + \sqrt{2P_1} \sum_{l=2}^{L} \beta_l^{(1)} b_1(t-\tau_l^{(1)})\, a_1(t-\tau_l^{(1)}) \cos(\omega_c t + \varphi_l^{(1)}) \\
& + \sum_{k=2}^{K} \sum_{l=1}^{L} \sqrt{2P_k}\,\beta_l^{(k)} b_1(t-\tau_l^{(k)})\, a_1(t-\tau_l^{(k)}) \cos(\omega_c t + \varphi_l^{(k)}) \\
& + n(t),
\end{aligned}
\tag{4.9}
$$

where $n(t)$ is the channel AWGN which has two sided power spectral density $N_0/2$ Watt/Hz. The phase $\varphi_l^{(k)} = \omega_c t + \Phi_l^{(k)} + \theta_l^{(k)}$ is assumed to be an independent random variable distributed over $[0, 2\pi]$.

4.4 Receiver Model

As explained in Chapter 2, a RAKE correlator receiver is an optimum receiver for a multipath channel. As shown in Figure 4.2, the RAKE receiver consists of down converters, matched filters or correlators, and a combiner. The combiner that achieves the best performance is shown in Figure 4.3. In such a combiner, each path signal is multiplied by the corresponding complex-valued (conjugate) channel gain $\hat{g}_i = \hat{\beta}_i^{(k)} e^{-j\hat{\varphi}_i^{(k)}}$, where $1 \le i \le L$. The effect of this multiplication is to compensate for the phase shift in the channel and to weigh the signal by a factor that is proportional to its strength. Thus, a strong signal carries a larger weight than a weak signal.

In Figure 4.2, the output of I and Q sections of the matched filter correspond to the real and imaginary parts of the received baseband signal respectively. The real and imaginary parts of the received signals correspond to a transmitted 1 and 0 respectively. After the complex valued weighting operation is performed in the combiner, both combiner output are summed. This optimum combiner is called a Maximal Ratio Combiner (MRC). Of course, the realization of this combiner is based on the assumption that the channel attenuations $\beta_i^{(k)}$ and the phase shifts $\varphi_i^{(k)}$ are perfectly known. That is, the estimates of the parameters $\hat{\beta}_i^{(k)}$ and $\hat{\varphi}_i^{(k)}$ contain no noise. A RAKE receiver with perfect (noiseless)

estimates of the channel tap weights gives L^{th}-order diversity [5]. It is also assumed that all tap weights have the same mean-square value $E[(\hat{\beta}_l^{(k)})^2]$. These assumptions are used throughout this chapter.

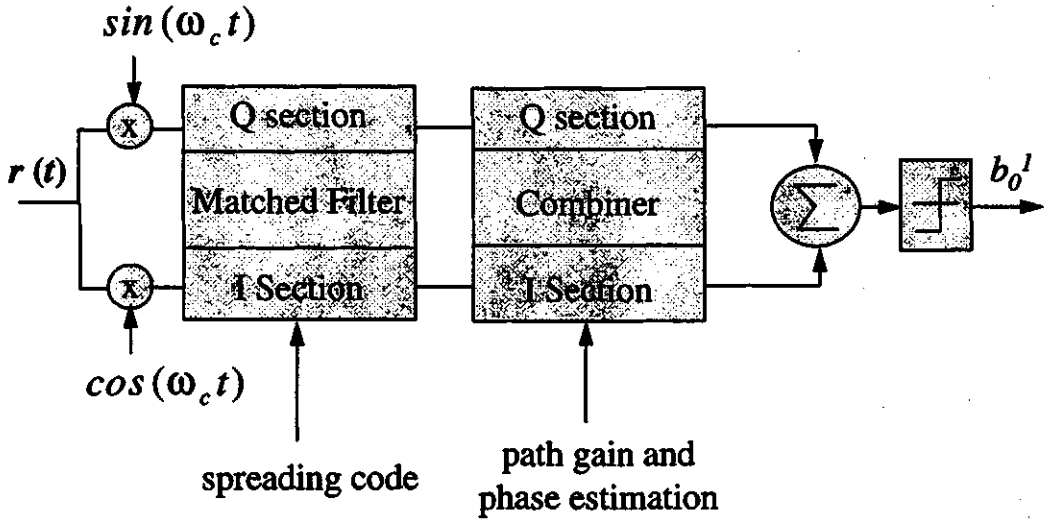

Figure 4.2 RAKE Receiver or RAKE Correlator receiver.

In Figure 4.2, the received signal $r(t)$ is down converted to the baseband in-phase signal $r_I(t)$ and quadrature phase signal $r_Q(t)$ by multiplying $r(t)$ with $\cos(\omega_c t)$ and $\sin(\omega_c t)$, respectively. The low-pass in-phase signal is given by

$$\begin{aligned} r_I(t) = & \sqrt{2P_1}\,\beta_I^{11} b_1(t-\tau_1^{(1)})\, a_1(t-\tau_1^{(1)}) \\ & + \sqrt{2P_1}\sum_{l=2}^{L} \beta_I^{l1} b_1(t-\tau_l^{(1)})\, a_1(t-\tau_l^{(1)}) \\ & + \sum_{k=2}^{K}\sum_{l=1}^{L} \sqrt{2P_k}\,\beta_I^{lk} b_1(t-\tau_l^{(k)})\, a_1(t-\tau_l^{(k)}) \\ & + n_I(t). \end{aligned} \tag{4.10}$$

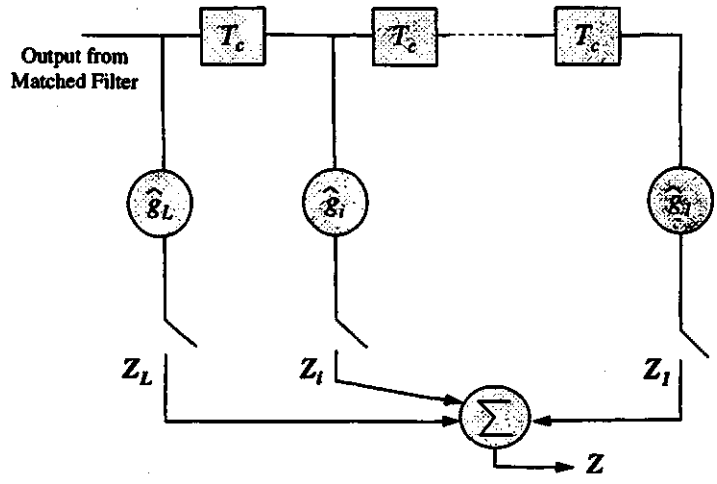

Figure 4.3 RAKE Receiver Combiner (Also known as the Transversal Filter).

The quadrature signal $r_Q(t)$ is obtained by setting I equal to Q in Equation 4.10, where $\beta_I^{lk} = \beta_l^{(k)}\cos(\varphi_l^{(k)})$, $\beta_Q^{lk} = \beta_l^{(k)}\sin(-\varphi_l^{(k)})$, and $n_I(t)$ is the low-pass equivalent thermal noise. As the VSAT tail circuit is a point-to-point communication, the receiver is designed only for the desired user or the first user. It is assumed that the receiver can ideally lock on to the delay $\tau_i^{(1)}$ and phase $\hat{\varphi}_i^{(1)}$, where $i = 1,2,...,L$ is the number of tap weights in the combiner as shown in Figure 4.3. The output Z_i of the i^{th} tap weight combiner for user 1 is given by

$$
\begin{aligned}
Z_i = & \sqrt{\frac{P_1}{2}}\, b_0^{(1)}\, T\, \beta_i^{(1)}\, \hat{\beta}_i^{(1)} \\
& + \sqrt{\frac{P_1}{2}} \sum_{l=2}^{L} \beta_l^{(1)}\, \hat{\beta}_l^{(1)} \cos(\varphi_l^{(1)} - \hat{\varphi}_i^{(1)}) \int_0^T b_1(t-\tau_l^{(1)})\, a_1(t-\tau_l^{(1)})\, a_1(t-\tau_i^{(1)})\, dt \\
& + \sum_{l=1}^{L} \sum_{k=2}^{K} \sqrt{\frac{P_k}{2}}\, \beta_l^{(k)}\, \hat{\beta}_l^{(k)} \cos(\varphi_l^{(k)} - \hat{\varphi}_i^{(1)}) \int_0^T b_k(t-\tau_l^{(k)})\, a_1(t-\tau_l^{(k)})\, a_1(t-\tau_i^{(1)})\, dt \\
& + \int_0^T n_I(t)\, \hat{\beta}_l^{(k)}\, a_1(t-\tau_i^{(1)}) \cos(\omega_c t + \hat{\varphi}_i^{(1)})\, dt,
\end{aligned}
\tag{4.11}
$$

where $b_0^{(1)}$ is the data bit to be detected and $\hat{\beta}_l^{(k)}$ is estimated $\beta_l^{(k)}$. Equation 4.11 may

rewritten as

$$
\begin{aligned}
Z_i = & \sqrt{\frac{P_1}{2}} b_0^{(1)} T \beta_i^{(1)} \hat{\beta}_i^{(1)} \\
& + \sqrt{\frac{P_1}{2}} \sum_{l=2}^{L} \beta_l^{(1)} \hat{\beta}_l^{(1)} \cos(\varphi_l^{(1)} - \varphi_i^{(1)}) \left[b_{-1}^{(1)} R_{11}(t_l^{(1)}) + b_0^{(1)} \hat{R}_{11}(t_l^{(1)}) \right] \\
& + \sum_{l=1}^{L} \sum_{k=2}^{K} \sqrt{\frac{P_k}{2}} \beta_l^{(k)} \hat{\beta}_l^{(k)} \cos(\varphi_l^{(k)} - \varphi_i^{(1)}) \left[b_{-1}^{(k)} R_{k1}(t_l^{(k)}) + b_0^{(k)} \hat{R}_{k1}(t_l^{(k)}) \right] \\
& + N_g,
\end{aligned}
\tag{4.12}
$$

where $t_l^{(k)} = \tau_l^{(k)} - \tau_i^{(1)}$, N_g is the AWGN term which is a zero mean Gaussian random variable. In Equation 4.12, $R_{kl}(\tau)$ and $\hat{R}_{kl}(\tau)$ are the continuous-time partial cross-correlation functions given by [10]

$$
\begin{aligned}
R_{k1}(\tau) &= \int_0^{\tau} a_k(t-\tau)\, a_1(t)\, dt \\
\hat{R}_{k1}(\tau) &= \int_{\tau}^{T} a_k(t-\tau)\, a_1(t)\, dt,
\end{aligned}
\tag{4.13}
$$

where $0 \le \tau \le T$. Equation 4.12 can be simplified as

$$
Z_i = D_s + S_s + F_c + N_g, \tag{4.14}
$$

where D_s is the desired signal, S_s is the self interference due to multipath components, and F_c is the co-channel or multi-user interference from other users.

4.5 Bit Error Rate Analysis

An approximation to calculate the probability of error or Bit Error Rate (BER) in CDMA system is known as the standard Gaussian approximation [10-12, 25]. In this

approximation, all the interference signals are assumed to result in Gaussian distributed noise with zero mean. The variance for this interference caused noise will be explained later. In deriving the probability of error, the probability of error conditioned on a fixed set of attenuation factors $\beta_i^{(1)}$ is first obtained. This conditional probability of error is next averaged over the probability density function of the $\beta_i^{(1)}$.

Let $P(e|\gamma)$ denote the conditional probability of error conditioned on γ, where γ is the combined Signal-to-Noise plus interference Ratio (SNR) per bit at the output of the RAKE receiver with L^{th} order of diversity. With the symbol $b_0^{(1)}$ equally likely, then

$$P(e|\gamma) = \frac{1}{2}\Pr(Z<0 \mid b_0^{(1)} = +1) + \frac{1}{2}\Pr(Z \geq 0 \mid b_0^{(1)} = -1), \tag{4.15}$$

where Z is the output of the maximal ratio combining as in Figure 4.3. Due to the symmetry of the problem, Equation 4.15 may be written as

$$P(e|\gamma) = \Pr(Z \geq 0 \mid b_0^{(1)} = -1). \tag{4.16}$$

For simplicity, the conditioning on $b_0^{(1)}$ is omitted, thus Equation 4.16 may be rewritten as [5]

$$P(e|\gamma) = Q\left(\sqrt{2\gamma}\right), \tag{4.17}$$

where

$$Q(x) = \frac{1}{\sqrt{2\pi}} \int_x^{\infty} e^{\frac{-u^2}{2}}\, du. \tag{4.18}$$

The combined SNR per bit, γ, is given by

$$\gamma = \sum_{i=1}^{L} \gamma_i, \tag{4.19}$$

where γ_i denotes the instantaneous SNR at the output of the i^{th} correlator. γ_i is given by

$$\begin{aligned} \gamma_i &= \frac{\mathrm{E}^2[Z_i]}{\mathrm{Var}[Z_i]} \\ &= \frac{E[D_s^2]}{\mathrm{Var}[S_s] + \mathrm{Var}[F_c] + \mathrm{Var}[N_g]} . \end{aligned} \tag{4.20}$$

For a fixed $\beta_i^{(1)}$, various components of Equation 4.20 are given by:

$$\begin{aligned} \mathrm{E}[D_s^2] &= \frac{PT^2}{2}(\beta_i^{(1)})^4 , \\ \mathrm{Var}[S_s] &= \frac{P}{2}\frac{\mathrm{E}\left[(\beta_i^{(1)})^4\right]}{2}(L-1)\,\mathrm{E}\left[\left(b_{-1}^{(1)}R_{11}(t_i^{(1)}) + b_0^{(1)}\hat{R}_{11}(t_i^{(1)})\right)^2\right], \\ \mathrm{Var}[F_c] &= \frac{P}{2}\frac{\mathrm{E}\left[(\beta_i^{(k)})^4\right]}{2}L(K-1)\,\mathrm{E}\left[\left(b_{-1}^{(k)}R_{k1}(t_i^{(k)}) + b_0^{(k)}\hat{R}_{k1}(t_i^{(k)})\right)^2\right], \\ \mathrm{Var}[N_g] &= \frac{\mathrm{E}\left[(\beta_i^{(k)})^2\right]N_0T}{4} . \end{aligned} \tag{4.21}$$

For rectangular chip waveform, the expectation involving even and odd cross-correlation functions is given by [25]

$$\mathrm{E}\left[\left(b_{-1}^{(k)}R_{k1}(t_i^{(k)}) + b_0^{(k)}\hat{R}_{k1}(t_i^{(k)})\right)^2\right] = \frac{2}{3N_c}T^2, \tag{4.22}$$

where N_c is the sequence length of the Golds codes introduced in Chapter 2. It was assumed

that $E[(\beta_l^{(k)})^2]$ is same over all the paths. It is also assumed that $G = E[(\beta_l^{(k)})^2]$ and $G^2 = E[(\beta_l^{(k)})^4]$ for l^{th} path of the k^{th} user for $l = 1,2,\ldots,L$ and $k = 1,2,\ldots,K$. Using bit energy $E_b = PT$ and from Equations 4.20, 4.21, and 4.22, γ_i is obtained as

$$\gamma_i = \frac{(\beta_1^{(1)})^4}{\frac{G^2(LK-1)}{3N_c} + \frac{N_0 G}{2E_b}}. \tag{4.23}$$

The average value of γ_i, denoted by $\bar{\gamma}_i = \mathrm{E}[\gamma_i]$, is assumed to be identical for all paths. That is,

$$\bar{\gamma}_i = \frac{1}{\frac{(LK-1)}{3N} + \frac{N_0}{2\bar{E}_b}}, \tag{4.24}$$

where $\bar{\gamma}_i$ is the SNR per combined path, $\bar{E}_b = GE_b$ is the received signal energy per bit, and E_b is the transmitted signal energy per bit.

The bit error probability can be obtained by averaging the conditional probability of error $P(e|\gamma)$, in Equation 4.17, over a probability density function $f(\gamma)$ so that

$$P(e) = \int_0^\infty P(e|\gamma)\, f(\gamma)\, d\gamma. \tag{4.25}$$

In a Rayleigh fading channel, the instantaneous SNR γ_i of the i-path is distributed according to a chi-squared distribution with two degrees of freedom [5]. Thus, the combined SNR (γ) with a diversity order of L has a probability density function of chi-square distribution with $2L$ degree of freedom given by

$$f(\gamma) = \frac{1}{(L-1)!\ (\bar{\gamma}_i)^L}\ \gamma^{L-1}\ e^{-\gamma/\bar{\gamma}_i}. \tag{4.26}$$

Substituting Equation 4.17, 4.19, and 4.26 into Equation 4.25 results in a closed-form solution [5, 12] for $P(e)$ as

$$P(e) = \left[\frac{1}{2}(1-\mu)\right]^L \sum_{i=1}^{L}\binom{L-1+i}{i}\left[\frac{1}{2}(1+\mu)\right]^i, \tag{4.27}$$

where, by definition,

$$\mu = \sqrt{\frac{\bar{\gamma}_i}{1+\bar{\gamma}_i}}\ . \tag{4.28}$$

4.6 Numerical Results

In Figure 4.4, the computed results for $P(e)$ in Equation 4.27 are plotted for Gold codes of length $N_c = 31$ and for several different values of K and L. The average probability of bit error of the RAKE receiver is plotted as a function of the expected received energy per bit-to-noise density ratio $\bar{E}_b / N_0$. For notation simplicity, N_c is denoted by C and $\bar{E}_b / N_0$ is denoted by Er/No. Notice that as the transmitted power, and hence the parameter Er, is increased beyond a certain level, the performance of the system does not continue to improve significantly. This is because all transmitters are increasing the transmitted power together. Hence, the multiple-access interference increases as the power of each transmitter increases. It is also shown in Figure 4.4 that the multipath diversity in the receiver can increase the performance of the system significantly.

In Figure 4.5, the average probability of bit error versus the number of active transmitters K is plotted for a fixed value of Er/No = 10 dB, and number of resolved paths $L = 3$. The bit error results are plotted for various lengths of Gold codes assuming

rectangular waveform. As C becomes large, the portion of the multipath and multiuser interference energy in the information bandwidth, after de-spreading, decreases. On the other hand, the desired signal and white noise energy remain the same. Consequently, the combined signal-to-noise-plus-interference ratio increase and the probability of bit error decreases. Also, the effect of interference in the desired signal becomes small in comparison to the white noise as C increases.

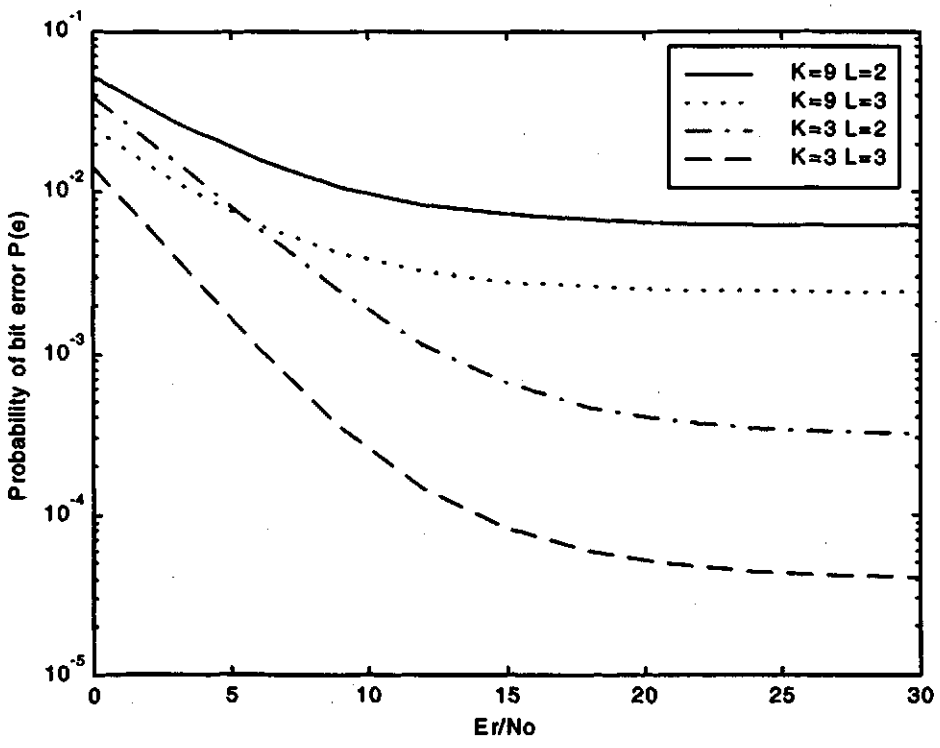

Figure 4.4 The computed results for average probability of bit error versus Er/No for $C = 31$. The two values of user number ($K = 9$, $K = 3$) and number of resolved paths ($L = 3$, $L = 2$) are used.

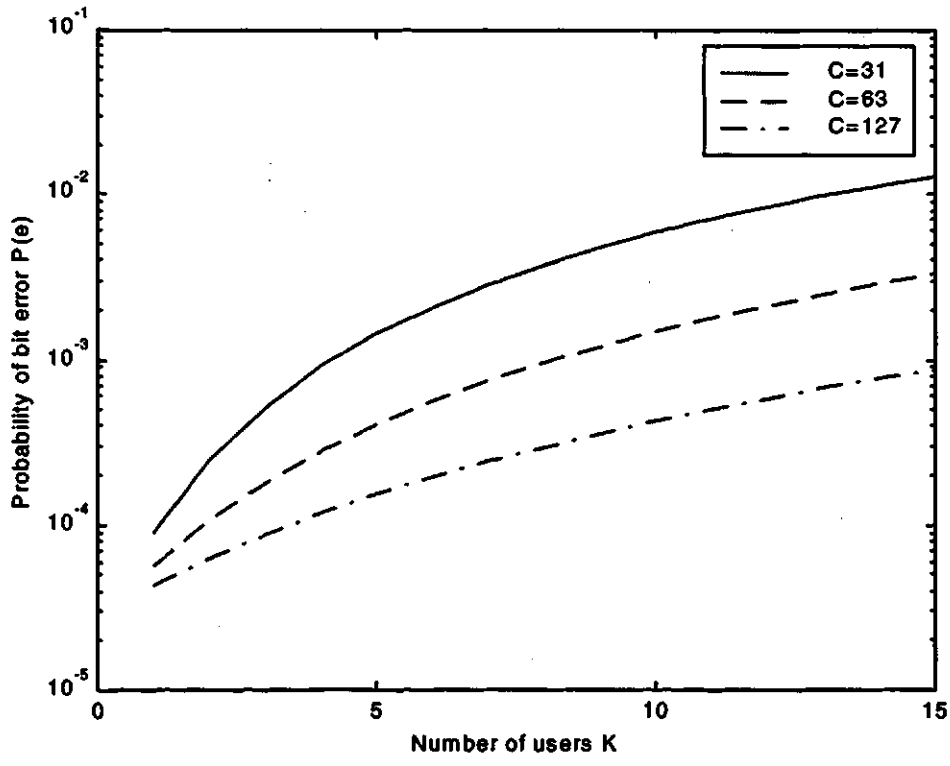

Figure 4.5 The average probability of bit error versus K for Er/No=10 dB and $L = 3$ with code length C as the parameter.

5. Performance of Generalized Stop-and-Wait ARQ Protocols

5.1 Introduction

In the previous chapter, it was seen that the bit error rate performance of a Binary Phase Shift Keying Direct Sequence Code Division Multiple Access (BPSK DS-CDMA) communication system degrades rapidly as the equivalent noises increase. This noises result from the combined effect of multiuser interference, multipath fading, and thermal noise. The Automatic Repeat Request (ARQ) error control strategies are widely used to mitigate the effect of transmission errors. It was shown in Chapter 3 that the stop-and-wait ARQ protocol has the simplest implementation but has low throughput efficiency. In this chapter, improved ARQ methods known as the generalized stop-and-wait ARQ protocols are proposed and analyzed for a wireless CDMA communication system. The key common feature of these methods is that they retain the general simplicity of stop-and-wait ARQ protocol while achieving a significant improvement in throughput efficiency by reduction of waiting states.

5.2 Generalized Stop-and-Wait Type-1 (GSW-1) ARQ Protocol

The operation of the Generalized Stop-and Wait Type-1 (GSW-1) ARQ protocol, proposed first in [32], is illustrated in Figure 5.1. As shown in this figure, the data to be transmitted are divided into fixed-length data blocks. Each sequence of k information-bearing bits is encoded through an (n,k) code into a codeword of length n. Each data block is transmitted, or if necessary retransmitted, by sending a set of M identical copies rather

than just a single copy. This technique reduces the influence of the round trip propagation delay on the throughput efficiency resulting in a higher throughput. After each transmission of a set of M copies of a data block, the transmitter is idle, as it waits for acknowledgment signals from the receiver. At the receiver, an error detection is performed on each received copy. For each received copy, an acknowledgment signal is sent back to the transmitter through the feedback channel. A positive acknowledgment (ACK) is sent for a correctly received codeword or if a correctable error pattern is detected and a negative acknowledgment (NACK) is sent in case of erroneous data blocks for which a correct reconstruction is not possible. The feedback channel of the communication system is assumed to be noiseless, i.e., all the acknowledgment signals are received without errors at the transmitter.

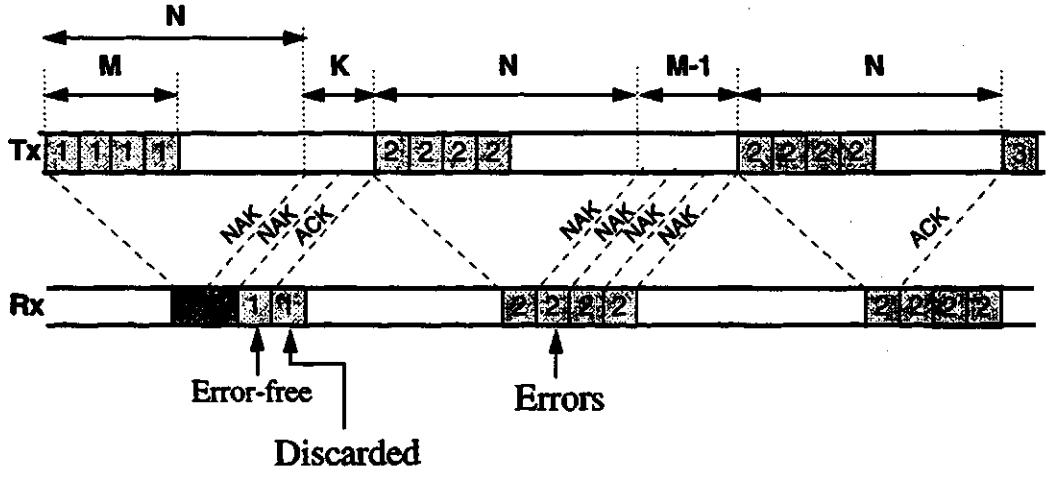

Figure 5.1 The Generalized Stop-and-Wait Type one (GSW-1) ARQ Protocol.

In GSW-1 protocol, the transmitter starts sending the next data blocks as soon as an ACK message for a copy in the previous block arrives at the transmitter. It is a waste of time to continue waiting for the remaining acknowledgment signals, since they are of no further use. Also, it is useless to continue sending the remaining copies of the codewords. If all M

acknowledgment signals are negative, a retransmission of the current data block is required and a new set of M copies of that block is sent.

The throughput efficiency of the GSW-1 ARQ protocol is given by [32]

$$\eta = \frac{k}{n\,E[\alpha]}, \tag{5.1}$$

where $E[\alpha]$ is the average number of data blocks which could be sent during the time needed to deliver one correct block. The random variable α denotes the total number of data blocks required to deliver one correct data block. In the analysis below, it is assumed that transmission errors from block to block are statistically independent and are identically distributed with a constant block error probability P.

In order to derive an analytical expression for $E[\alpha]$, discrete random variable F is introduced. F denotes the number of consecutive erroneous copies in a set of M copies of a data block before the first correct copy or before the end of the set. The variable F has the following probability distribution:

$$Pr[F = f] = \begin{cases} (1-P)\,P^f, & 0 \le f < M \\ P^M, & f = M \\ 0, & f > M. \end{cases} \tag{5.2}$$

Using this variable F, α can be expressed as follows :

$$\alpha = \begin{cases} N + F, & 0 \le F < M \\ N + M - 1 + \alpha', & F = M, \end{cases} \tag{5.3}$$

whereby α' denotes the number of data blocks needed to deliver a correct data block, which are counted from the start of the first retransmission of the block. Since transmission errors

in consecutive blocks are, in the first instance, assumed to occur independently with a constant block error probability P, the random variables α and α' are identically distributed and $E[\alpha] = E[\alpha']$. Based on the definition of α in Equation 5.3, its expectation $E[\alpha]$ may be derived as

$$E[\alpha] = Pr[F<M]\ E[N+F \mid F<M] + Pr[F=M]\ E[N+M-1+\alpha' \mid F=M], \tag{5.4}$$

where,

$$Pr[F<M] = 1 - Pr[F=M]. \tag{5.5}$$

Substituting for $Pr[F<M]$ from Equation 5.5 into 5.4 yields

$$\begin{aligned} E[\alpha] = {} & E[N+F \mid F<M] - Pr[F=M]\ E[N+F \mid F<M] \\ & + Pr[F=M]\ E[N+M-1+\alpha' \mid F=M]\ . \end{aligned} \tag{5.6}$$

Combining of Equations 5.2, 5.3, and 5.6 results in

$$E[\alpha] = \frac{N - 1 + E[F] + (1 - P^M)}{(1 - P^M)}\ . \tag{5.7}$$

$E[F]$ can be evaluated using the moment generating function. Let $F(z) = z^f$ denote the probability generating function of the random variable F, then

$$\begin{aligned} E[F(z)] &= \sum_{f=0}^{\infty} Pr[F=f]\ z^f \\ &= \sum_{f=0}^{m-1} Pr[F=f \mid f<M]\ z^f + Pr[F=f \mid f=M]\ z^M \\ &= \frac{(1-P) + P^{M+1} z^M (1-z)}{1 - Pz}\ . \end{aligned} \tag{5.8}$$

The moment generating function can be obtained by differentiating Equation 5.8 with respect to z. If it is denoted by $E'[F(z)]$ then it can be expressed as

$$E'[F(z)] = \frac{\left(1 - P + P^{M+1} z^{M} (1 - z)\right) P}{(1 - Pz)^2} . \tag{5.9}$$

For convergence, $Pz \leq 1$ is a prerequisite. Since $P \leq 1$, z can be chosen as one. Then $E[F]$ can be written as

$$\begin{aligned} E[F] &= E'[F(1)] \\ &= \frac{P\ (1 - P^{M})}{1 - P} . \end{aligned} \tag{5.10}$$

From Equations 5.1, 5.7, and 5.10, the throughput efficiency η is obtained as

$$\eta = \frac{k}{n} \left(\frac{(1 - P^{M})\ (1 - P)}{(N - 1)\ (1 - P) + (1 - P^{M})} \right). \tag{5.11}$$

5.3 Generalized Stop-and-Wait Type-2 (GSW-2) ARQ Protocol

In the Generalized Stop-and-Wait Type-2 (GSW-2) protocol, first proposed in [9], the codewords to be transmitted are divided into groups, each composed of M codewords, where $M \geq 1$. Once a group of M codewords has been sent, the transmitter enters the waiting state, as illustrated in Figure 5.2. The number of time-slots that the transmitter spends in the waiting state varies, according to the ACK and NAK sequence that it receives via a feedback channel.

The receiver can be either in the decoding state or the waiting state. In the decoding state, the receiver analyzes the received codeword. If the received codeword is errorless or contains a correctable error pattern, the receiver sends an ACK to the transmitter.

Conversely, if the codeword contains an uncorrectable error pattern, the receiver sends NAK so that all the successive received codewords are discarded, regardless of whether they are error-free or not. Thus, there would be only one erroneous codeword in the i^{th} transmission.

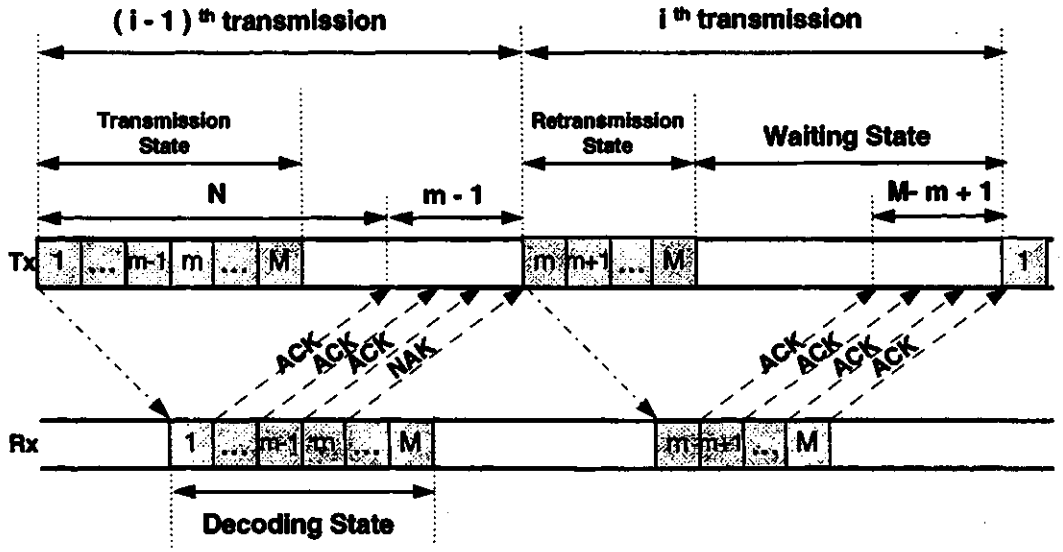

Figure 5.2 The Generalized Stop-and-Wait Type two (GSW-2) ARQ Protocol.

Because the time spent by the transmitter in the waiting state is significantly reduced, the GSW-2 protocol can increase the throughput efficiency performance of the classical stop-and wait protocol. On the other hand, the GSW-2 protocol retains the implementation simplicity of the classical stop-and-wait protocol.

The throughput efficiency η of the GSW-2 ARQ protocol is given by

$$\eta = \frac{kM}{nE}, \tag{5.12}$$

where k is the number of information bits, n is the length of a codeword, and E is the

average number of time-slots required to transmit a group of M codewords. E may be expressed as

$$E = \sum_{i=1}^{\infty} n_i P_s(i). \tag{5.13}$$

In this expression, i is the index of transmission and n_i is the number of codeword time slots required to transmit M codewords. $P_s(i)$ is the probability that at the i^{th} transmissions, all the M codewords have been received successfully.

To obtain the throughput efficiency of GSW-2 protocol consider a typical case shown in Figure 5.2. At the $(i-1)^{th}$ transmission, the first $(m-1)$ codewords have been positively acknowledged, while the m^{th} codeword is negatively acknowledged. Following the reception of the NAK signal, the transmitter immediately enters the retransmission state, then sends the m^{th} codeword followed by successive $(M-m+1)$ codewords. When all the M codewords have been positively acknowledged, the transmitter sends the next M codewords.

After i transmission, it is assumed that c_i codewords have been positively acknowledged, and for the $(c_i+1)^{th}$ codeword, an NAK signal has been received. The transmitter repeats a $(c_i+1)^{th}$ codeword and all of the successive codewords, and then enters the waiting state such that $c_{i-1} \le c_i \le M$, where c_{i-1} is the number of codewords that have been positively acknowledged after $i-1$ transmission . If $c_i = M$, then all the M codewords have been successfully transmitted.

The probability that during the i^{th} transmission c_i codewords are correctly received given c_{i-1} codewords were positively acknowledged is denoted by $Pr(c_i | c_{i-1})$. This probability may be written as

$$Pr(c_i|c_{i-1}) = P(1-P)^{c_i - c_{i-1}}, \tag{5.14}$$

where P is the codeword error probability which is assumed to be same for each transmitted codeword. The probability $P_s(i)$ that after i transmissions all the M codewords have been successfully received can be expressed as

$$P_s(i) = \sum_{c_1=0}^{M-1} \sum_{c_2=c_1}^{M-1} \cdots \sum_{c_{i-1}=c_{i-2}}^{M-1} P(1-P)^{c_1} \times P(1-P)^{c_2-c_1} \cdots P(1-P)^{c_{i-1}-c_{i-2}} (1-P)^{M-c_{i-1}}. \quad (5.15)$$

In general, $P_s(i)$ can be simplified as

$$P_s(i) = \binom{M+i-2}{i-1} P^{i-1} (1-P)^M. \quad (5.16)$$

If M codewords are recovered after i transmissions, the number of time slots n_i required after i transmissions is given by

$$n_i = i(N-1)+M. \quad (5.17)$$

Combining Equation 5.13, 5.16, and 5.17 results in

$$E = (1-P)^M \sum_{i=1}^{\infty} [i(N-1)+M] \binom{M+i-2}{i-1} P^{i-1}. \quad (5.18)$$

Equation 5.18 may be written as

$$E = (1-P)^M \{M\, E[A] + (N-1)(E[A] + E[B])\}, \quad (5.19)$$

where

$$E[A] = \sum_{i=0}^{\infty} \binom{M+i-1}{i} P^i , \tag{5.20}$$

and

$$E[B] = E[i] = \sum_{i=0}^{\infty} \binom{M+i-1}{i} i P^i . \tag{5.21}$$

$E[A]$ in Equations 5.20 can be evaluated as follows:

$$\begin{aligned} E[A] &= \sum_{i=0}^{\infty} \binom{-M}{i} (-1)^i P^i \\ &= (1-p)^{-M}. \end{aligned} \tag{5.22}$$

$E[B]$ in Equation 5.21 can be evaluated using moment generating function described in the previous section as follows:

$$\begin{aligned} E[t^i] &= \sum_{i=0}^{\infty} \binom{-M}{i} (-1)^i (tP)^i \\ &= (1-tP)^{-M}. \end{aligned} \tag{5.23}$$

Differentiating Equation 5.23 with respect to t and setting $t = 1$ results

$$E[B] = \frac{PM}{(1-P)^{M+1}} . \tag{5.24}$$

Combining Equations 5.12, 5.19, 5.22, and 5.24 yields

$$\eta = \frac{k M (1-P)}{n \{(1-P)(M+N-1) + PM(N-1)\}} . \tag{5.25}$$

An example for $P_s(i)$ evaluation is next described to illustrate the method. Considered that a group of four codewords ($M = 4$) is transmitted and the total number of transmissions where all of the M codewords that have been successfully received are three ($i = 3$). Assuming that each transmitted codeword has the same probability of being received in error, the probability that some codewords are correctly received and another codeword is in error can be described in Table 5.1. This table also shows all possibilities of combination of error-free codewords received in each transmission.

Table 5.1: $P_s(i)$ computation example for Generalized Stop-and-Wait Type-2 ARQ

1st transmission			2nd transmission			3rd transmission		
pac(1)	c_1=pac(1)	Pr(c_1)	pac(2)	c_2=pac(2)+c_1	Pr(c_2/c_1)	pac(3)	c_3=pac(3)+c_2	Pr(c_3/c_2)
0	0	P	0	0	P	4	4	$(1-P)^4$
0	0	P	1	1	$P(1-P)^1$	3	4	$(1-P)^3$
0	0	P	2	2	$P(1-P)^2$	2	4	$(1-P)^2$
0	0	P	3	3	$P(1-P)^3$	1	4	$(1-P)^1$
1	1	P (1-P)	0	1	P	3	4	$(1-P)^3$
1	1	P(1-P)	1	2	$P(1-P)^1$	2	4	$(1-P)^2$
1	1	P(1-P)	2	3	$P(1-P)^2$	1	4	$(1-P)^1$
2	2	$P(1-P)^2$	0	2	P	2	4	$(1-P)^2$
2	2	$P(1-P)^2$	1	3	$P(1-P)^1$	1	4	$(1-P)^1$
3	3	$P(1-P)^2$	0	3	P	1	4	$(1-P)^1$

In Table 5.1, $pac(i)$ denotes the number of codewords that are positively acknowledged during the i^{th} transmission and $Pr(c_i \mid c_{i-1})$ denotes the probability that during the i^{th} transmission c_i codewords are correctly received given c_{i-1} codewords were positively acknowledged as explained in Equation 5.14. Condition for the ninth row of Table 5.1 is explained using Figure 5.3. The first transmission shows that after two codewords have been successfully transmitted, the third codeword is detected in error. In the second transmission, the third codeword is received successfully and the fourth codeword is in error. Finally, the fourth codeword is successfully transmitted in the third transmission trial. Thus, the

probability that after three transmission $P_s(3)$, the four codewords are successfully received, can be expressed as

$$\begin{aligned} P_s(3) &= \sum_{1}^{10} Pr(c_3 \mid c_2)\ Pr(c_2 \mid c_1)\ Pr(c_1) \\ &= 10\ P^2\ (1-P)^4 \\ &= \binom{5}{2}\ P^2\ (1-P)^4. \end{aligned} \tag{5.26}$$

As may be seen from Equation 5.26 it is a typical case that could have been obtained from the general case of Equation 5.16.

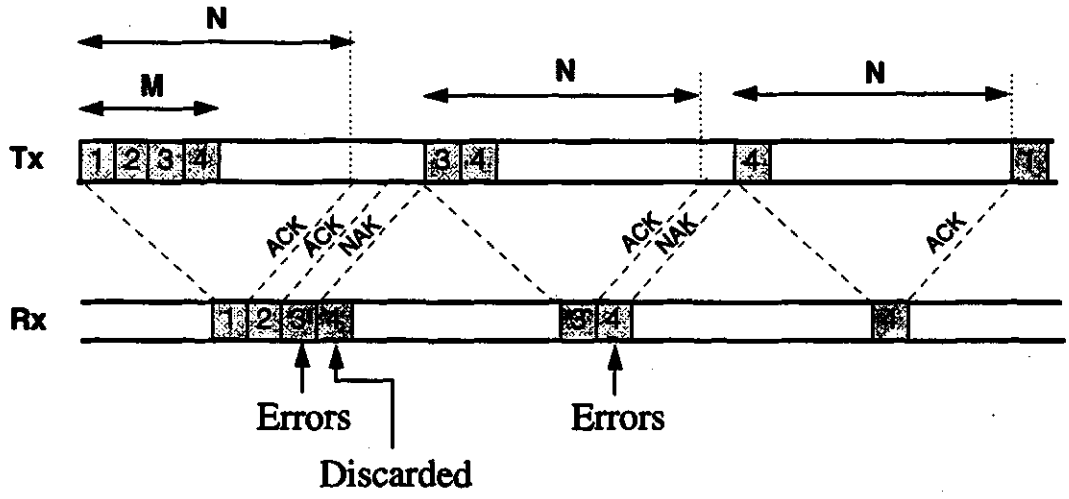

Figure 5.3 The Generalized Stop-and-Wait Type two (GSW-2) ARQ protocol for M=4 and i=3.

5.4 Numerical Results

The throughput efficiency performance of GSW ARQ protocols was computed for a CDMA channel model described in Chapter 4. The results are computed for various combinations of CDMA system parameters, such as K the number of active transmitters, L

the maximum number of paths, and N_c the length of the Gold code. Again, for notational simplicity, the expected received energy per bit-to-noise density ratio $\bar{E}_b/N_0$ is replaced by Er/No. Two ARQ parameters that influence the throughput are varied. These being N, the round trip delay in codewords and M, the set of codewords sent by the transmitter.

In Chapter 3, N was defined as

$$N = \left\lfloor \frac{TR}{n} \right\rfloor + 1 , \tag{5.27}$$

where $\lfloor x \rfloor$ denotes the largest integer that is less than or equal to x, R denotes the transmission rate, and T denotes the round-trip delay in second. T can be calculated for Time Division Duplexing (TDD) links [33] by finding the sum of:

$$T = T_{pd} + T_{md} + T_{rr} + T_{ta} + T_{rt} + T_{rd} , \tag{5.28}$$

where T_{pd} is the forward plus reverse path time delay propagation, T_{md} is the modem data delay, T_{rr} is RTS/CTS delay in the receiving modem, T_{ta} is the time taken to transmit an acknowledgment, T_{rt} is RTS/CTS delay in transmitting modem, and T_{rd} is two receiver reaction delays. Since the distance between transmitter and receiver in this thesis is set to be 30 km, then T_{pd} = 2 ms. T_{md} and T_{rd} are usually very small and can be assumed to be zero. Since the acknowledgment signal only takes one bit period, T_{ta} is also negligible. For data rate R = 64 Kbps, T_{rr} or T_{rt} are between 20 and 75 ms [33]. Thus T_{rr} and T_{rt} are the major contributors to the round trip delay. From Equation 5.28, T lies between 42 and 152 ms corresponding to minimum and maximum values of T_{rr} and T_{rt}, respectively. Finally N can be evaluated from Equation 5.27 and for the 64 Kbps data rate, it is in between 7 and 25 codewords.

In Figure 5.4, the throughput efficiency η of the GSW-1 protocol is plotted as a function of Er/No in decibels (dB) for different values of N and M. For notational simplicity, the throughput efficiency η is denoted by *throughput* that will be used throughout this thesis. As may be seen from this figure, the propagation delay N is the dominant factor influencing the throughput performance. The throughput of GSW-1 protocol degrades severely as N increases. It may be observed that performance significantly improves as M increase. This is particularly true for low values of Er/No. This improvement results from the reduction of the round trip propagation delay.

In Figure 5.5, the throughput of the GSW-2 protocol is plotted as a function of Er/No for different values of N and M. Obviously, the throughput of the GSW-2 protocol increases as M increases. It is also seen that the degradation performance caused by additional propagation delay can be mitigated by increasing the number of M when Er/No>12 dB. The impact of higher M reduces for low Er/No. The performance improvement occurs due to the time reduction of the transmitter in the waiting state.

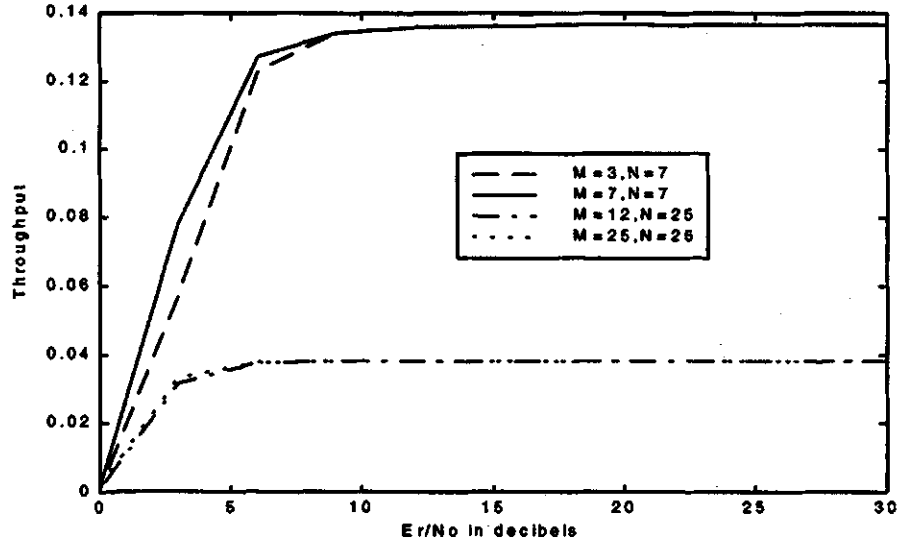

Figure 5.4 Throughput of GSW-1 protocol versus Er/No over a CDMA system with number of user K=3, number of resolved paths L=3, and code length N_c=31.

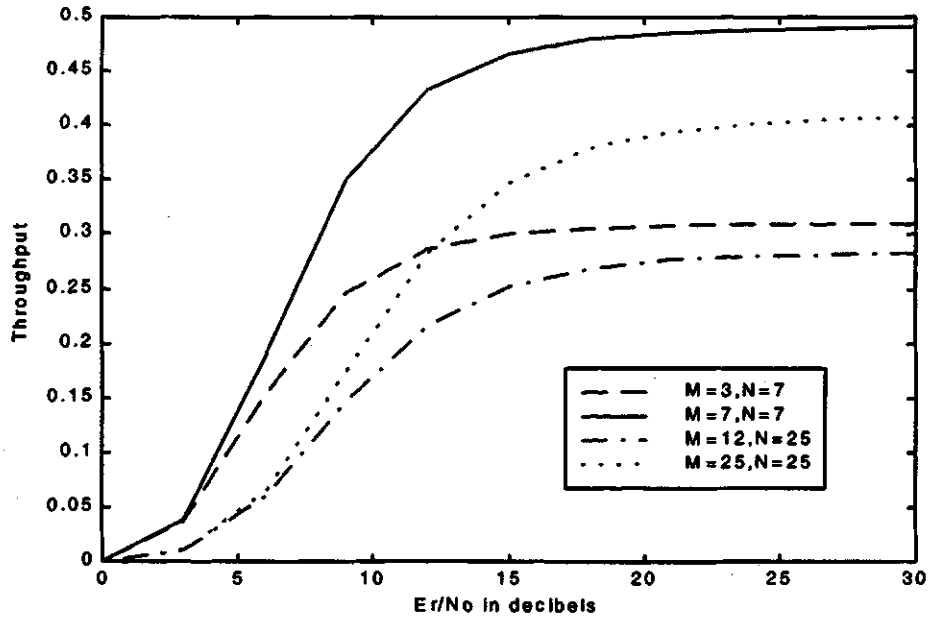

Figure 5.5 Throughput of GSW-2 protocols versus Er/No over a CDMA system with number of user K=3, number of resolved paths L=3 and code length N_c= 31.

Figures 5.6, 5.7, and 5.8 show the throughput of two GSW protocols as a function of Er/No for N = 7, M=3; N = 7, M=7; and N = 25, M=12. The results for classical ARQ protocols SW ARQ and GBN ARQ are also shown for comparison. For low Er/No, the GSW protocols outperform the classical protocols. At low Er/No, the GSW-1 achieves significant performance improvement over classical protocols and has higher efficiency than GSW-2. At high Er/No, the GBN performs the best, followed by GSW-2, GSW-1, and SW, respectively.

The gain in throughput with GSW-2 over the classical SW protocol is significant for medium and high Er/No if M is chosen suitably. For all values of Er/No, the GSW-2 protocol presents throughput values near the GBN protocol. It has the advantage of simpler implementation and lower complexity than the GBN protocol.

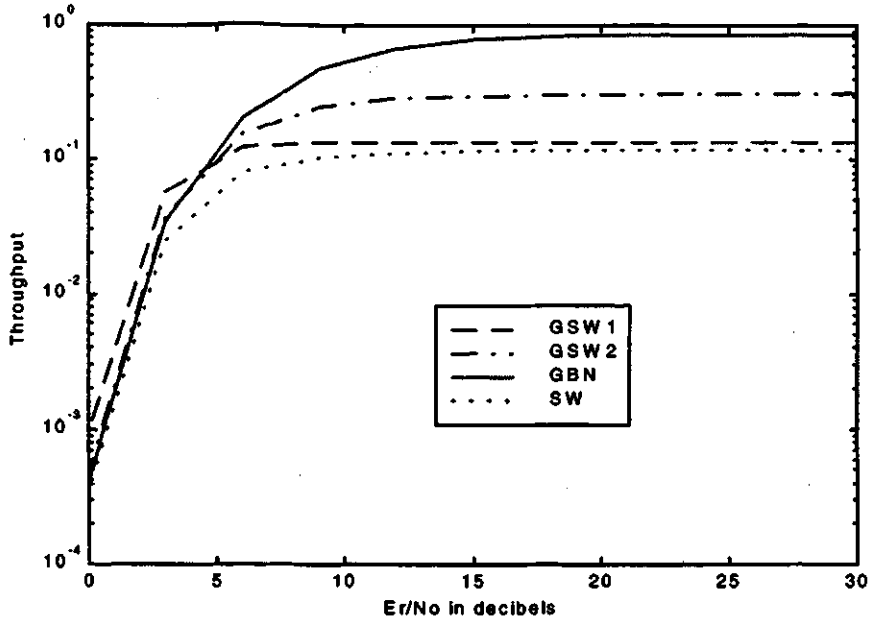

Figure 5.6 Throughput of four ARQ protocols versus Er/No over a CDMA system with number of user K=3, number of resolved paths L=3, and code length N_c=31. The propagation delay N=7 and number of successive blocks M=3.

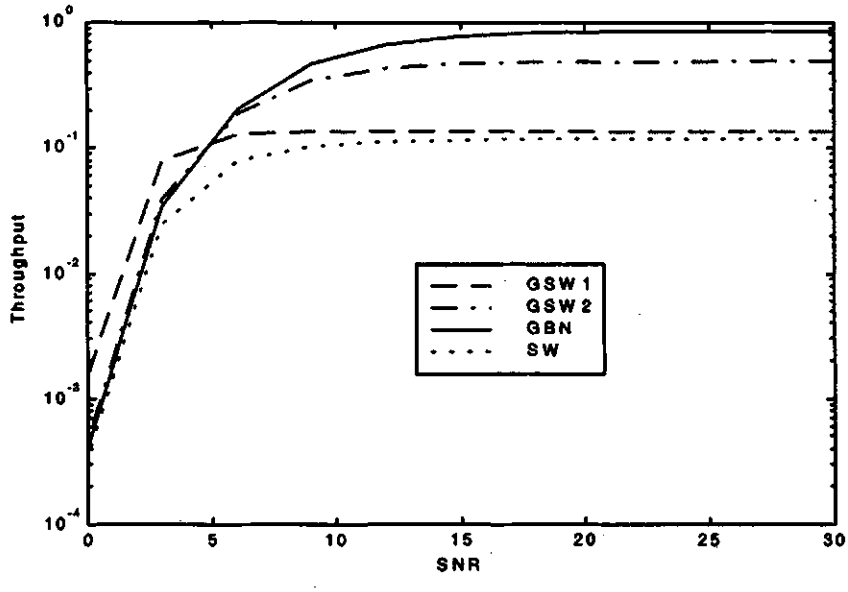

Figure 5.7 Throughput of four ARQ protocols versus Er/No over a CDMA system with number of user K=3, number of resolved paths L=3, and code length N_c=31. The propagation delay N=7 and number of successive blocks M=7.

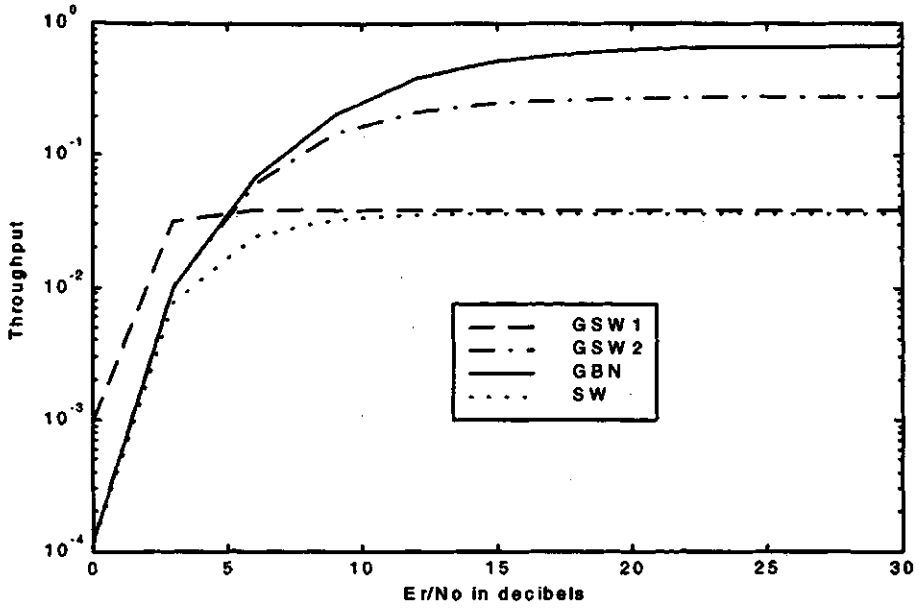

Figure 5.8 Throughput of four ARQ protocols versus Er/No over a CDMA system with number of user K=3, number of resolved path L=3, and number of code length N_c=31. The propagation delay N=25 and number of successive blocks M=12.

In Figures 5.9 and 5.10, the throughput of GSW protocols is plotted as a function of Er/No for N=7, M=7 and N=25, M=25, respectively. The throughput of GSW protocols severely degrades when the number of the co-users K in a CDMA increases. The GSW-1 protocol achieves higher throughput than GSW-2 protocol for a CDMA system with K=9, at any values of Er/No. On the other hand, the GSW-2 protocol outperforms GSW-1 protocol for K=3, especially for high Er/No. This advantage does not occur at low Er/No. For high round trip delay N and high number of co-users, GSW-1 protocol performs better than the GSW-2 protocol. This performance improvement is realized at all values of Er/No.

These results can be attributed to the CDMA channel model characteristics. As the number of co-users in CDMA increase, the probability of channel error ϵ and the probability of codeword error P increase. Consequently, to achieve the same level of throughput, a CDMA channel with number of co-users K=9 requires a higher average

energy per bit than the one with K=3.

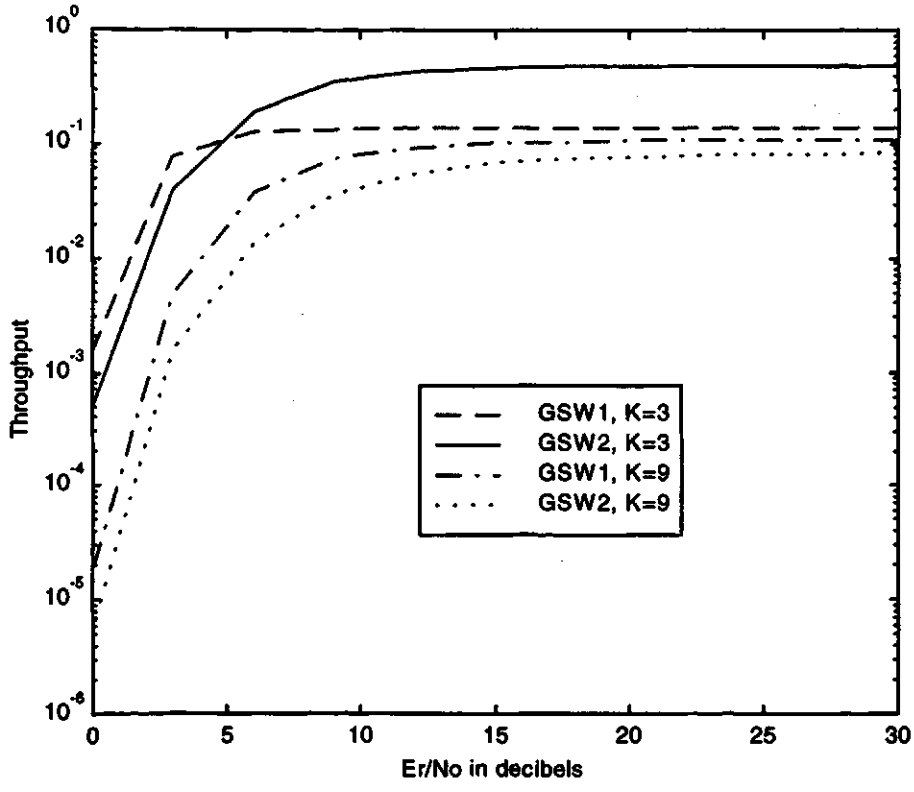

Figure 5.9 The throughput comparison of two GSW protocols versus Er/No for a CDMA system with number of resolved paths L=3, and code length N_c=31. The propagation delay N=7 and number of successive blocks M=7.

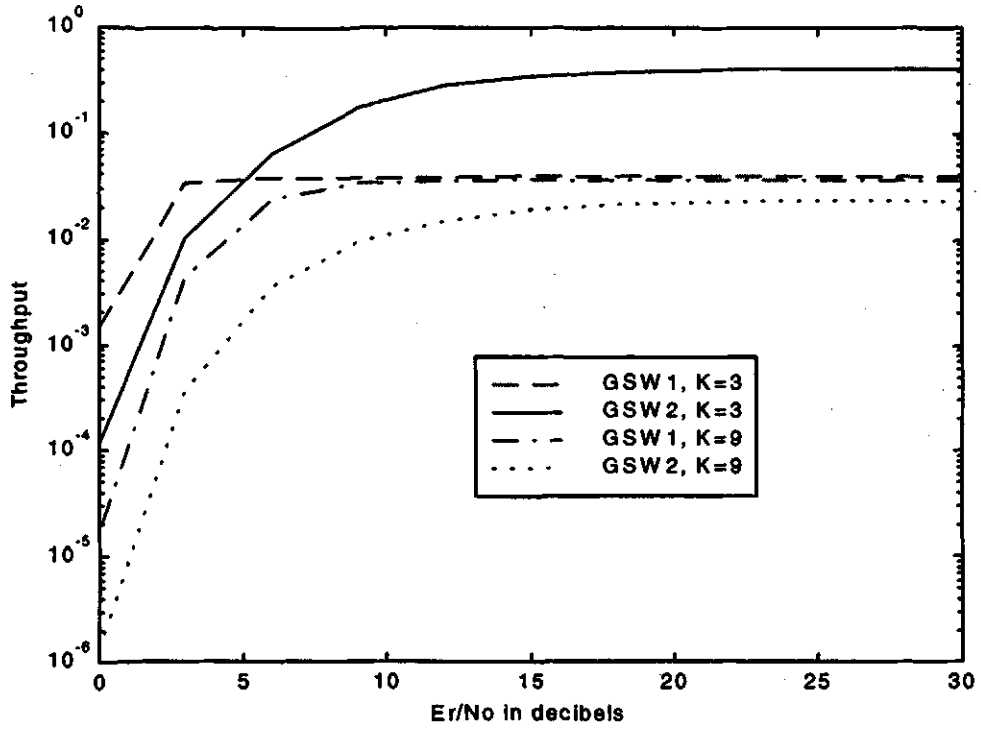

Figure 5.10 The throughput of some GSW protocols versus Er/No for a CDMA system with number of resolved paths L=3, and code length N_c=31. The propagation delay N=25 and number of successive blocks M=25.

6. Simulation Results

Over the past decade or so, it has become increasingly common to resort to computer-aided techniques to estimate the performance of digital communication systems. This trend has became common because of the difficulties of getting a closed form solution for the performance without using approximations. An example is the Gaussian approximation used to model multiple access interference in the previous chapters. The performances measures commonly used are the Bit Error Rate (BER) or the bit error probability and throughput efficiency or simply the throughput.

In this chapter, a time-domain simulation is developed to analyze urban radio Code Division Multiple Access (CDMA) system performance using MATLAB simulation software. The simulation programs are used to estimate the BER performance of the CDMA RAKE receiver as well as the throughput performance for different ARQ protocols. To establish the accuracy of simulation, BER results are obtained for a simple Binary Phase Shift Keying (BPSK) modulation system with Additive White Gaussian Noise (AWGN) as well as for a more complex CDMA system. These results are then compared to well known analytical results given in Chapters 3, 4, and 5 to establish the accuracy of simulation. This is followed by the throughput simulation for different new Automatic Repeat Request (ARQ) protocols presented in the previous chapters. A comparative analysis is presented based on the simulation results.

6.1 BER simulation for CDMA

Several techniques are available for simulating the BER of CDMA systems [34]. The Monte Carlo method is the most commonly used technique and this method is used to

estimate the BER of the urban CDMA RAKE receiver. This method is based on counting the errors. Since an error can be expected to occur every ϵ^{-1} bits, ϵ being the BER, the length of a Monte Carlo run must increase as ϵ decreases. For sufficiently small ϵ the simulation time will be prohibitively long. It is practical to verify BER of, as low as, about 10^{-5}, using the Monte Carlo simulation [35].

The number of bits required for estimating BER using a Monte Carlo simulation is of the order of $10/\epsilon$. Such a sample will produce a confidence interval of about $(2\epsilon, 0.5\epsilon)$ at 0.95 confidences level [34]. This means that about one million symbols are necessary to simulate a BER of 10^{-5}.

6.1.1 System model of a CDMA system

The system model described here consists of a Direct Sequence Spread Spectrum (DS-SS) transmitter model, an urban CDMA radio channel model, and a RAKE receiver model, as shown in Figure 6.1. The lowpass equivalent representation is used in the simulation. The simulation is based on drawing samples from the probability distributions that model different random processes in the CDMA urban radio system. This is performed a sufficient number of times and errors are counted.

Several assumptions are used in the simulation model. The first is that the data bits of the different users independently take value of -1 or 1. Another assumption is that different users K transmit asynchronously in $[0, T_b]$. Four samples per chips are used. The path gains β are assumed to be independent Rayleigh random variables with a variance $\sigma = 0.5$ and the path phases Φ are independent random variables uniformly distributed over $[0, 2\pi]$. The number of multipaths L considered is three. Since a multipath Rayleigh fading channel has a slow fading rate, the gain and phase are assumed to remain constant over 400 data bits. Perfect power control, perfect channel parameter estimation, and perfect spreading code phase estimation are also assumed for the simulation.

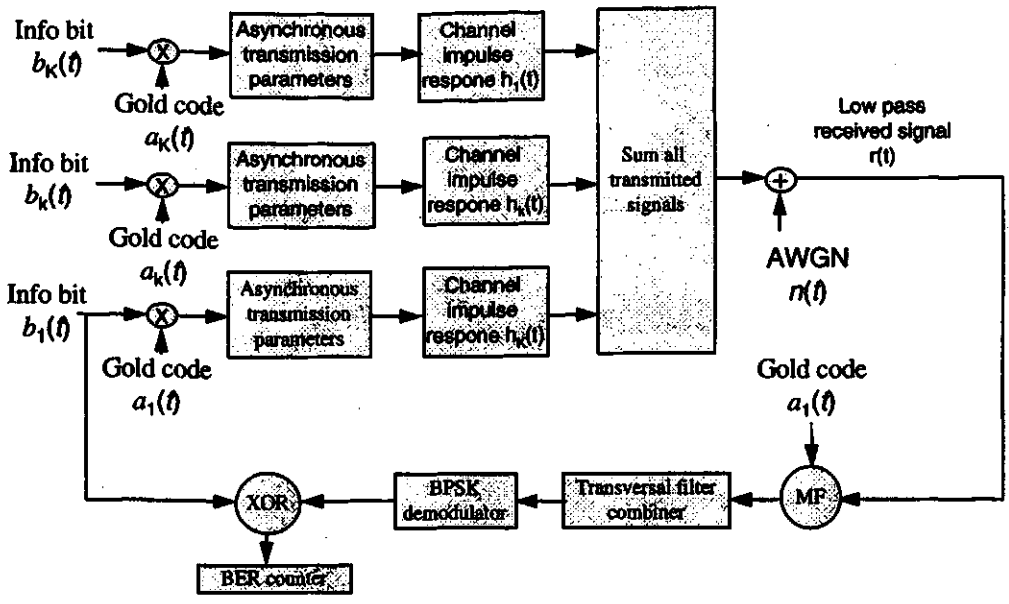

Figure 6.1 Low-pass equivalent of the simulated urban CDMA system.

As shown in Figure 6.1, the transmitter consists of a data source with waveform $b_k(t)$, a spread spectrum code waveform $a_k(t)$. Both of these waveforms take on a value of -1 or 1. The data waveform is first multiplied by the spread spectrum sequence which is a Gold code with length $N_c = 31$. The resulting waveform is then sampled and delayed by a delay between 0 and T_b.

The complex lowpass equivalent impulse response of the channel for the link between the k^{th} user and the RAKE receiver was given in Equation 4.6. The channel is characterized using a discrete-time impulse response model. In this model, the maximum multipath delay spread T_m is divided into a small time interval called bins. Each bin is assumed to contain either one multipath component or no multipath component. A possibility of more than one path in a bin is excluded. A bin size of chip duration T_c is used in the simulation. Thus, the maximum number of bins possible for the system being simulated is 16. Thus there are 16 resolved paths. The number of resolved paths in the receiver was assumed to be three, so that three out of sixteen bins are assumed to be

occupied. In order to reduce complexity in the multipath tracking software, the three resolved paths are assumed to occupy the first three bins as shown in Figure 6.2.

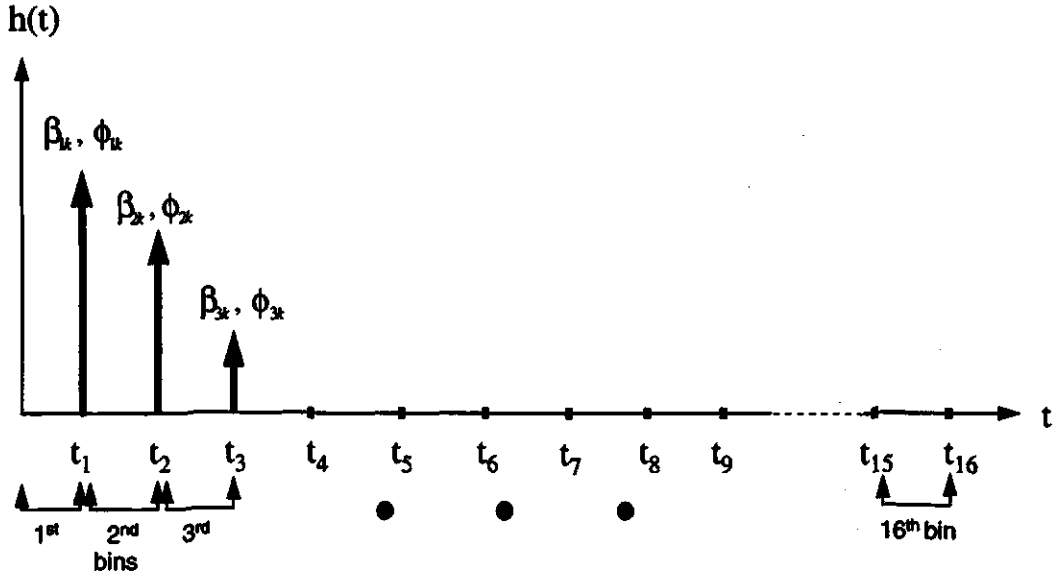

Figure 6.2 A multipath channel model of the urban CDMA system.

The path phases Φ_{lk} are uniformly distributed over $[0, 2\pi]$. The Rayleigh distributed path gain β_{lk} in Equation 4.6 is generated using the method discussed below. The Rayleigh distribution function $F(\beta)$ may be written as [36]

$$F(\beta) = 1 - e^{-\beta^2/2\sigma^2}. \tag{6.1}$$

In this case,

$$\beta = \sqrt{-2\sigma^2 \ln(1 - F(\beta))}. \tag{6.2}$$

Since $F(\beta)$ is in the range of zero to one, $1 - F(\beta)$ can be replaced by y, where y is a random variable with uniform distribution over [0, 1]. Thus the Rayleigh distributed random variable can be generated using

$$\beta = \sqrt{-2\sigma^2 \ln(y)}. \tag{6.3}$$

The multipath diversity combining rake receiver consists of a filter matched to the first users's spreading code, a diversity combiner, and a BPSK demodulator. The matched filter is implemented as a bank of correlators. The function of the correlator is implemented in the simulation by multiplying the lowpass received signal with a spreading code aligned with each path. The diversity combiner is implemented as a transversal filter with a number of taps equal to the number of paths of the user, as shown in Figure 4.3. Maximal ratio combiner is realized by applying weights that are equal to the corresponding path gains at each tap point and then summing the weighted outputs. This is followed by a data decision detector for the combined output.

6.1.2 Program Structure of a CDMA system

As shown in Figure 6.3, the program can be constructed in a straightforward way [37]. First, initialization parameters such as the number of bits per block, number of users, a block counter, error counter, and all other variables are set up. Gold codes with period 31 are generated for each user. Thirdly, there is a loop that is used repeatedly. This loop consists of a transmitter section, a channel section, receiver, error detector, and counter section. Finally, the estimate of the bit error probability is obtained by dividing the number of errors observed by the number of times that the loop was repeated.

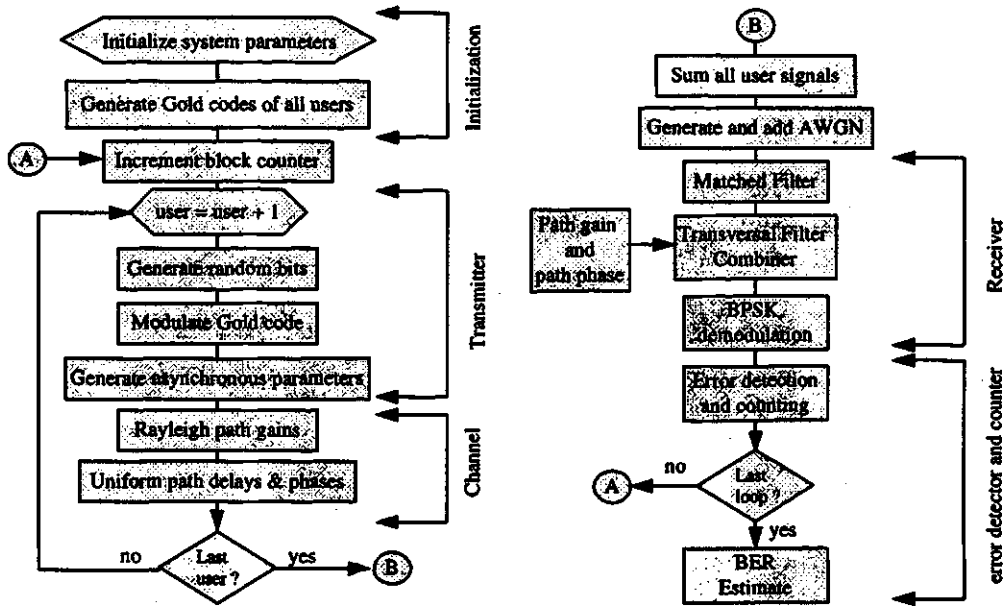

Figure 6.3 Flowchart of the simulation program for BER performance evaluation of a CDMA RAKE receiver in urban radio environment.

In the transmitter section, the random data bits for all K users are generated and multiplied by the corresponding Gold code. The asynchronous nature of the user transmission is taken into account by shifting the blocks by an amount equal to their transmitter delay. In the channel section, the uniformly distributed path phases and Rayleigh distributed path gains for all L resolvable paths of all K users are generated. The output of the k^{th} transmitter is convolved with the k^{th} channel model. The white Gaussian noise is generated and then added to the sum of the K user signals to obtain the total received signal at the receiver. In the final stage, at the RAKE receiver section, the received signal is put through a matched filter that is matched to the Gold code of user one. The outputs of the matched filter are maximal-ratio combined, using transversal filter combiner that is provided with the perfect estimation of path gains and phases. The combiner output is then BPSK demodulated.

6.1.3 Simulation of BER Performance Results

In this section, simulation results are presented together with the analytical results obtained in Chapter 4. The simulation results were obtained for six values of the Er/No of 0, 5, 10, 15, 20, 25, and 30 decibels. Figure 6.4 depicts the analytical and simulation results for two values of simultaneous users $K=3$ and $K=9$. The number of resolvable paths L is taken as 3. The 95% confidence interval of $(2\epsilon, 0.5\epsilon)$ is also shown. The simulated BER results agree with analytical results quite well for low Er/No. The agreement is not so good at the higher Er/No values. This could be explained by the fact that the analytical approach, a Gaussian approximation of the multi-user interference was used. For the low Er/No, where the contribution of the thermal noise to the total amount of noise is relatively large, the total noise is almost white Gaussian noise. For higher Er/No, this is not the case. In spite of this assumption, the BER obtained by analysis lies within the confidence interval of the simulated BER estimate. This agreement between the simulated and analytical result justifies the approximation used in the analysis. Therefore, the Gaussian approximation for MUI can be used to obtain the performance analytically. This results in much lower simulation time. For example, the numerical computation using Gaussian approximation takes a few seconds of the computer time, while Monte Carlo simulation of BER performance with a rake receiver takes approximately 14 to 18 hours of computer time if this assumption is not used.

6.2 Techniques for Estimating Throughput Efficiency of ARQ protocols.

The Monte Carlo method is used to estimate the throughput efficiency of different ARQ protocols. The estimated throughput efficiency is obtained by counting the total number of data blocks required to deliver one correct block. To achieve higher confidence, the number of blocks to be delivered correctly is taken to be $10/\epsilon$. These blocks are divided into M frames where each frame consists of $10/\epsilon M$ blocks. These number of blocks are required to produce results with a confidence interval of about $(2\epsilon, 0.5\epsilon)$ at 0.95

confidences level. Finally, the simulated results are compared with the analytical results. For the SW and GBN protocols, M is assumed to be one.

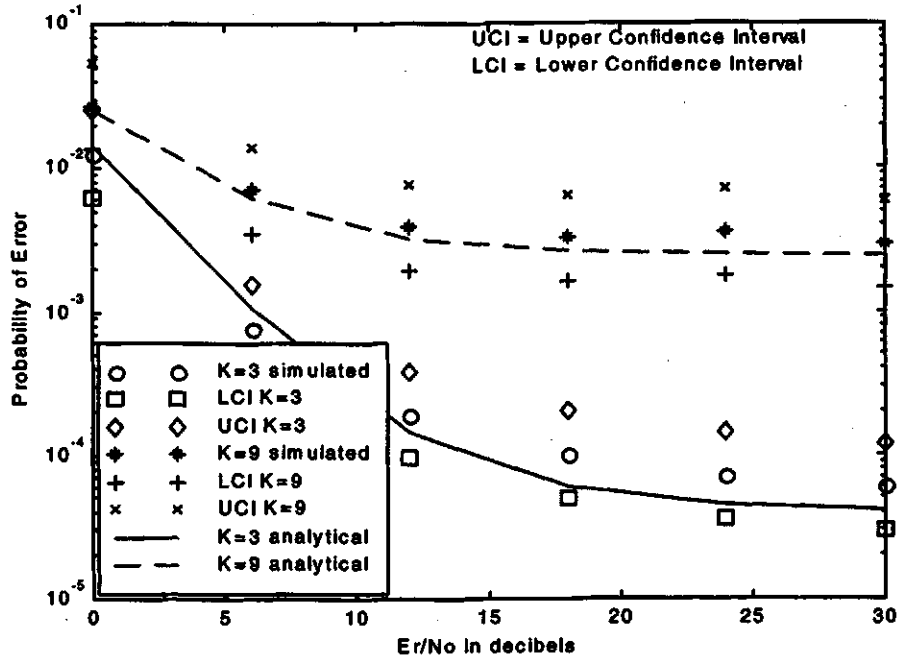

Figure 6.4 Probability of error versus Er/No for a CDMA RAKE receiver. Results were computed for L=3 and N_c=31. The 95% confidence level interval is superimposed.

6.2.1 System model of an ARQ simulation for a BPSK system with AWGN

In this section, the throughput of some ARQ protocols such as SW, GBN, GSW-1, and GSW-2 are simulated over a BPSK-modulation system with AWGN. The simulation results are then compared with the analytical results derived in Chapters 3 and 5. The system model described here consists of a digital information source, a CRC-16 coder, a channel coding, a CRC-16 decoder, and a digital Information sink, as shown in Figure 6.5. The channel coding consists of a BPSK modulator, AWGN channel model, and a correlator.

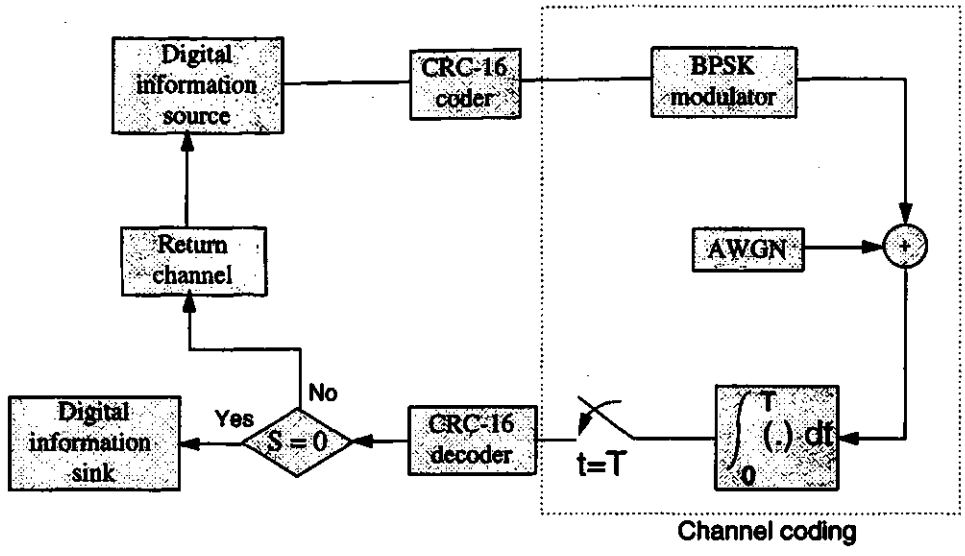

Figure 6.5 A BPSK modulation system with ARQ.

The CRC-16 encoder and decoder use a shift register circuit with feedback connections, as explained in Chapter 3. The BPSK modulator, AWGN, and a correlator are described in Chapter 2. The data is delivered from an information source to the CRC-16 encoder that attaches 16 parity bits to 384 message bits. The output of the CRC-16 encoder is a 400-bits data block that is ready to be sent through a channel coding. The encoded block is then delivered to the BPSK modulator and transmitted over the AWGN channel. At the receiving end, the block is demodulated and delivered to the information sink through a CRC-16 decoder that computes the syndrome of the received data. If an erroneous data block is detected, the receiver sends an NAK through the return channel. Conversely, an ACK is sent if an error-free block is detected. The erroneous data is delivered to the destination only if the decoder fails to detect the presence of errors. The return channel is assumed to be an error-free channel.

6.2.2 Program Structure of ARQ simulations for a BPSK system with AWGN

The protocol programs are different from one protocol to another, but they can be constructed in a somewhat similar way, as shown in Figure 6.6 to 6.9. At first, initialization parameters such as the number of bits per block, number of blocks per frame, a block counter, frame counter, round-trip delay, and some channel coding variables need to be set up. Next, one needs to generate and to transmit a frame or a block through a BPSK system with AWGN. The syndrome of the received block has to be calculated in order to detect the errors. In the SW and GBN protocols, if the received blocks are error-free the receiver sends an ACK to the transmitter to send the next block. In the GSW-1 protocol, the receiver requests a new frame to the transmitter as soon as it receives an error-free block. On the other hand, in the GSW-2 protocol, the receiver will request a new frame if all blocks of a frame have been received correctly.

6.2.3 Simulation Results of ARQ protocols for a BPSK system with AWGN

In this section, simulation results, together with the analytical results, are presented for a BPSK modulated system with AWGN for four values of the Er/No. In Figure 6.10, the effect of the delay N on the SW and GBN throughput performance is presented. As calculated in Chapter 6, N=7 represents 42 ms delay and N=25 represents 152 ms delay. From the plot, it may be seen that the simulated results fit the analytical results quite well for all value of Er/No. Figures 6.11 and 6.12 show the throughput of GSW-1 and GSW-2 protocols for different values of M and N. Once again, the plots show good agreement between analytical and simulation results.

In the analysis of the ARQ throughput efficiency, the effect of undetected codeword error was not considered. The results presented in Figure 6.10, 6.11, and 6.12 show a good agreement with the analytical results. Based on this, it may be concluded that the undetected codeword error has an insignificant effect in the throughput simulation of an ARQ protocol.

Therefore, the simulation of the CRC-16 coder and decoder can be removed from the system model and replaced by much simpler XOR operation. This will reduce simulation complexity and time. The results below were obtained using this approach.

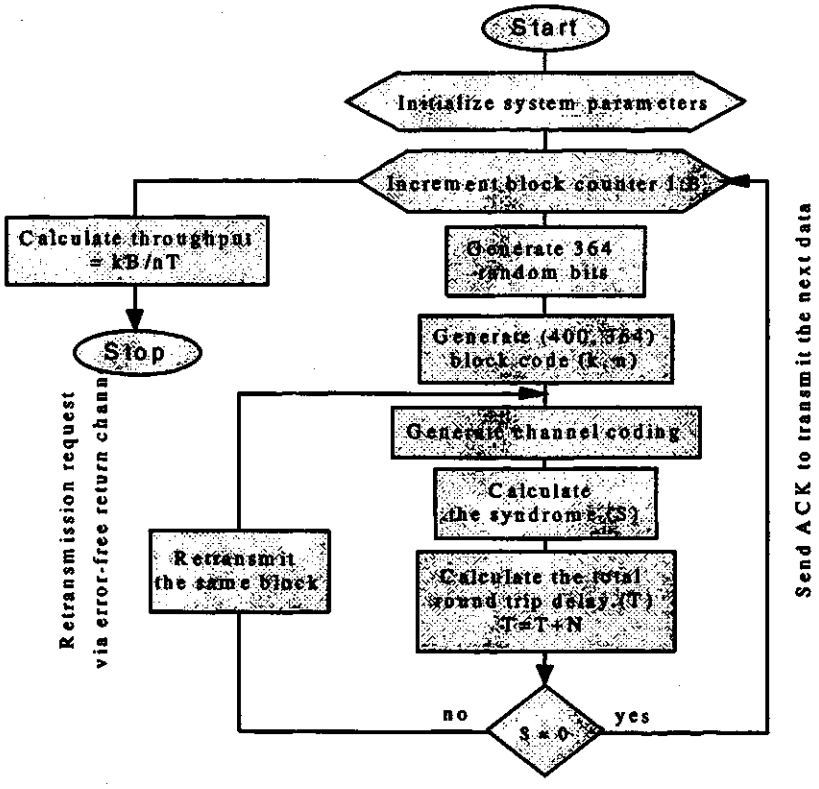

Figure 6.6 Flowchart of the simulation program for SW ARQ Protocol.

6.3 New Generalized Stop-and-Wait ARQ Protocols

As stated before, the modified versions of GSW-1 and GSW2 protocols were designed to improve the throughput efficiency under severe channel conditions. These new protocols, designated GSW-3 and GSW-4, retain the simple implementation of the previous protocols, while reducing the transmitter waiting state time. Since these proposed protocols are fairly difficult to analyze, only simulated results were obtained.

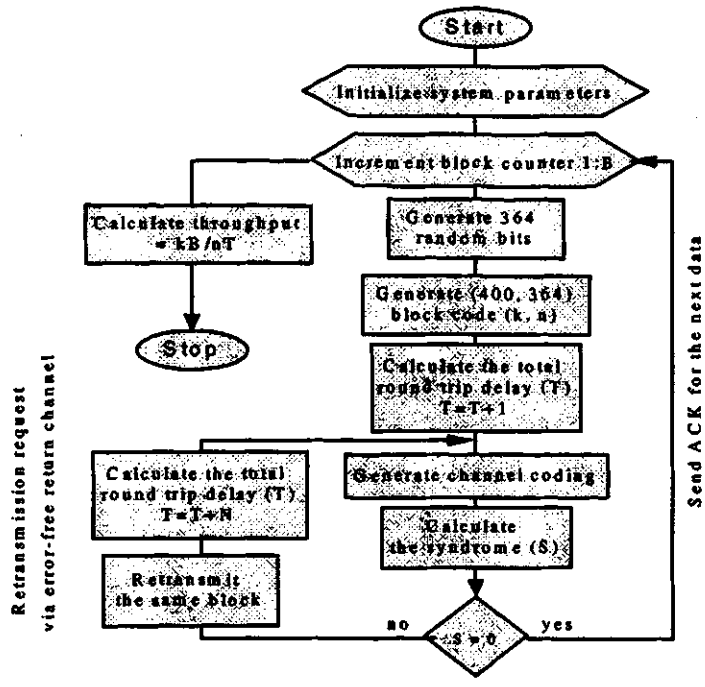

Figure 6.7 Flowchart of the simulation program for GBN ARQ Protocol.

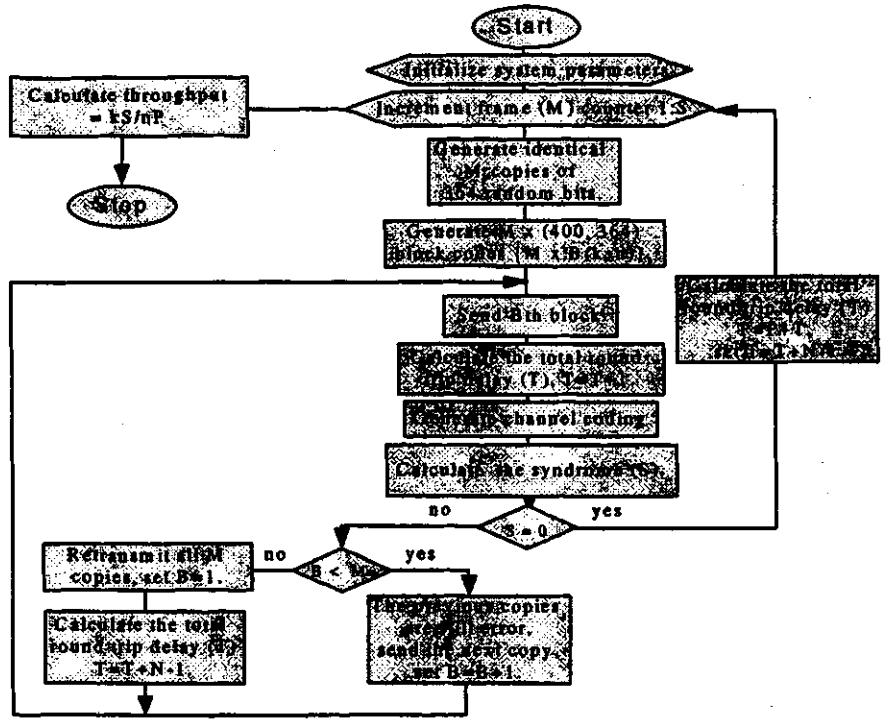

Figure 6.8 Flowchart of the simulation program for GSW-1 ARQ Protocol.

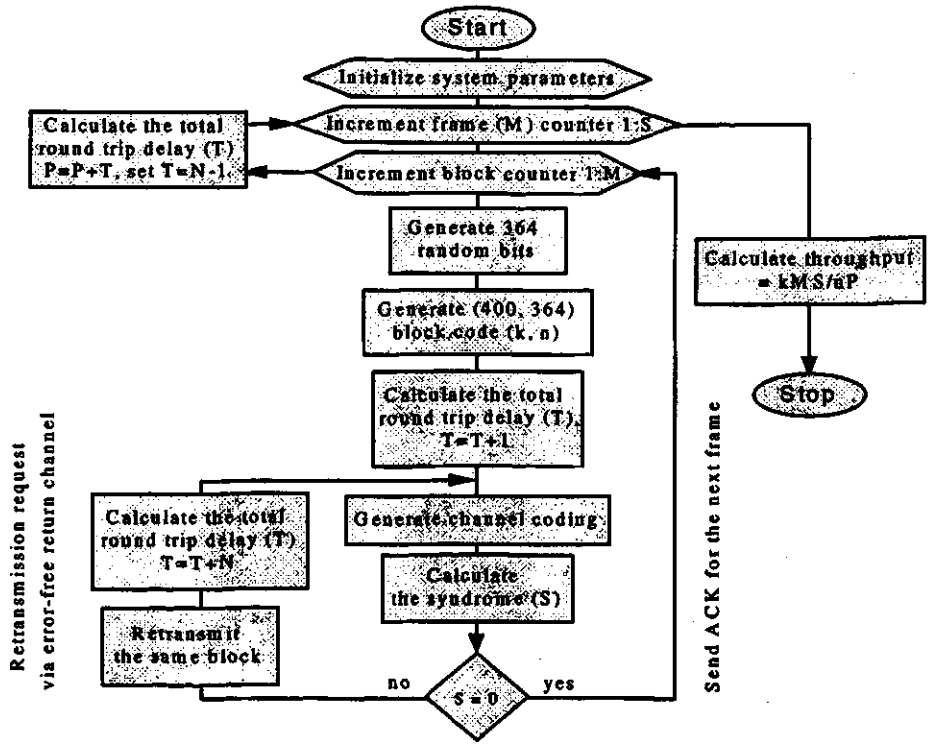

Figure 6.9 Flowchart of the simulation program for GSW-2 ARQ Protocol.

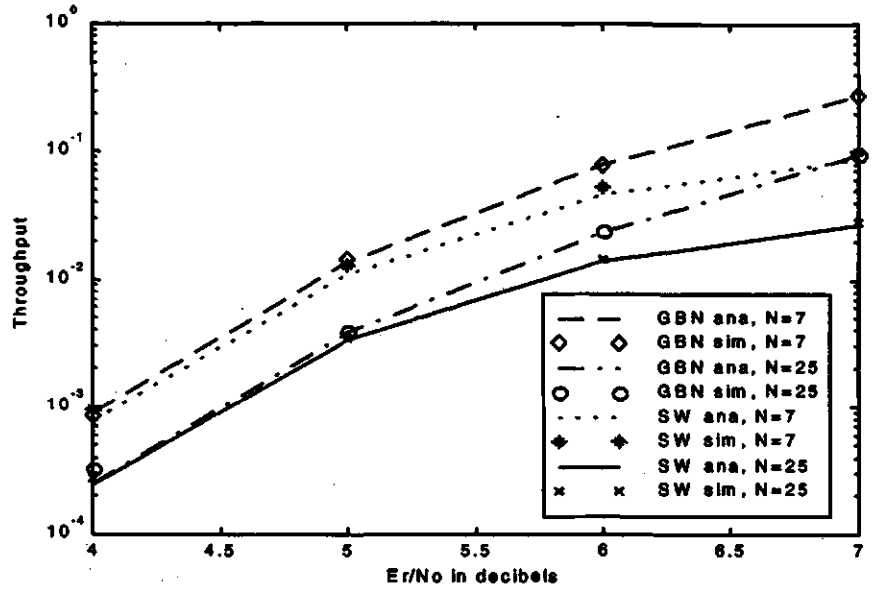

Figure 6.10 Throughput of SW and GBN protocols versus Er/No obtained by analysis and simulation over a BPSK system with AWGN for N=7 and N=25.

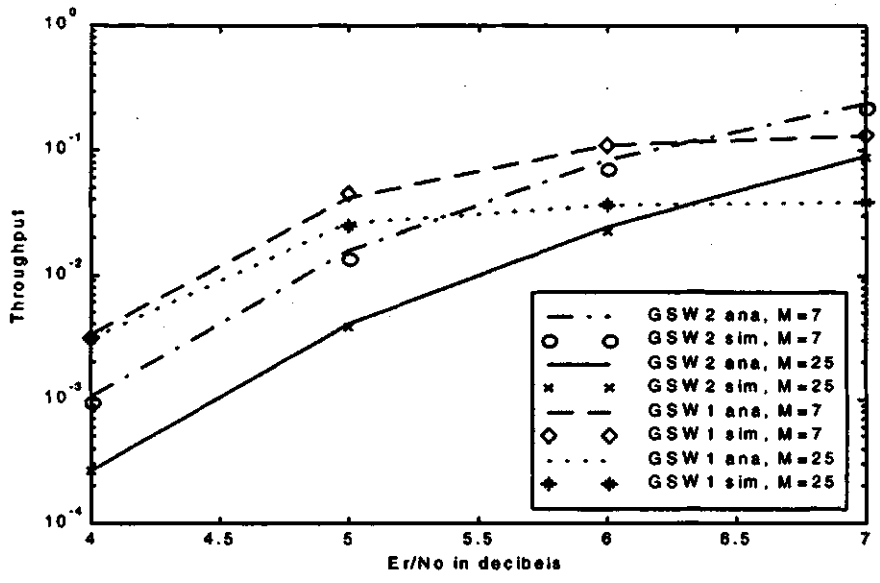

Figure 6.11 Throughput of GSW-1 and GSW-2 protocols versus Er/No obtained by analysis and simulation over a BPSK system with AWGN. Results were computed for N=7 for M=7 and N=25 for M=25.

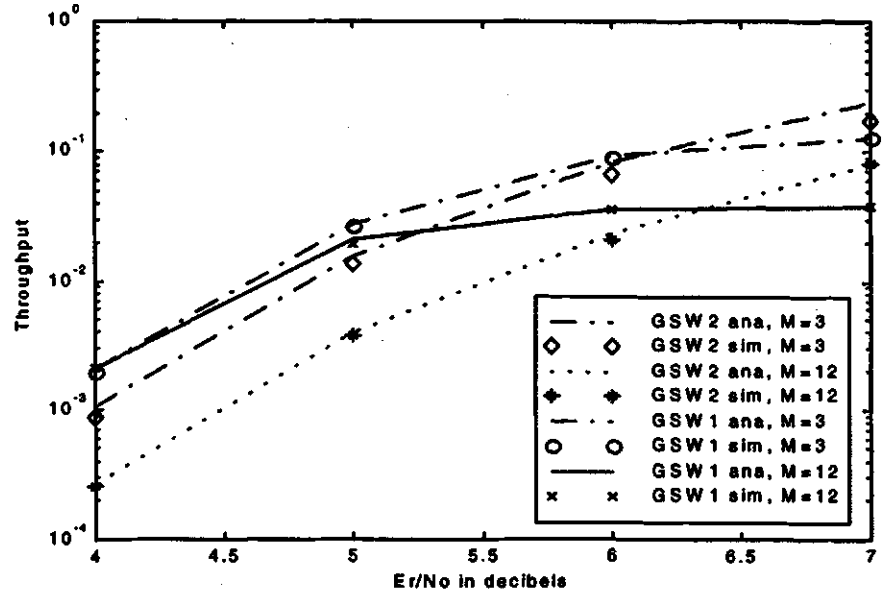

Figure 6.12 Throughput of GSW-1 and GSW-2 protocols versus Er/No obtained by analysis and simulation over a BPSK system with AWGN. Results were computed for N=7 for M=3 and N=25 for M=12.

6.3.1 Generalized Stop-and-Wait Type-3 (GSW-3) ARQ Protocol

In the GSW-3 protocol, a buffer is introduced at the receiver so that codewords received without error or with detectable error patterns can be stored. This solution seems somewhat contradictory, as the SW protocol is generally selected because of its simplicity. However, since the buffer required in the GSW-3 protocol is meant to store M codewords and M can be set low in relation to N, its implementation complexity can be kept to an acceptable level for many applications. Compared to this, the SR requires a buffer length at least equal to N and is more complex, particularly for higher values of N.

As shown in Figure 6.13, for GSW-3 protocol, the transmitter sends M codewords and enters the waiting state, while the receiver decodes all the M vectors and sends the transmitter the ACK or NAK signals for the M codewords. The transmitter remains in the waiting state until all the M acknowledgments have been received before entering the retransmission state, during which only the negative acknowledged codewords are retransmitted. Thus, the transmitter will resend only the error codewords.

6.3.2 Generalized Stop-and-Wait Type-4 (GSW-4) ARQ Protocol

As shown in Figure 6.14, for the GSW-4 protocol, each codeword that is negatively acknowledged in the first transmission is retransmitted twice consecutively. This increases the probability of receiving an error free codeword. Thus, the throughput efficiency of the GSW-4 can be improved over GSW-3. In the GSW-4 protocol, the transmission length (the number of codewords in a transmission cycle) can vary, depending on the number of negatively acknowledged codewords in the previous transmission.

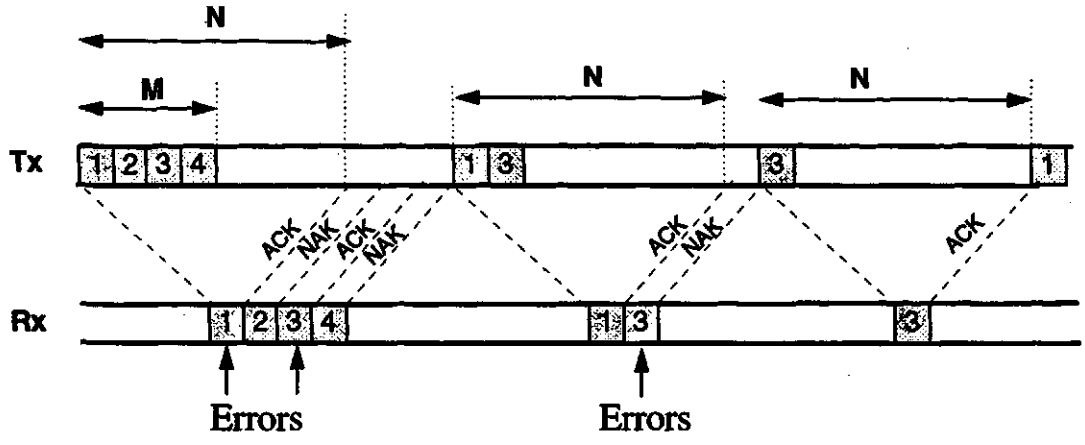

Figure 6.13 The Generalized Stop-and-Wait Type three (GSW-3) ARQ protocol.

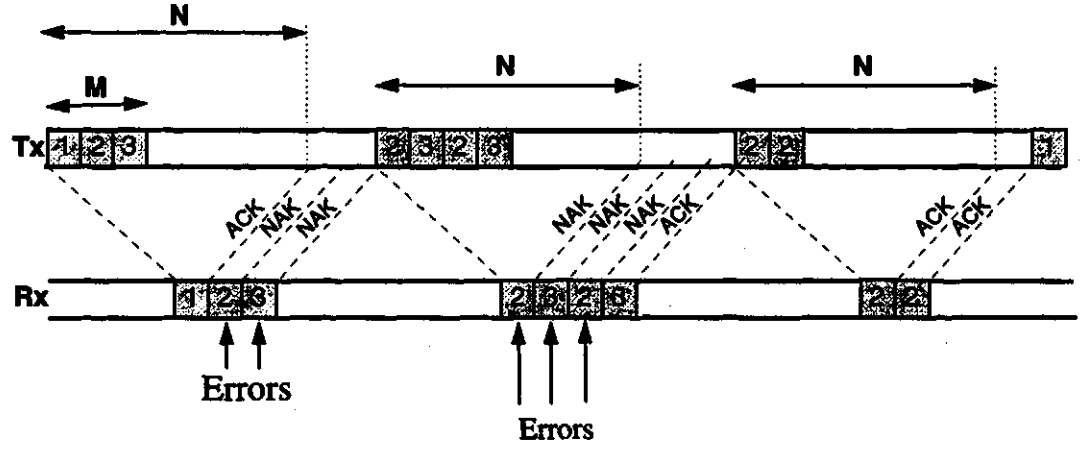

Figure 6.14 The Generalized Stop-and-Wait Type four (GSW-4) ARQ protocol.

6.3.3 System model of an ARQ simulation for a CDMA system

The throughput of SW, GBN, GSW-1, GSW-2, GSW-3, and GSW-4 protocols were simulated for CDMA system shown in Figure 6.15 below. The system model described here consists of a digital information source, a channel coding block, a XOR operation, and a digital information sink. The channel coding block consists of DS-SS transmitters, an urban channel model with AWGN, a matched filter, a transversal filter, and a BPSK demodulator.

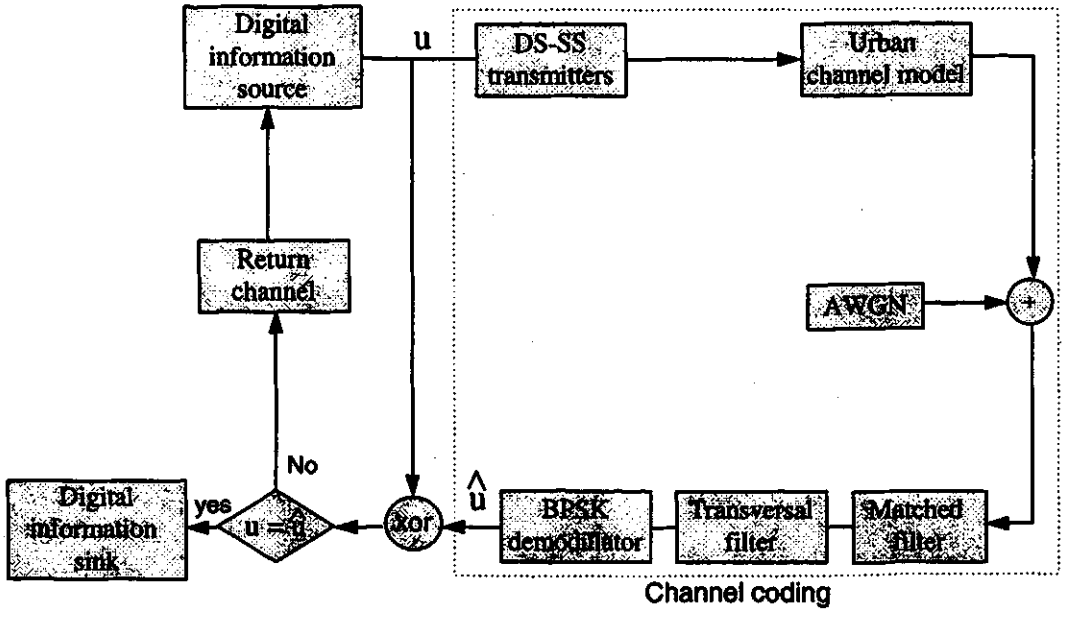

Figure 6.15 An urban radio CDMA system with ARQ.

The 400-bit data blocks are delivered from an information source to the transmitters over an urban channel model with AWGN. At the receiver, the lowpass equivalent received signals are delivered to the matched filter that is matched to the first user and passed through a transversal filter. At the receiving end, the combined signals of the first user are demodulated by a BPSK demodulator and delivered to the XOR operator, which compares them with the original data block. If there are no discrepancies, the block is delivered to the

information sink and the receiving terminal notifies the sending terminal, through a suitable return channel, that the block has been correctly received. If discrepancies exist, the sending terminal is so notified and the block is retransmitted (it is assumed that the block is stored at the sending terminal until acknowledgment or retranmission request is received).

6.3.4 Simulation results of ARQ protocols for a CDMA system

The flowchart for the simulation program structures for the GSW-3 and GSW-4 protocols are presented in Figure 6.16 and 6.17. These charts are similar to the previous structures described in Section 6.2.2. The only difference is in the introduction of a buffer for erroneous blocks and the procedure of copying the identical error blocks before requesting for retransmission.

Figures 6.18 and 6.19 show the throughput performance of the SW, GBN, GSW-1, and GSW-2 versus Er/No over a CDMA system for different values of K, N, and M. The plots show good agreement between the analytical and simulation results, especially in the high signal to noise ratios (Er/No > 10 decibels) and low user number, K=3. For K=9, the performances of a CDMA system degrades severely, the analytical results of the throughput do not fit well with the simulation results shown in Figure 6.19. This could be explained by the difference between the analytical and simulation BER results for the CDMA system, in Section 6.1.3.

In Figures 6.20 to 6.27, the simulation results for various ARQ protocols for a CDMA system are presented. Figures 6.20 and 6.21 show the throughput versus Er/No with K=3 and N=7 for M=3 and M=7. The plots depict that GBN outperforms the other ARQ protocols for Er/No > 4.3 decibels when M=3 and for Er/No > 7 decibels when M=7. For fairly low Er/No, the GSW-4 protocols outperforms the other protocols. Even the GSW-3 performance is higher than that of the GBN and it requires only a simple buffer. The GSW-1 yielded the best performance for very low Er/No values.

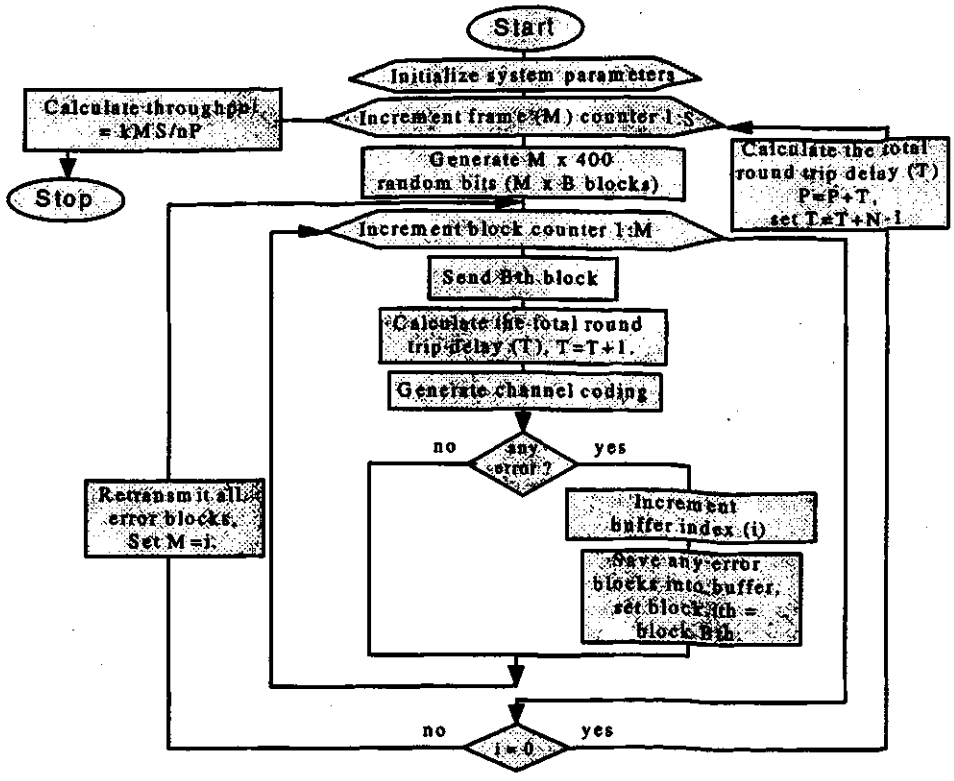

Figure 6.16 Flowchart of the simulation program for GSW-3 ARQ Protocol.

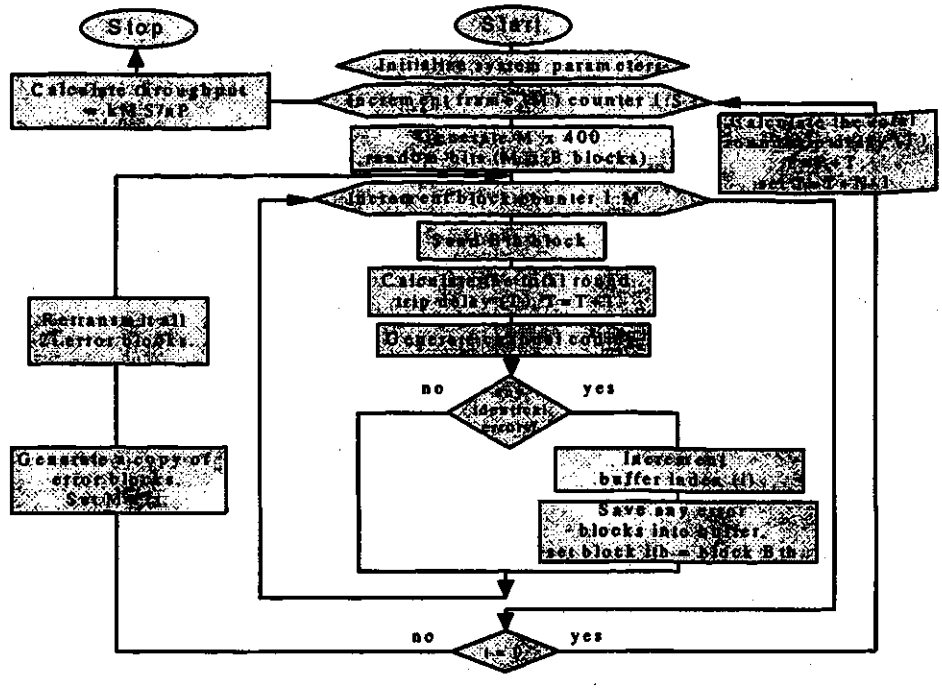

Figure 6.17 Flowchart of the simulation program for GSW-4 ARQ Protocol.

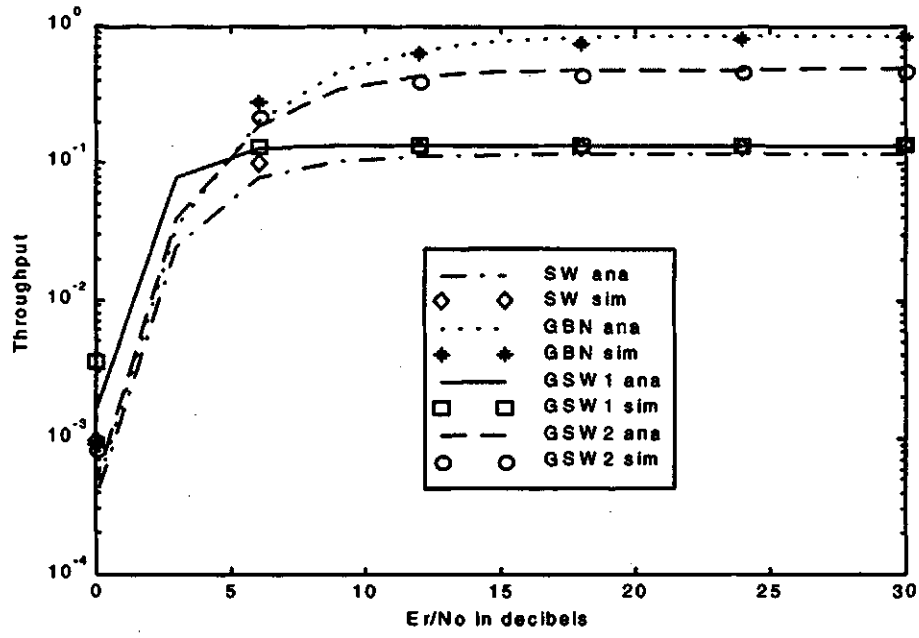

Figure 6.16 The simulated and analytical results for throughput of ARQ protocols plotted as a function of Er/No for a CDMA system with K=3, L=3, and N_c=31. Results were computed for N=7 and M=7.

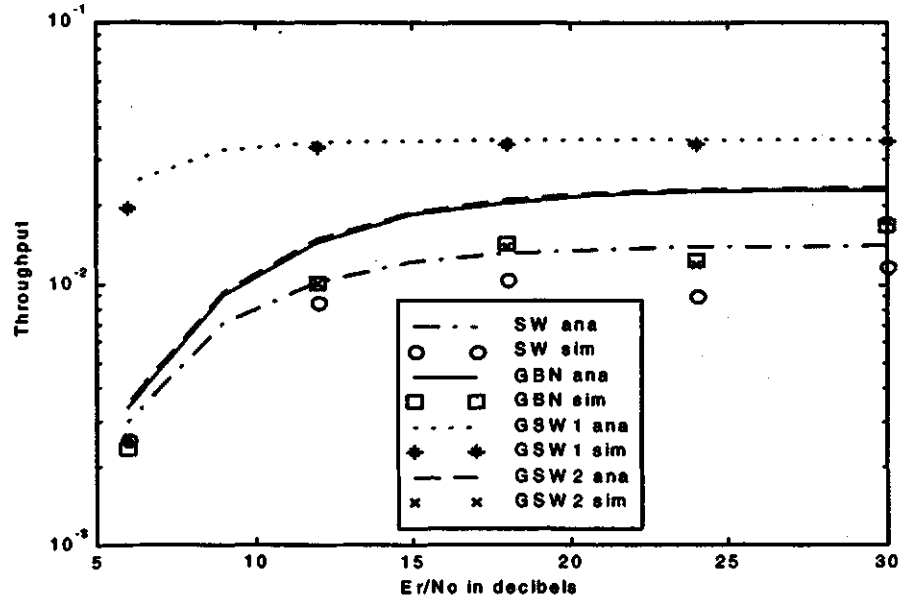

Figure 6.19 The simulated and analytical results for throughput of ARQ protocols plotted as a function of Er/No for a CDMA system with K=9, L=3, and N_c=31. Results were computed for N=25 and M=25.

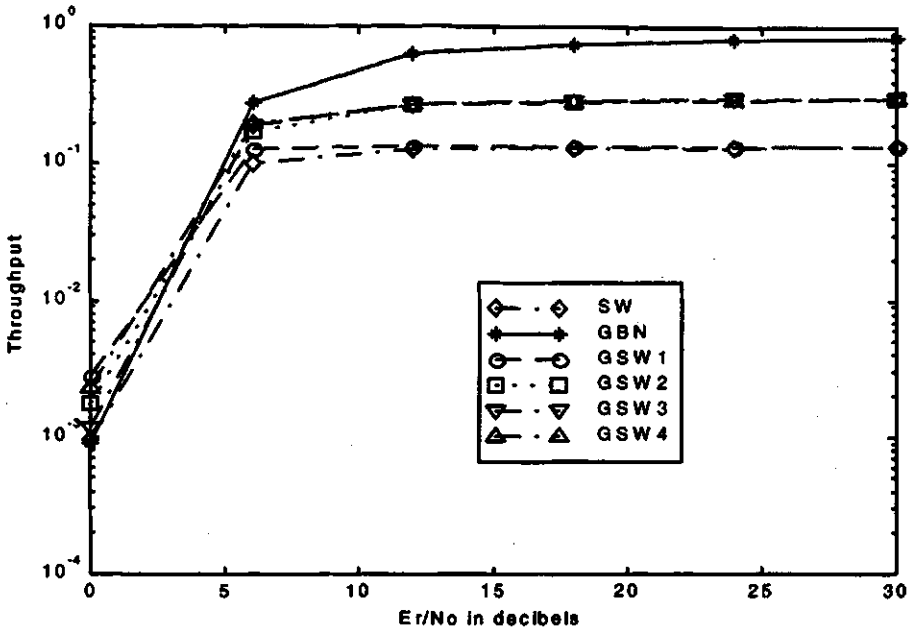

Figure 6.20 The simulated results for throughput of ARQ protocols plotted as a function of Er/No for a CDMA system with K=3, L=3, and N_c=31. Results were computed for N=7 and M=3.

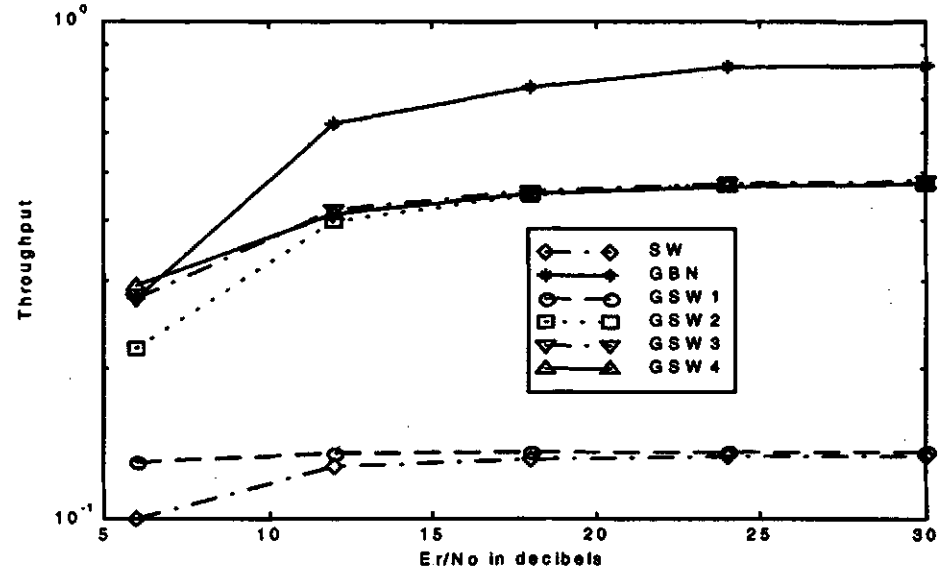

Figure 6.21 The simulated results for throughput of ARQ protocols plotted as a function of Er/No for a CDMA system with K=3, L=3, and N_c=31. Results were computed for N=7 and M=7.

Figures 6.22 and 6.23 show the throughput versus Er/No with K=3 and N=25 for two values of M=12 and M=25 respectively. The performances of the GSW-4, GSW-3, and GSW-2 protocols are comparable to that of the classical GBN protocol for high values of M. However, even with N=M, the GSW-2 protocol requires a lower signal to noise ratios per bit than the GBN protocol because of N-length wait periods required in GBN. The throughput of the GSW-3 and the GSW-4 protocols is higher than other protocols for 1.5 < Er/No < 9.5 dB with M=12 and 2.5 < Er/No < 12 dB with M=25. The GSW-3 and GSW-4 protocols require 1 dB lower energy for the same throughput as M increases from 12 to 25. Furthermore, the GSW-1 performs better when Er/No is low.

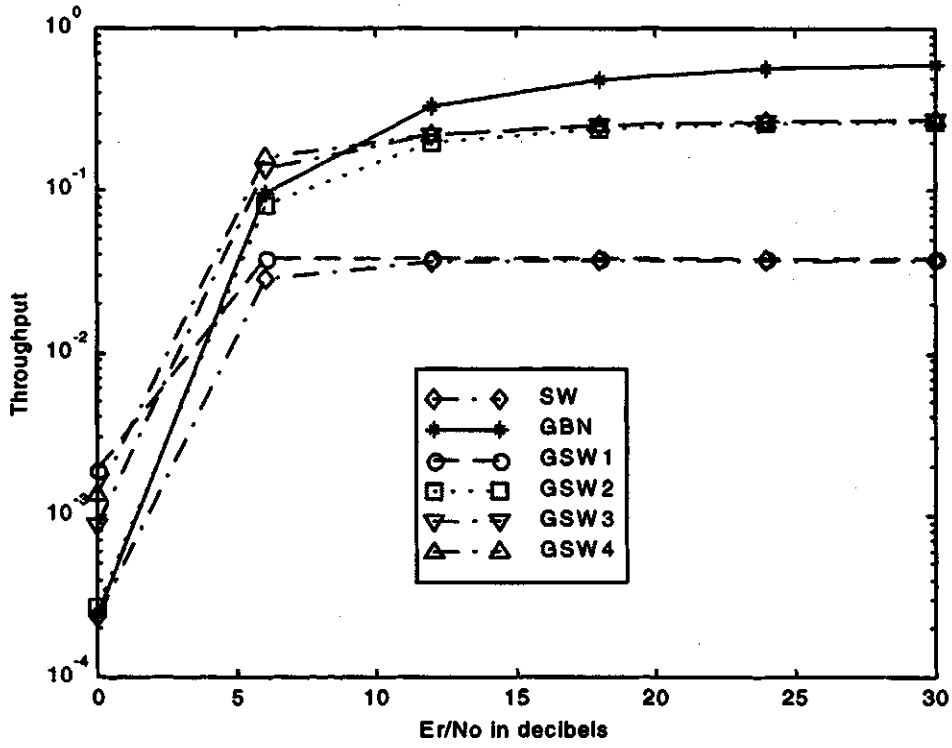

Figure 6.22 The simulated results for throughput of ARQ protocols plotted as a function of Er/No for a CDMA system with K=3, L=3, and N_c=31. Results were computed for N=25 and M=12.

Figures 6.24 and 6.25 show the throughput versus Er/No for K=9, N=7 for two values of M=3 and M=7 respectively. The figures show that for this case, with respect to the throughput performance, the protocols could be ordered as: The GSW-4 followed by the GSW-1, GSW-3, GBN, GSW-2, and SW.

Figures 6.26 and 6.27 show the throughput versus Er/No with K=9, N=25 for M=12 and M=25. For this case, the throughput performances results indicate the following order: The GSW-4 followed by the GSW-3, GSW-1, GBN, GSW-2, and SW protocols. Obviously, the GSW-4 shows the best performance under severe channel conditions. This is because of the fact that an identical copy of the erroneous block can give a better chance of error-free reception. The GSW-3 protocol outperforms the GSW-1 protocol as the delay increases. This advantage is achieved because the received codewords in the GSW-3 are discarded only if erroneous. The GSW-2 performance is comparable to the GBN protocol for different parameter values especially for high values of N, M and K. However, the GSW-1 protocol, that is the simplest generalized stop-and-wait protocol, outperforms the other protocols in the low Er/No for any values of N and M, except for the small delay N=7 and small number of frame M=3, as shown in Figure 6.24. This advantage is achieved because a set of M identical copies are sent rather than only a single copy of block. Thus, this technique will reduce the influence of the delay on the throughput. Figure 6.26 shows somewhat surprising result in that the throughput of the GBN protocol is even lower than much simpler SW protocol for very low Er/No values.

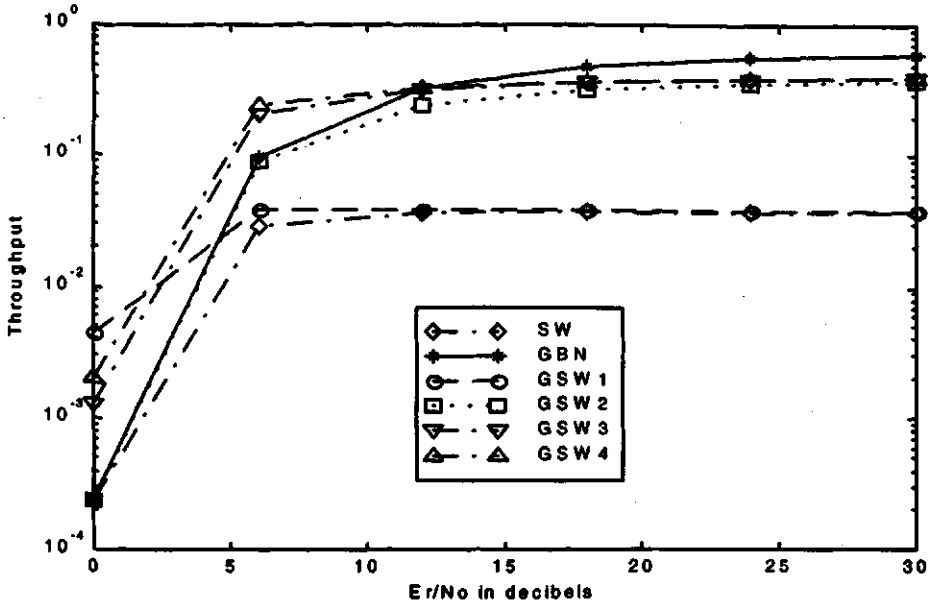

Figure 6.23 The simulated results for throughput of ARQ protocols plotted as a function of Er/No for a CDMA system with K=3, L=3, and N_c=31. Results were computed for N=25 and M=25.

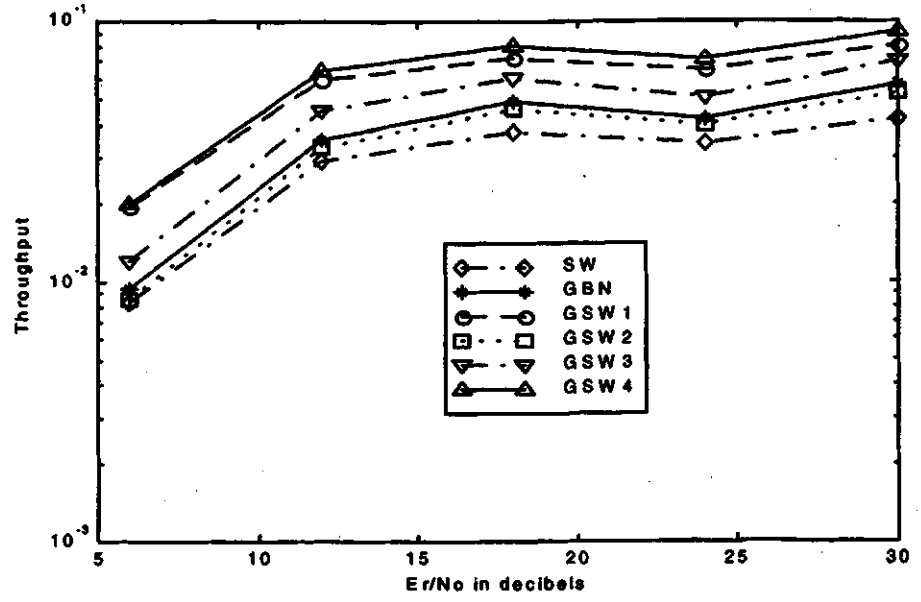

Figure 6.24 The simulated results for throughput of ARQ protocols plotted as a function of Er/No for a CDMA system with K=9, L=3, and N_c=31. Results were computed for N=7 and M=3.

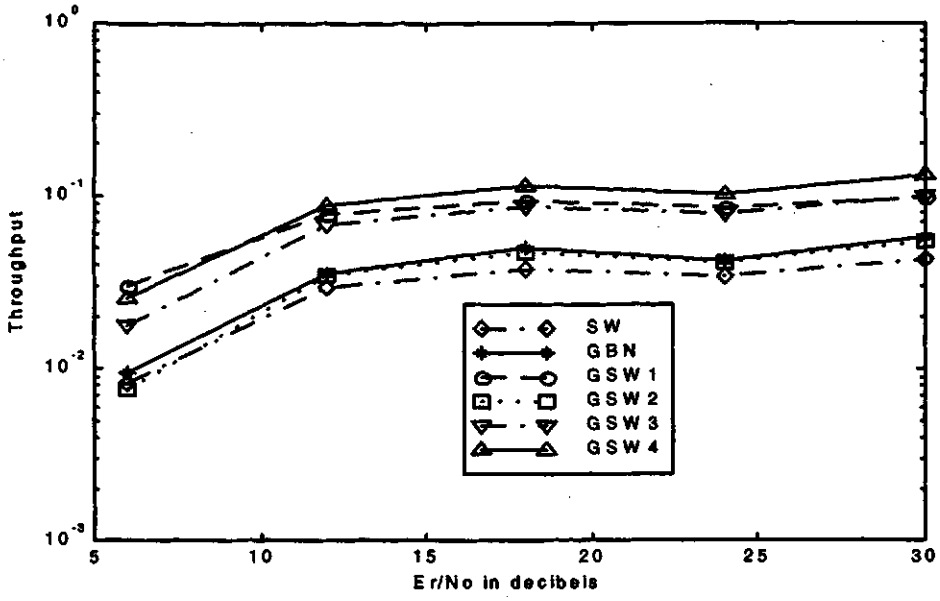

Figure 6.25 The simulated results for throughput of ARQ protocols plotted as a function of Er/No for a CDMA system with K=9, L=3, and N_c=31. Results were computed for N=7 and M=7.

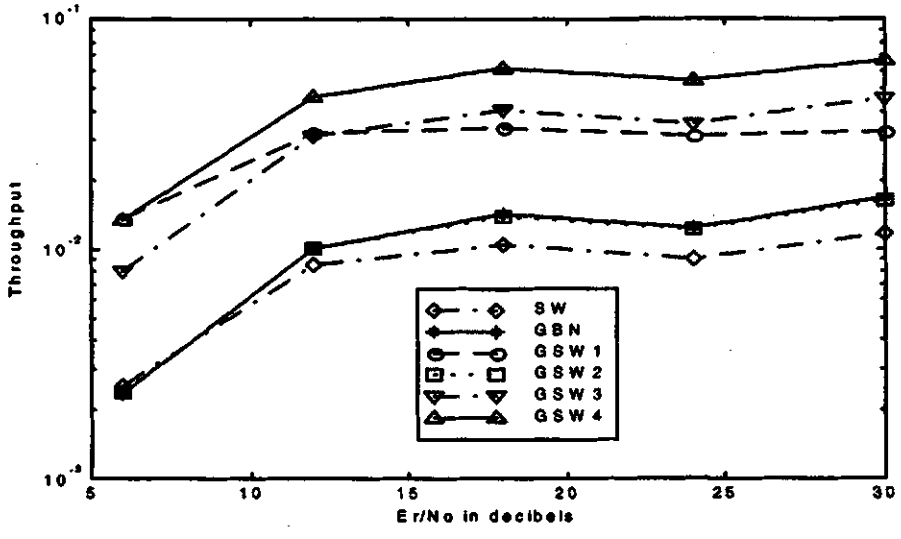

Figure 6.26 The simulated results for throughput of ARQ protocols plotted as a function of Er/No for a CDMA system with K=9, L=3, and N_c=31. Results were computed for N=25 and M=12.

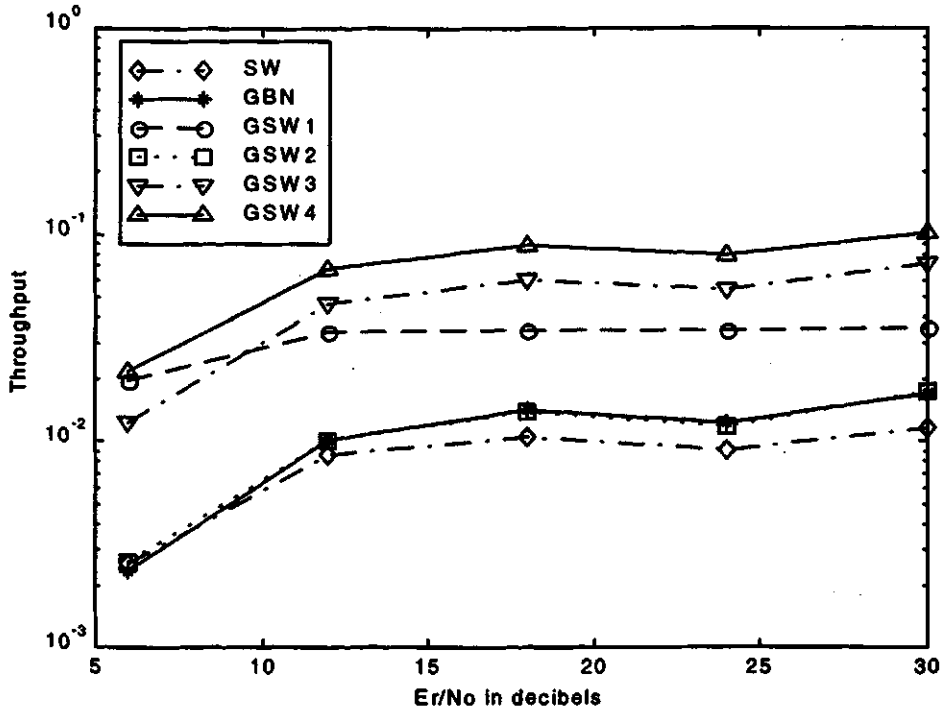

Figure 6.27 The simulated results for throughput of ARQ protocols plotted as a function of Er/No for a CDMA system with K=9, L=3, and N_c=31. Results were computed for N=25 and M=25.

7. Conclusions

In Chapter 1 the objectives of this thesis were laid down as follows:

1. Analyze different ARQ error correction methods for the CDMA systems. Identify/ propose an ARQ that is particularly suitable for CDMA.

2. Using computer simulation, verify analysis results obtained in the first objective. Based on the analysis and simulation, perform a comparison of various ARQ methods for CDMA.

Based on the work reported in this thesis, it can be said that both objectives were realized. The conclusions may be summarized as follows:

The BER performance of a CDMA urban radio system has been analyzed and the results obtained were comparable to those developed by K. Ben Letaief et al [31]. The BER performance analysis of the CDMA systems was used to get channel error probability results required for derivation of the throughput efficiency of SW, GBN, GSW-1, and GSW-2 protocols.

The computer simulation of the CDMA urban radio system was carried out to verify the BER performance analysis derived previously. The simulated BER fits the analytical results within confidence interval of $(2\epsilon, 0.5\epsilon)$ with a confidence level of 95%. The simulation of a CDMA urban radio system was then used to simulate the ARQ protocol performance analysis.

The ARQ protocol communications were simulated to verify the throughput performance analysis of the SW, GBN, GSW-1, and GSW-2 protocols for a BPSK

modulation with AWGN. The analytical results, once again, agree quite well with the simulation results. The simulation results also show that the effect of undetected error on the throughput performance is insignificant. Therefore, the assumptions used in the throughput analysis are valid.

Other computer programs were developed to simulate SW, GBN, GSW-1, and GSW-2 protocols over a CDMA urban radio system. The analytical and simulation results again show an excellent agreement. Because of the close agreement between the simulation and analytical results for these protocols, it was concluded that the simulation only could be relied on for more complex generalized ARQ protocols for which no analytical results were available. Derivation of analytical results for these protocols was out of scope of this research work.

The GSW-3 and the GSW4 protocols have been previously proposed for CDMA systems with severe channel conditions. These protocols are more complex than any classical or previous generalized stop-and-wait protocols as buffers are required to store error-free codewords. However, these protocols have an advantage over the other methods as only erroneous codewords are retransmitted to correct the errors. These protocols are expected to reduce the waiting state thereby improving the throughput performance. Finally, the simulated throughput performance of GSW-3 and GSW-4 ARQ protocols was evaluated and compared with that for the SW, GBN, GSW-1, and GSW-2 protocols. The results are summarized below:

- Under the severe channel conditions, the GSW-4 and GSW-3 protocol prove to be superior to SW, GBN, GSW-1, and GSW-2 protocols. The GSW-1 protocol is a fairly simple protocol that requires no buffer. Yet it provides the best solution for low signal to noise ratios. The GSW-2 protocol is more complex than the GSW-1 protocol but less complex than the GSW-3 and GSW-4 protocols and it has a performance comparable to the GBN protocol for any value of parameters N and M

(N = Propagation delay, M = Number of successive blocks).

- For a fairly good channel, GBN outperforms other protocols for high Er/No (> 10 decibels). For high Er/No, the performance of GSW-4, GSW-3, and GSW-2 protocols is inferior to that of GBN but is quite similar. This similarity ends as Er/No decreases. The GSW-4 protocol shows the best performance for low Er/No. The throughput of GSW-1 is comparable to the SW protocol for high Er/No and is higher than other protocols for very low Er/No.

7.1 Suggestions For Future Study

The throughput performance of the GSW ARQ protocols over a CDMA urban radio system could be further improved using the following suggestions:

- By combining GSW-1 and GSW-4 protocols, the throughput performance of the new protocol could be better for high and low Er/No as well as for different values of parameters K, M, and N.
- Memory coding could be introduced in GSW protocols to combine several copies of the same block in the decoding process at the receiver.

To reduce the computer time, importance sampling method should be implemented in the simulation and a Markov chain channel model could be used to simulate the CDMA system.

References

[1] T. S. Rappaport, *Wireless Communications: Principles and Practice*, Prentice-Hall PTR, Upper Saddle River, New Jersey, 1996.

[2] H. Hashemi, "Simulation of the Urban Propagation Channel," *IEEE Transaction on Vehicular Technology*, Vol. VT-28, No. 3, August 1979, pp. 213-225.

[3] G. L. Turin, "Introduction to Spread-Spectrum Antimultipath Techniques and Their Application to Urban Digital Radio," *Proceedings of the IEEE*, Vol. 68, No. 3, March 1980, pp. 328-353.

[4] L. W. Couch II, *Digital Analog Communication Systems Fourth Edition*, Macmillan Publishing Company, New York, USA, 1993.

[5] J. G. Proakis, *Digital Communications Third Edition*, McGraw-Hill, Inc., USA, 1995.

[6] S. Lin, D. J. Costello, Jr., M. J. Miller, "Automatic-Repeat-Request Error Control Schemes," *IEEE Communication Magazine*, Vol. 22, No. 12, December 1984, pp. 5-17.

[7] S. Lin, D. J. Costello, *Error Control Coding Fundamentals and Applications*, Prentice-Hall, Inc., Englewood Cliffs, New Jersey, 1983.

[8] P. E. Boudreau, W. C. Bergman, D. R. Irvin, "Performance of a Cyclic Redundancy Check and its interaction with a Data Scrambler," *IBM Journal of Research and Development*, Vol. 38, No. 6, November 1994, pp. 649-743.

[9] F. Argenti, G. Benelli, A. Garzelli, "Generalised Stop-and-Wait Protocol," *Electronics Letters*, Vol. 28, No. 9, April 1992, pp. 861-863.

[10] M. B. Pursley, "Performance Evaluation for Phase-Coded Spread-Spectrum Multiple-Access Communication-Part I: System Analysis," *IEEE Transactions on Communications*, Vol. COM-25, No. 8, August 1977, pp. 795-799.

[11] G. L. Turin, "The Effects of Multipath and Fading on the Performance of Direct-Sequence CDMA systems," *IEEE Journal on Selected Areas in Communications*, Vol. SAC-2, No. 4, July 1984, pp. 597-603.

[12] M. Kavehrad, P. J. McLane, "Performance of Low-Complexity Channel Coding and Diversity for Spread Spectrum in Indoor, Wireless Communication," *AT&T Technical Journal*, Vol. 64, No. 10, October 1985, pp. 1927-1965.

[13] A. R. K. Sastry, "Improving Automatic Repeat-Request (ARQ) Performance on

Satellite Channels Under High Error Rate Conditions," *IEEE Transactions on Communications,* Vol. COM-23, April 1975, pp. 436-439.

[14] M. Moeneclaey, H. Bruneel, I. Bruyland, D. Chung, "Throughput Optimization for a Generalized Stop-and-Wait ARQ scheme," *IEEE Transactions on Communications*, Vol. COM-34, No. 2, February 1986, pp. 205-207.

[15] G. Benelli, A. Garzelli, "New Modified Stop-and-Wait ARQ Protocols for Mobile Communications," *Wireless Personal Communications*, Vol. 1, 1995, pp. 117-126.

[16] R. C. Dixon, *Spread Spectrum Systems,* John Wiley & Sons, Inc., USA, 1984.

[17] M. K. Simon, J. K. Omura, R. A. Scholtz, B. K. Levitt, *Spread Spectrum Communications Handbook,* McGraw-Hill, Inc., USA, 1994.

[18] D. L. Schilling, L. B. Milstein, R. L. Pickholtz, M. Kullback, F. Miller, "Spread Spectrum for Commercial Communications," *IEEE Communications Magazine*, Vol. 29, No. 4, April, 1991, pp. 66-79.

[19] D. L. Schilling, L. B. Milstein, R. L. Pickholtz, "Theory of Spread-Spectrum Communications - Tutorial," *IEEE Transactions on Communications*, Vol. COM-30, May 1982, pp. 855-884.

[20] D. C. Cox, "910 Mhz Urban Mobile Radio Propagation: Multipath Characteristics in New York City," *IEEE Transactions on Vehicular Technology*, Vol. VT-22, No. 4, November 1973, pp. 104-110.

[21] B. Sklar, "Rayleigh Fading Channels in Mobile Digital Communication Systems Part I: Characterization," *IEEE Communications magazine,* Vol. 35, No. 7, July 1997, pp. 90-100.

[22] B. Sklar, "Rayleigh Fading Channels in Mobile Digital Communication Systems Part II: Mitigation," *IEEE Communications magazine,* Vol. 35, No. 7, July 1997, pp. 102-109.

[23] R. Gold, "Optimal Binary Sequences for Spread Spectrum Multiplexing," *IEEE Transaction on Information Theory*," Vol. IT-13, October 1967, pp.619-621.

[24] R. Gold, "Maximal Recursive Sequences with 3-Valued Recursive Cross-Correlation Functions," *IEEE Transaction on Information Theory*, January 1968, pp.154-156.

[25] M.B. Pursley, D.V. Sarwate, "Performance Evaluation for Phase-Coded Spread Spectrum Multiple-Access Communication - Part II: Code Sequences Analysis," *IEEE Transactions on Communications,* Vol. COM-25, No. 8, August 1977, pp. 800-803.

[26] D. C. Cox, "910 Mhz Urban Mobile Radio Propagation: Multipath Characteristics in New York City," *IEEE Transactions on Vehicular Technology*, Vol. VT-22, No. 4, November 1973, pp. 104-110.

[27] B. Sklar, *Digital Communications Fundamentals and Applications,* Prentice Hall, Englewood Cliffs, New Jersey, 1988.

[28] P. Sweeney, *Error Control Coding: An Introduction,* Prentice Hall International Ltd, UK, 1991.

[29] T. Kasami, T. Klove, S. Lin, "Linear Block Codes for Error Detection," *IEEE Transactions on Information Theory*, Vol. IT-29, No. 1, January 1983, pp. 131-136.

[30] M. A. Do, S. Y. Wu, "Hybrid Diversity Combining Techniques for DS-CDMA over a multipath fading channel," *Wireless Networks*, No. 3, March 1997, pp. 155-158.

[31] K. Ben Letaief, M. Hamdi, "Efficient Simulation of CDMA System in Wireless Mobile Communications," *IEEE Global Communications Conference*, Vol. 3, 1995, pp. 1799-1803.

[32] H. Brunneel, C. Tison, "Improving the Troughput of Sop-and-Wait ARQ schemes with Repeated Transmissions," *AEU International Journal on Electronics and Communications*, Vol. 51, No. 1, 1997, pp. 1-8.

[33] J. R. Freer, *Computer Communications and Networks*, Plenum Press, New York, 1988.

[34] M. C. Jeruchim, "Techniques for Estimating the Bit Error Rate in the Simulation of Digital Communication Systems," *IEEE Journal on Selected Areas in Communications,* Vol. SAC-2, No. 1, 1984, pp. 153-170.

[35] P. M. Hahn, M.C. Jeruchim, "Developments in the Theory and Application Techniques of Importance sampling," *IEEE Journal on Selected Areas in Communications,* Vol. SAC-2, No. 1, 1984, pp. 153-170.

[36] A. Papoulis, *Probability, Random Variables, and Stochastic ProcessesThird Edition*, McGraw-Hill, Inc., New York, 1991.

[37] H. S. Misser, A. Kegel, R. Prasad, "Spectrum for Indoor Radio Communication in a Rician Fading Channel," *IEE Proceedings-I*, Vol. 139, No. 6, 1992, pp. 620-624.